# Clinical Low Field Strength Magnetic Resonance Imaging

## A Practical Guide to Accessible MRI

Hans-Martin Klein

Springer

# Clinical Low Field Strength Magnetic Resonance Imaging

hansmartin.klein@mz-siegerland.de

Hans-Martin Klein

# Clinical Low Field Strength Magnetic Resonance Imaging

## A Practical Guide to Accessible MRI

Springer

Hans-Martin Klein
Department of MRI
Medical Center at Siegerland Airport
Burbach
Germany

ISBN 978-3-319-16515-8 ISBN 978-3-319-16516-5 (eBook)
DOI 10.1007/978-3-319-16516-5

Library of Congress Control Number: 2015949266

Springer Cham Heidelberg New York Dordrecht London


Printed on acid-free paper

Springer International Publishing AG Switzerland is part of Springer Science+Business Media (www.springer.com)

*To Lisa, Annika, Jonas, and Lars*

hansmartin.klein@mz-siegerland.de

# Foreword

## The Great Wave at Low Field Strength

“The great wave at Kanagawa” is a famous color woodcut by the Japanese artist Katsushika Hokusai which has inspired music and poetry, but also my personal view on medical imaging.

During the 25 years that I gave lectures to students at Aachen University, Germany, I often started by showing this wonderful picture in order to illustrate that in essence, radiology is based on diagnostics using waves of different qualities and energy such as electromagnetic waves, a physical principle MRI is also based on.

I also used to tell this to my former residents, one of whom was Hans-Martin Klein, the author of this book. The wave of enthusiasm for diagnostic imaging has evidently spilled over leading to – among others – an intensive engagement particularly in low-field-strength MRI and ultimately to this book. An attractive field, a true clinical demand, as well as great personal expertise and a lot of enthusiasm are indispensable ingredients for the success of such an undertaking – qualities which can be taken for granted in this project.

The topic is particularly appealing since low-field-strength MRI has tangible advantages, but it is undervalued and underestimated in a world dominated by high-field-strength MRI. For this reason it is important to write a book like this in order to demonstrate the feasibilities of this technique and to let this tidal wave gently roll ashore the radiological readership.

Aachen/Berlin, Germany
2015

Rolf W. Günther

# Preface

MR imaging is a little bit like playing electric guitar. The higher the string tension (field strength), the higher the frequency and the stronger the signal induced in the pickup (coil). On the other hand, low frequency has a better potential for (tissue) penetration, as everybody who tried to shield a sound studio knows: only solid substances can attenuate the volume of bass drum or bass guitar. No musician would dare to say that low frequency is less valuable than high frequency (particularly on a dance floor). But, however, radiologists do: since the early 1980s, technical development of MR systems has been focused on systems with high field strength.

High magnetic field strength provides additional signal and therefore enables to reduce imaging time and/or increase spatial resolution. However, lower-field-strength MR imaging provides some important advantages: smaller siting, no need for helium, better access to the patient, low power consumption, improved T1 contrast, less missile effects, reduced susceptibility artifacts, and far lower RF exposure.

Therefore, it seems to be justified to take a look at the low end of the field strength scale: Low- and mid-field-strength MR systems have taken profit from the technical progress in signal and image processing as well. Gradient performance has been improved. Multichannel systems and parallel imaging are available.

The question is: How much field strength do we really need for clinical imaging?

And to make this perfectly clear: I play bass guitar.

Burbach, Germany Hans-Martin Klein



hansmartin.klein@mz-siegerland.de

# Contents

# List of Contributors

At this point, I'd like to express my gratitude to those who helped in preparing this book.

Prof. Dr. Christiane Kuhl, director of the Clinic of Diagnostic and Interventional Radiology, RWTH Aachen, Germany, who allowed me to use some of her very instructive graphic material.

Dr. med. Willy Loretan and his colleague Dr. med. Michael Kolbe from "Medizinische Radiologie/Radiodiagnostik" in Brig, Switzerland. They impressed me 14 years ago with their imaging on a 0.2 T GE Signa Profile.

Dr. med. Brigitte Redeker-Standke from "Jade-Weser Imaging," Varel, Germany, sent me excellent imaging examples of her 0.4 T Hitachi Aperto.

Dr. Frieder Mauch, Sportklinik Stuttgart, forwarded some very illustrative musculoskeletal low-field-strength MR images.

Esaote Biomedica Deutschland GmbH; Fonar, Melville, USA; Hitachi Medical Systems, Germany; and Siemens Medical Solutions, Erlangen, Germany, provided additional image material.

My son Lars, who was the most important reviewer of the manuscript.

Rolf W. Günther for so much help and advice, not only for this book.

# 1 Introduction

Magnetic resonance imaging is one of the most fascinating methods of medicine. It has become a symbol of medical progress, as well as the efficiency and potential of modern diagnosis and therapy.

Basically, commercially available MR systems can be divided in two groups: systems with high- and low-field magnetic field strength (Tavernier and Cotten 2005). What is this parameter field strength? What is addressed usually as "field strength" is more precisely, but a little academically, the magnetic flux density. For reason of simplicity, we stick to the expression field strength. It is measured in Tesla (T). The old unit Gauß (G) is still used occasionally. The rate of conversion is 1 T equals 10,000 G.

One G is earth magnetic field strength at equator level.

High-field systems represent the standard – at least in Europe and the USA. They usually possess a closed-bore, superconducting magnet with a magnetic field strength (flux density) of 1.5 or 3 T. There are some stronger magnets (7 T, 9.3 T), but the music plays up to 3 T.

Low-field MRI systems have become rare in German radiological institutes. They are more frequent in countries with government-controlled medical systems (Parizel et al. 1995). These machines usually have an open-designed, permanent magnet with less than 0.5 T field strength.

Leon Kaufman, as an early developer of open MRI, advocated low-field imaging (Kaufman et al. 1989):

> Freed from the physical constraints imposed by high field superconducting magnets, opportunities other than lowered cost present themselves. (…), we achieve a considerable reduction in siting needs, services, and increased patient comfort, safety, and access.

Reading this article of Dr. Kaufman, after years of working with high-field MR systems, I wondered whether magnetic field strength is really as decisive for image quality as traditionally assumed. So I asked a good friend, Uwe Thomas, who was working with GE Medical Systems at that time, about their best clinical low-field



H.-M. Klein, *Clinical Low Field Strength Magnetic Resonance Imaging: A Practical Guide to Accessible MRI*, DOI 10.1007/978-3-319-16516-5_1

MRI site in Europe. He told me to see the practice of Drs. Kolbe and Loretan in Brig/Switzerland. On my way to Montreux Jazz Festival, I visited this small, beautiful institute and was deeply impressed by the image quality of the 0.2 T MR system with permanent magnet. While scanning was not as fast as with a high-field system, the device operated very silently and created a pleasant atmosphere. The open design and low noise level predestinated it for patients with claustrophobia or for children. The colleagues told their patients that they used low field strength and were very careful with RF exposure to their body. They took their time, and if the doctor takes time, the patient can take time too. For an abdominal MRI, the patients had to visit twice – and appreciated it – a totally alternative approach in our time, characterized by stress and hecticness.

And image quality was surprisingly good.

As a consequence, I convinced my hospital CEOs to invest in a 0.35 T system, and a few years later in an additional 3 T MRI. This was a dream come true. Every system had its own strengths and weaknesses, and the two machines complemented each other beautifully, working perfectly in combination – clinically, ecologically, and economically. This does not mean that every hospital would be wise to buy three MRI machines, but modern healthcare tends to create networks of larger structures that can easily accommodate a variety of systems – not only to play the high keys, but to play the whole piano.

MR imaging is also a symbol of expensive medicine and for the restriction of medical resources. Despite it may be wishful, not everyone who needs MR imaging has immediate access to it.

The most important cost-driving factor of MRI is field strength (Kaufman et al. 1989). On the other hand, if you ask a manufacturer how to improve MRI quality, the answer in (almost) every aisle of every congress is the same: “increase field strength.”

Public health science demands that, for allocation of medical resources, the rules of cost-effectiveness have to be considered (Töpfer 2007). This is expressed in the so-called economic principle.

There is a tendency to change from “procedure-based” (pay per MRI examination) to “value-based” (high-quality diagnosis and treatment of an appendicitis) payment in medicine. Now, what is value in medicine? The answer to this question could fill another book. To make it short, each medical procedure is subject to cost-effectiveness evaluations. These studies reduce medicine to the essential question: at which price can an additional “quality-adjusted” life year (QALY) be bought? A QALY is a life year with full quality, without disease-related “value reduction.” So one year in intensive care is expensive but no full-value (quality adjusted) life year. A devoted physician knows that medicine doesn’t work this way. But in a time of vanishing resources and a growing number of patients, there has to be some kind of resource distribution control.

This concept can be applied to each medical procedure. For example, MRI is a well-established diagnostic step before knee surgery. But is it cost-effective and is it economical? Mather and coworkers found that alternative strategies without MRI may provide equivalent service at lower costs (Mather et al. 2015). MRI may be an adjunctive, but its cost-effectiveness was found to be suboptimal.

There are two main causes for economic disapproval of a medical method: the method is insufficient (definitely not true for knee MRI) and too expensive. In both cases, the price of an additional QALY is too high. The authors of the abovementioned study work at Duke University. So, if MRI is too expensive for North Carolina, how much true is this for Myanmar or the Ivory coast?

In the USA, the affordable care act (ACA) is changing the role of diagnostic imaging. Radiology becomes more a “cost center” than a revenue generator (Barnes 2013). Radiology, like laboratory medicine, is sometimes considered a “commodity,” a standard good, not appreciated for quality but just by the price (Borgstede 2008).

This will provoke a number of new questions. Are the medical procedures and the way in which they are performed still optimal, or do we need a change?

Of course, an expensive high-field MRI offers considerable marketing potential: The bigger the machine, the better the diagnosis. But is this really true? The patient expects the best possible diagnostic safety, particularly with an expensive method like MRI, but does this really depend on field strength? Don’t we, by emphasizing the importance of large high-field systems, support those who say, “It’s the machine that makes the diagnosis, not the doctor.” Is Radiology a commodity, simply judged by the price? Is it the field strength or the doctors’ skills that make the difference?

In roentgenology, we try to minimize patient exposure to radiation. The “ALARA” principle demands that radiation has to be “as low as reasonably achievable.” We optimize tube voltage and reduce tube current by every means. Of course, more tube current means less noise, but no one would dare to say that increasing tube current is a really good idea for improving image quality in CT. And increasing tube current leads to linear increase of radiation exposure; increasing field strength leads to an increase in RF exposure by a power of 2 (Litmanovich et al. 2014). 3 T MRI means 100 times higher RF exposure than 0.3 T.

How much field strength does an experienced well-trained radiologist really need for high-quality MR imaging? Are the low-field MRI systems as good as possible, or has their development been neglected a little bit, in favor of the high end of the field strength scale?

## 1.1 History

The first MR imaging systems, built by Bruker, in Karlsruhe/Germany, used huge circular permanent magnets made from iron and weighing up to 100 tons. These systems had a field strength of about 0.1 T.

Alternatively, resistive electromagnetic MR systems were developed enabling to achieve up to 0.35 T. The field strength was limited due to overheating of the magnet.

In 1980 the company EMI, who also built the first clinical CT scanner, invented the concept of a superconducting magnet, cooled by liquid helium and nitrogen. With this system, field strengths of more than 1.0 T could be easily achieved (Fig. 1.1). EMI went bankrupt at this time and was bought by General Electric, which demonstrates that there is a substantial economic component in the history of MRI.

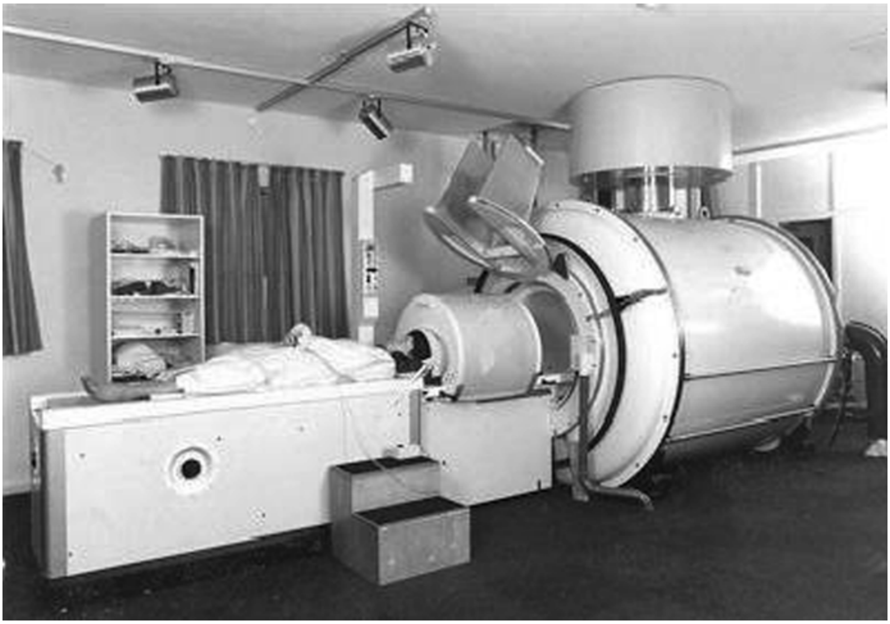

**Fig. 1.1** Cryogenic magnet in Hammersmith hospital

After introduction of superconducting magnets, the scale of MR imaging systems widened.

Per definition, ultralow-field MR systems work at a field strength of less than 0.1 T and low field use magnets with 0.1–0.5 T. In ultralow- and low-field systems, permanent magnets are dominant. In fact, it is possible to perform imaging even with the field strength of the earth magnetic field (about 1 G or 0.1 mT) or lower (Hilschenz et al. 2013). Mid-field systems use 0.5–1 T, high-field systems use 1–2 T, and ultrahigh-field systems work at more than 2 T field strength (up to 9.3 T).

These values may be better appreciated if we consider that at 14 T the magnetic field can hold a frog in water in the center of the magnet and at about 35 T a patient would fly in the center of the magnet bore. So with ultrahigh-field imaging systems, we are not far away from considerably coarse physical effects to the patient.

During the early 1980s, a controversy took place concerning the optimal field strength for imaging systems. In 1996, Derek Shaw, a General Electric employee and one of the leading MR experts in Europe called this controversy the "field strength war" (Shaw 1996).

Two arguments were in favor of higher field strength.

The signal–noise ratio was improved with increasing field strength. The better the SNR, the better the image quality. Additionally, stronger gradients are needed, which enhances spatial resolution. Scan time is regularly shorter on high-field machines and they facilitate functional MRI (blood oxygen level dependent, BOLD). Furthermore, MR spectroscopy (MRS) takes profit from higher field strength. The spectral difference between tissue substances is proportional to the resonance frequency, which is proportional to field strength. However, MR spectroscopy did not manage to establish an important role in clinical routine imaging.

All other arguments were in favor of lower field strength (Table 1.1).

Nevertheless, the "field strength war" was clearly won by the high-field fraction. All main manufacturers decided for the higher side of the street.

MR imaging in Europe and the USA became more and more dominated by high-field machines, which are large, complex, and expensive. The whole technical development, coil design, gradient performance, and sequence tailoring, was optimized for high-field systems.

In the 1990s, some companies changed their politics a little. They provided mid-field systems with 0.5–1 T field strength. It was realized (but not officially promoted) that the relation between magnetic field strength and SNR is not linear; it is overproportional. But RF energy deposition in the body increases, proportional to the square of field strength. Therefore, as said above, at 3 T the RF exposure is 100 times higher than at 0.3 T. In 2009 the European Commission published a guideline for RF protection of employees and patients in static MRI fields (http://ec.europa.eu). If this guideline had not been retracted, low-field systems would have experienced a renaissance.

The top of the scale is represented by 7 T or even 9.3 T systems (KFA Jülich/Germany). At this extremely high magnetic field strength, side effects become an issue. However, only few studies report on patient acceptance (Theysohn et al. 2008). Since the market is small and the applications restricted, it is difficult to find a manufacturer for magnets > 3 T.

There is a multitude of further advantages for smaller systems: reduced costs and space requirements, open design for better patient comfort, less or no helium consumption, less missile effects, susceptibility, and motion artifacts.

**Table 1.1** Advantages and disadvantages of low-field MRI systems

| Advantages | Disadvantages |
|---|---|
| Lower RF energy deposition | Lower signal/noise ratio |
| Lower energy consumption | No spectroscopy |
| No helium | Inferior spectral fat saturation |
| Smaller siting | |
| Better T1 contrast | |
| Shorter T1 times | |
| Independent from high power supply | |
| Less missile effects | |
| Less dielectric effects | |
| Less susceptibility/metal artifacts | |
| Low maintenance | |
| Better patient access/open design | |
| Less motion artifacts (more convenience) | |

If these specific advantages of lower field strength had been appreciated 20 years earlier, MR systems could look significantly different, both smaller and cheaper.

In the evaluation of low-field MRI, there were of course studies showing the weaknesses of this technique (Friedman et al. 1995; Woertler et al. 2000), but newer systems with improved performance renewed the interest in low-field systems (Cotten et al. 2000; Tavernier and Cotten 2005). Sometimes it is necessary to rethink what has been established as standard. After 25 years of high-field supremacy, a new look at the lower side of the field strength scale is justified.

It was one of Aachen's most famous sons, Mies van der Rohe, who said "Less is more!" and based his fascinating architectural style on this concept. Can this be true for MRI?

- There was an intense controversy on the best field strength in the 1980s and 1990s: the field strength war. The standard is now 1.5 T
- RF exposure grows with the square of field strength. 3 T has 100 times higher RF power than 0.3 T
- Field strength is the most important cost-driving factor in MRI
- High-field MRIs require infrastructure, reliable electricity, and helium, which is not available in all parts of the world
- If all other parameters are equal (gradients, coils, sequences, matrix, etc.), is there a considerable difference in diagnostic safety?
- Is a system with lower field strength sometimes the better choice?

## References


Barnes E (2013) Obamacare's effect on radiology: big, but gradual. AuntMinnie.com

Borgstede JP (2008) Radiology: commodity or specialty. Radiology 247:613–616

Cotten A, Delfaut E, Demondion X et al (2000) MR imaging of the knee at 0.2 and 1.5T: correlation with surgery. AJR Am J Roentgenol 174:1093–1097

Friedman DP, Rosetti GF, Flanders AE et al (1995) MR imaging: quality assessment method and ratings at 33 centers. Radiology 196:219–226

Hilschenz I, Koerber R, Scheer HJ, Fedele T, Albrecht HH, Mario Cassará A, Hartwig S, Trahms L, Haase J, Burghoff M (2013) Magnetic resonance imaging at frequencies below 1 kHz. Magn Reson Imaging 31(2):171–177

European commission (2009). http://ec.europa.eu/health/scientific_committees/opinions_layman/en/electromagnetic-fields/

Kaufman L, Arakawa M, Hale J, Rothschild P, Carlson J, Hake K, Kramer D, Lu W, Van Heteren J (1989) Accessible magnetic resonance imaging. Magn Reson Q 5(4):283–297

Litmanovich DE, Tack DM, Shahrzad M, Bankier AA (2014) Dose reduction in cardiothoracic CT: review of currently available methods. Radiographics 34(6):1469–1489

Mather RC 3rd, Garrett WE, Cole BJ et al (2015) Cost-effectiveness analysis of the diagnosis of meniscus tears. Am J Sports Med 43(1):128–137

Parizel PM, Dijkstra HA, Geenen GP et al (1995) Low field vs. high field MR imaging of the knee: a comparison of signal behavior and diagnostic performance. Eur J Radiol 19:132–138

Shaw D (1996) From 5-mm tubes to man. The objects studied by NMR continue to grow. In: Gran DN, Harris RK (eds) Encyclopedia of nuclear magnetic resonance, vol 1. John Wiley and Sons, Chichester, pp 623–624

Tavernier T, Cotten A (2005) High- versus low field MR imaging. Radiol Clin North Am 43:673–681

Theysohn JM, Maderwald S, Kraff O et al (2008) Subjective acceptance of 7 Tesla MRI for human imaging. MAGMA 21:63–72

Töpfer A (2007) Betriebswirtschaftslehre: Anwendungs- und prozessorientierte Grundlagen. Springer, Berlin, p 64. ISBN 3540493948

Woertler K, Strothmann M, Tombach B, Reimer P (2000) Detection of articular cartilage lesions: experimental evaluation of low- and high field strength MR imaging at 0.18 and 1.0 T. J Magn Reson Imaging 11:678–685

# MRI System

# 2

Since introduction in the early 1970s by Lauterbur, Damadian, and Mansfield, MRI has experienced a tremendous progress. A lot of "brainpower" was invested to optimize this fascinating and important imaging technique.

To understand the differences in the variety of available (Rinck 2009) systems and their effect on imaging, let us at first have a look at the functional principle of MR imaging.

The basic system architecture of a magnetic resonance imaging system is given in Fig. 2.1.

The MRI magnet is positioned in a faraday cabin, shielding it from external influences as well as exterior areas from RF radiation.

MR imaging is a complex procedure. In the following lines, the process steps are described (Vlaardingerbroek and den Boer 2002, Stark and Bradley 1992).

1. The user (radiologist) selects the scan sequences and defines the scan geometry data.
2. The gradient power, as a function of time and direction, is computed by the host computer, stored, and transferred to the so-called spectrometer.
3. The "spectrometer" comprises the control computer (controlling the magnet, the gradients, RF transmitting and receiving, RF coils, and AD converter) and is responsible for data acquisition by the receiver.
4. Before the scan process can start, some further steps have to be performed: shimming the frequency generator on the resonance frequency (Larmor frequency), shimming the RF coils, and adjusting receiver and transmitter sensitivity.
5. After the initialization process, the slice selection gradient is switched (usually concerning the $z$-axis) and the scan sequence is started. All other components of the system are deactivated at this time.
6. After the slice selection gradient reaches its final value, the RF (radiofrequency) amplifier is activated. The input signal is given by the frequency generator, producing a harmonic signal of the frequency $\omega_o$. This signal is modulated in the function generator (amplitude modulation). The amplitude-modulated RF



H.-M. Klein, *Clinical Low Field Strength Magnetic Resonance Imaging: A Practical Guide to Accessible MRI*, DOI 10.1007/978-3-319-16516-5_2

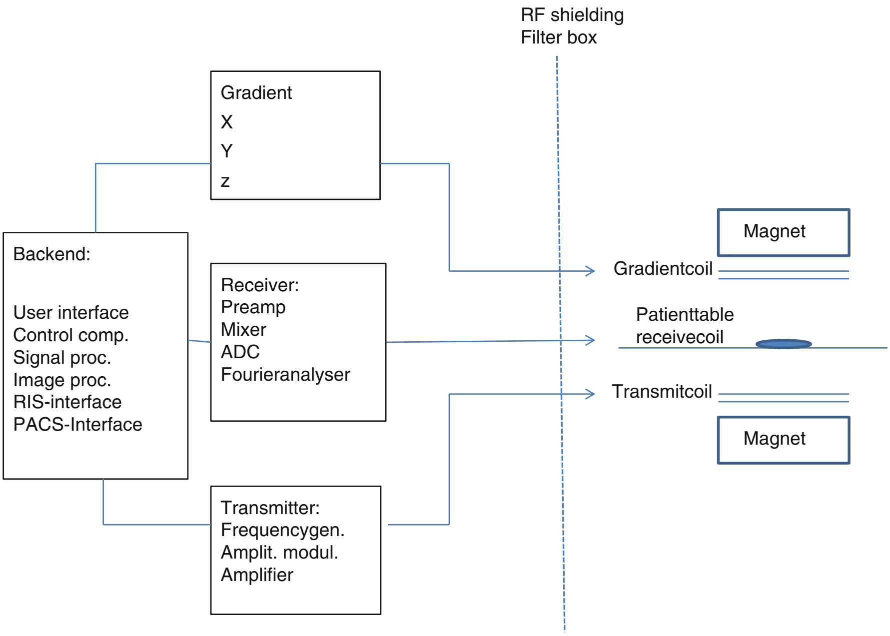


**Fig. 2.1** MRI system architecture

signal is transferred to the RF coil and the excitation pulse is emitted to the patient, producing the RF magnetic field $B_{RF}$. During this time, receiver coils in the preamplifier are detuned and blocked, to provide destruction of the receiver circuits by the large RF signal.

7. The phase-encoding gradient is switched on, until the required gradient strength is reached. Then, the 180° refocusing pulse is started. It is usually slice selective and has two times the strength of the 90° excitation pulse.
8. Next, the readout gradient is applied. During the readout gradient time, the receiver circuit is active. The magnetization is measured, and the A/D converter is scanning the receiver signal. Following a short delay, the next element of the scan sequence is started.
9. After completion of the scan procedure, the signal data are submitted to a Fourier transformation, and the computer image is displayed on the monitor. The user can adjust the image concerning window and level.
10. Further image processing like 3D reconstruction, filtering, and signal intensity measurements is possible.

Besides magnetic field strength, the quality of MRI depends on several other technical features of the system: homogeneity, gradient power, send and receive coils, speed, and noise level of transmitter and receiver electronics (Rinck 2009).

In the following, the major technical components of the system are addressed.

## 2.1 Magnet

A constant magnetic field can be achieved by continuous electric current (electromagnets) or a permanent ferromagnetic material.

Usually, up to 0.4 T permanent magnets are used.

Resistive electromagnetic scanners have become very rare and are used in specially dedicated systems like the FONAR upright MRI or the PARAMED MR open.

Superconducting electromagnets are the current standard, mostly with a closed-bore geometry and an opening of 60 cm. Early cardiac MRI systems had smaller bores, since smaller openings lead to a considerable increase in signal.

In recent years, so-called wide-bore magnets with an opening of 70 cm have been introduced and are now widely accepted for high-field MRI scanners.

### 2.1.1 Permanent Magnets

Permanent magnets are produced from permanently ferromagnetic materials. The magnetic material is mounted on a C- or H-shaped carrier, made from conventional steel (Fig. 2.2). The C form gives excellent access to the patient.

They are characterized by the relation between magnetic flux and magnetic field strength. The total magnetic energy per volume unit is defined by the material.

To increase the magnetic field strength in the room between the magnetic poles by a factor of 2, the amount of magnetic material has to be increased by a factor of 4.

Increasing the linear extension of the homogeneous magnetic field (homogeneous sphere) by 1.2 requires 1.7 times more magnetic material.

The magnetic material regularly consists of a neodyne–bor–iron alloy (NdBFe) and is very expensive. Magnets produced from this material are limited to a maximum strength of 0.35 T, due to high costs and weight of the magnet.

A further requirement is to keep the magnet temperature very constant, since magnetic field strength changes occur at about 1000 ppm/K.

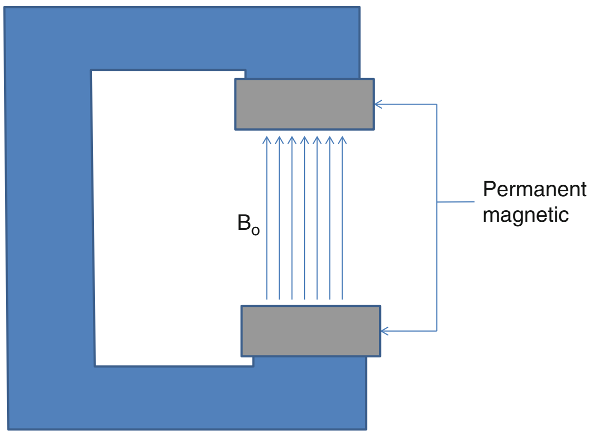


**Fig. 2.2** Permanent magnet with C-shaped iron ridge

Permanent magnets can also be produced in a cylindrical form. This magnet type is called “prisma” magnet (Zijlstra 1985). It produces a transversal magnetic field, requiring a special RF coil design.

A major advantage of the C-shaped open permanent magnets is good accessibility to the patient during the MR procedure (Fig. 2.3).

### 2.1.2 Electromagnets

Electromagnets consist of an arrangement of coils. Electric current in the magnetic core induces a magnetic field.

The magnetic flux ($B_o$) in the coil is proportional to the number of coil windings per meter ($N_m$) and the intensity of the electric current I (Vlaardingerbroek and den Boer 2002).

$$B_o = \mu_o I N_m$$

If a magnetic coil had infinite length, the magnetic field would be perfectly homogeneous. Real coils have limited length; therefore the homogeneity is imperfect. The magnetic field of a single coil magnet is quite in homogeneous. For practical purposes, a typical example would be a four-coil magnet design, where the coil arrangement creates a field with maximal homogeneity (Vlaardingerbroek and den Boer 2002). A disadvantage of this geometry is that an exterior fringe field exists, which can interact with other measurement systems, magnetic material, data storage media, or pacemakers.

**Fig. 2.3** Open low-field MRI with a permanent magnet (Hitach Aperto 0.4 T)

To compensate for this fringe field distortion, the magnet has to be shielded using either large amounts of iron around the coil (passive shielding) or external additional coils with electric current in the opposite direction for compensation (active shielding).

Both methods of shielding reduce the primary magnetic field strength so that a shielded magnet has to use a little more electric current than an unshielded magnet of the same magnetic strength.

So-called resistive magnets consist of two coil sets. These coils are connected with an iron ridge, increasing the efficiency (Tesla/A) by a factor of 4, compared with a system without such an iron ridge (Fig. 2.4).

A magnet with only one ridge bow is called C-arm magnet; a magnet with two bows is called H magnet.

### 2.1.3 Superconducting Magnets

Conventional electromagnets, using copper wire, with a field strength of more than 0.3 T, require tremendous amounts of electric power and a highly reliable electric power supply.

The solution to this problem was the development of superconducting magnets, which only need very few electricity to preserve the magnetic field.

The typical closed-bore MR magnet with horizontal field is a superconducting magnet (Fig. 2.5). It possesses six field excitation coils and two shielding coils with larger diameter to compensate for the fringe field.

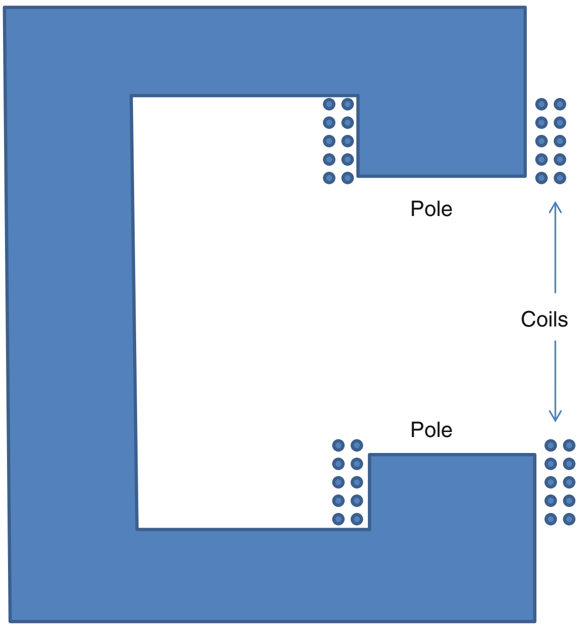


**Fig. 2.4** Electromagnet using an iron ridge. Instead of permanent magnets, the ridge carries two resistive magnets

**Fig. 2.5** 1.5 T wide-bore superconducting magnet (GE Optima 450 w. Courtesy GE Healthcare Inc.)

The coil wire usually consists of a niob–titanium alloy with a copper mantel. This material is superconducting below a certain maximum temperature (<12 K). The temperature always has to be lower than this maximum, even at the highest electric currents.

Additionally, electric flux density and field strength have to be limited.

Without these mandatory constructional criteria, the superconductivity is lost and a critical process of heat production takes place, leading to a complete boil-off of the cooling agent (helium). This process is called "quench." A quench process is dramatic but fortunately very rare in clinical practice.

With correct construction of the magnet system, the boil-off rate is well controlled.

To reduce heat conduction between the helium can and the surrounding air, there are two cooling shields (or vessels) for the helium compartment, in which temperature is kept at 15 or 60 K rsp, using a cryocooler.

Those three vessels are positioned in an outer vacuum container, fixed with thin wires to reduce heat conduction. Due to these thin and sensitive wires, transport of MR magnets is only possible with careful use of special transporting mobiles.

Every magnet has a specific boil-off rate, leading also to a slow reduction of the electric energy by non-Ohm effects. This means, that the resonance frequency is also reduced and the frequency generator has to be re-tuned. From time to time, the coil current has to be corrected. This is mostly combined with the helium refilling and system maintenance.

Only during the helium reloading process the magnet is connected to external energy supply.

The same type of superconducting magnets can be built with a niob–zinn conductor with a copper coverage. This material is much more expensive, but it has the advantage that the critical temperature is about 18 K. These superconducting systems do not need helium and can be run simply with a cryocooler.

There are very few superconducting MR systems with an open architecture and vertical magnetic field.

Toshiba used magnet coils consisting of erbium–3Ni in the 0.35 T open MRI OPART. The system is no longer available.

GE and Philips built open superconducting MRI system with vertical field orientation, the GE Signa 0.7, the Philips Panorama 0.6, and the Panorama HFO (high field open).

These systems had two superconducting magnets above and below the scan plane. The 0.6 T system used a C-shaped steel carrier.

At 0.6 T, the magnetic attraction causes a force of about 100 tons between the magnetic poles.

Therefore, the Panorama HFO with 1.0 T magnets is mounted on two columns to improve weight distribution at the cost of reduced accessibility.

Production of these systems is presently ceased, since the achievable market prices do not cover the production costs.

### 2.1.4 Dedicated Systems

For special purposes, so-called dedicated MR scanners with custom magnet designs have been developed.

Extremity scanners, mainly for musculoskeletal imaging, are much smaller and less expensive (Fig. 2.6).

For functional diagnosis of joint and spine disorders, considering the weight and position of the patient, an upright MR scanner was presented in 1996 by FONAR

**Fig. 2.6** Dedicated extremity scanner. *Left* O-scan, *right* G-scan with moveable patient table to enable upright scanning (Courtesy: Esaote Biomedical Imaging Inc.)

Inc., a company founded in 1978 by Dr. Raymond Damadian, M.D., one of the discoverers and pioneers of MR imaging (Fig. 2.7). For a standing or sitting patient, the alignment of the field axis is similar to a vertical magnet system.

This scanner uses an iron frame electromagnet and is open on top and at the front. The patient can sit or stand in the magnet and weight-bearing or functional studies can be performed.

Another innovative FONAR design is the so-called "open sky" MRI, with one magnetic pole hanging from the room ceiling (Fig. 2.8). Dedicated systems can improve convenience and safety for the patient during MRI procedures (Shellock 1999, 2000).

### 2.1.5 Homogeneity

Since magnetic resonance imaging depends highly on exact resonance frequency, and since frequency depends on field strength, a homogeneous magnetic field is of crucial importance for image quality.

In Germany, regulatory guidelines demand a field homogeneity of less than 5 ppm in a sphere of 40 cm diameter.

**Fig. 2.7** FONAR upright MRI, built for weight-bearing and functional MR imaging (Courtesy FONAR Inc., Melville, USA)

**Fig. 2.8** Fonar "open sky" (Courtesy FONAR Inc., Melville, USA)

This parameter is critical for low-field systems with vertical field orientation: as described above, the pole distance is smaller than 40 cm, to improve field strength (e.g., Siemens Magnetom C!, 36 cm; Hitachi Aperto, 38 cm).

Correction of field inhomogeneity is called shimming and can be achieved in permanent magnets by mounting small iron magnets on the magnetic poles.

Outside this homogeneity plane, magnetic field inhomogeneity increases rapidly to unacceptable values.

External influences on the magnetic field play an important role, particularly in low-field imagers. Moving ferromagnetic objects like cars or elevators close to the magnets can cause severe image deterioration. An EFI device (electric field intensity) can help to measure and partially compensate some of the field irregularities.

### 2.1.6 Vertical or Horizontal Magnetic Field?

Basically, we have two main concepts for MR magnets: Closed bore superconducting systems with horizontal field, helium consumption and high field strength option. Open permanent magnets with vertical field and limited field strength.

Besides all other arguments for permanent magent low field MRI, are there advantages of the vertical field orientation?

Vertical fields allow to use solenoid coils instead of saddle coils, which have a higher inherent SNR. This comparison was particularly true for the classic linear polarized 1-channel coil. The use of multichannel-array coils has changed the situation, since these coils have better SNR than a single solenoid coil. However, if solenoid coils are combined to multichannel arrays, as in the four-channel Magnetom C!, the game is open again (Blasche and Dale 2005).

The main advantage of these magnets is the fact, that the coil is not wrapped around the patient, enabling open design with more patient convenience, safety and better access for interventional procedures (Kaufman et al. 1989).

## 2.2 Gradients

The gradient field, which adds to the main magnetic fields, in order to encode the position of the emitting proton spins, is produced by resistive gradient coils.

Gradient field strength is usually measured in mT/m.

### 2.2.1 Gradient Chain

Along the *z*-gradient, the magnetic field should increase linearly with the distance from the isocenter and should be at least as large as the homogeneous area of the main magnetic field. X- and *y*-gradients are rotated around *z*-axis by 90°. They consist of two pairs of saddle coils. Open C- and H-arm magnets have gradient coils parallel to the magnetic pole shoes.

The voltage U in an ideal coil is proportional to the derivate of the current I with respect to time: dI/dT. In a real component, the coil resistance has to be taken into consideration as well.

At the required fast rise time, a rapid change of electric current results. Therefore, the inductivity of the coil has to be restricted. A compromise has to be found between inductivity and linearity of the gradient field.

A critical point is the free space inside the gradient coils. On one hand, narrow magnets cause claustrophobia. On the other hand, the necessary gradient power is increasing proportionally to the fifth power of the radius *r*. These facts explain some of the problems in manufacturing wide-bore closed-magnet systems.

In open MR systems, the gradient coils have a slightly different but related geometry.

### 2.2.2 Rise Time and Slew Rate

To achieve good gradient performance with a short rise time and high-gradient amplitude, strong-gradient amplifiers are necessary, which represent a large part of the power consumption of the MRI system (Mansfield and Morris 1982).

Using a gradient coil with an inductivity of L = 200 μH and a sensitivity $C^{-1}$ = 30 A (mT/m), the induction of a gradient field of 12 mT/m at a rise time of 600 ms requires a power of *43 kW*. This represents a slew rate of 20 mT/m/s (Vlaardingerbroek and den Boer 2002).

### 2.2.3 Eddy Currents

A change of the electric current in the gradient coils leads to a change in the gradient field and induces eddy currents in the surrounding conducting wires.

The magnetic fields, induced by these eddy currents, are oriented against the original gradient field and reduce the field rise time.

This can be partially compensated by well-controlled increase of the gradient power. Incorrect compensation of these eddy currents leads to severe image artifacts. Another option is shielded gradient coils, which are widely free of eddy current artifacts.

## 2.3 RF Chain

To produce, transmit, and receive a resonance signal of a body positioned in the magnet, we need an RF chain, consisting of transmitter, RF coils, and receiver.

### 2.3.1 Transmitter

The transmit circuit starts with a frequency generator. This generator produces a signal at the Larmor frequency of the magnet $\omega_o$, 21 MHz for 0.5 T or 128 MHz for 3 T. Frequency generation is followed by amplitude modulation of the signal and finally amplification at about 5–30 kW.

### 2.3.2 Coils

The signal is transferred to the emission coil, a large coil with homogeneous field. During emission of the signal, all pure receive coils are switched off to avoid damage of the sensitive receive electronics.

The receive coil is tuned to the resonance frequency of the magnet. If it's switched off, the coil is detuned. The coil contains a preamplifier, which increases signal intensity before transfer over a relatively long cable wire to the receiver electronics.

The design of RF coils is, despite all physical and technological skills, more of an art than a technique (Carlson et al. 1992, Edelstein et al. 1990).

Multiple causes of signal distortion are omnipresent, particularly in large coils.

#### 2.3.2.1 Solenoid Coils

The most simple coil is the so-called solenoid coil. It has a round or rectangular shape and is wrapped around or lying close on the relevant body part (Fig. 2.9).

It is a physical fact that electric coils produce the highest signal-to-noise ratio (SNR), when their axis is positioned perpendicular to the main magnetic field ($z$-axis). In a vertical field, for the head, extremities, and joints, the solenoid coil can be used in optimal orientation.


**Fig. 2.9** Different solenoid coils, using array coil design. Shoulder array, wrist, knee, birdcage head coil (Magnetom C!, Siemens Inc. Erlangen/Germany)

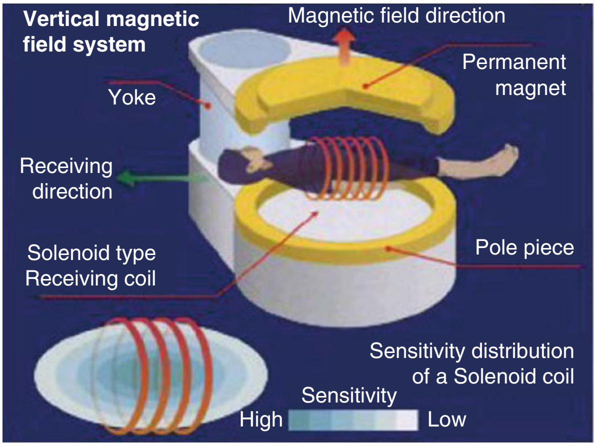


**Fig. 2.10** Sensitivity distribution in a solenoid coil

For the spine and abdomen, solenoid coils positioned cranially or caudally, left or right, are not optimal, since the coil axis is running parallel to the $z$-axis, and therefore the coil acquires no signal (Blasche and Dale 2005). Ventrally and dorsally positioned coils receive high signal amplitudes (Fig. 2.10).

#### 2.3.2.2 Helmholtz Coil

The Helmholtz coil is a special design of two solenoid coils lying parallel to each other. This increases signal and reduces coil inhomogeneities.

Saddle coils are a special version of the Helmholtz coil, one coil lying above and one below the patient, resulting in a transversal magnetic field (Fig. 2.11).

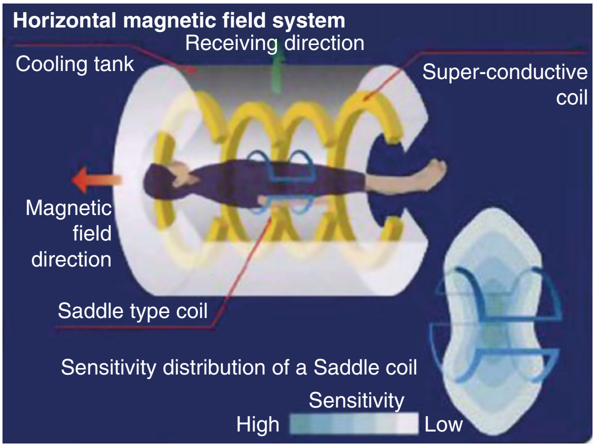


**Fig. 2.11** Sensitivity distribution in a saddle coil (Helmholtz coil)

A disadvantage of this concept is severe inhomogeneities in the marginal areas of coil coverage, causing aliasing effects due to acquisition of signal from structures outside the coil.

#### 2.3.2.3 Quadrature/Birdcage Coil

These artifacts can be reduced using a circular polarizing cage coil, which is currently one of the most frequent coil designs for the head, joints, and extremities. This coil contains metal bars running parallel to the $z$-axis, connected with two rings.

The metal bars represent an inductivity, which can rotate around the $z$-axis in the form of a slow wave front. The frequency of the wave front can be adjusted to the coil diameter and work as a low- or high-band noise filter.

The main transmit coil, integrated in the magnet bore, is designed this way.

This coil design is also well suited for transmit–receive coils, for the so-called birdcage coil (Fig. 2.12).

Planar or solenoid coils could also take profit from the quadrature principle, like in the spine or breast coil (“butterfly coil”).

#### 2.3.2.4 Array Coil

At the RSNA 2003, Siemens introduced the TIM (total imaging matrix) system, and GE followed with the GEM (geometry-embracing method) in 2011, both systems enabling true whole-body imaging. Such multiple-coil or “coil array” systems have shown to be advantageous in all imaging indications.

Attempts have been made to patent a “coil suit” with multiple solenoid coils in a flexible clothing tissue (Engelhardt and Kuth 2003; Klein 2008).

There is an ongoing controversy about advantages of solenoid coils, as they are used in systems with vertical magnetic field, over classical saddle coil design.

**Fig. 2.12** Birdcage coil

Given equal scan conditions, the signal sensitivity of a solenoid coil is principally higher than a conventional single-channel linear polarized saddle coil.

Modern array coil concepts using the quadrature principle have made this controversy a little obsolete (see Fig. 2.9).

For the head, neck, extremities, and joints, solenoid coils (with > 1 channel) are well suited. For body imaging, solenoid coils are mostly wrapped around the body or positioned laterally. However, (array) coil design for low-field systems has been neglected up to date. This could definitely be a field of prosperous scientific and technological endeavor.

#### 2.3.2.5 A/D Converter

In the receiver, the scan signal is amplified further and then converted to a digital signal. Modern MRI scanners integrate the A/D converter in the magnet cabinet (GE Optrix) or even in the receive coil (Philips). This can further increase the SNR: GE claims an SNR increase by about 27 % for its OPTRIX concept. Until now these techniques have not been applied to open permanent systems.

An important feature is the number of receiver channels. The more channels, the more coil elements can receive signal at the same time. This is a major parameter for multichannel systems like TIM (Siemens Healthcare) or GEM (GE Healthcare).

## 2.4 Back End

Signal and image processing and the user interface are components of the MRI back-end system.

The user interface is usually a control program, implemented on a personal computer. It transforms user commands in control data for the front-end controller.

And it transfers system and image information to the user and the picture archiving and communication system (PACS) as well as the radiology information system (RIS, worklist management, scan data) (Bigwood et al. 1997).

The control computer handles and transfers the user input data to the front end of the MRI system.

Signal processing is basically a harmonic analysis (Fourier transformation) of the MR signal. This is done mostly, due to economical reasons, on a separate computer using an invariate fast Fourier transform (FFT) algorithm (Bracewell 1965).

Image computation includes a variety of data processing like windowing and filter functions or 3D reconstruction. This can be performed by the host computer or, for reason of speed, by a separate numeric processor.

## 2.5 Quality

In Germany, the MRI commission has formulated a couple of parameters, to be fulfilled by an MRI, for permission of service for social-insured patients.

In 2008, after 4 years of intensive work with a 0.35 T MRI, I applied for a certification of this system by the MRI commission. The initiative was supported by Walter Märzendorfer, the CEO for magnetic resonance systems of Siemens Healthcare at that time.

All conditions were fulfilled, except the homogeneity over a 40 cm sphere, which was impossible due to a limited opening of the magnet in vertical axis. The 40 cm phantom didn’t fit in the magnet. Permission was denied (Table 2.1).

There are a lot of obese patients, patients with examinations under anesthesia (children, claustrophobia), patients with RF-sensitive devices (pacemaker, hearing devices, etc.), or remote areas, in countries with less developed infrastructure or low medical care budget. They all would be happy with low-field systems – but they also need the best possible image quality.

- MRI magnets can be permanent or electromagnets
- Permanent magnets need only very few energy for temperature equalization
- Electromagnets are mostly superconducting magnets. They need energy for cooling the liquid helium gas
- The gradient system is of high importance for image quality
- Gradient amplifiers are the most power-consuming elements of MRI
- RF transmission can use the system body coil or dedicated transmit/receive coils
- RF coils can have different designs: solenoid coil, saddle and Helmholtz coils, and multi-coil arrays. Optimal coil design is crucial for image quality
- New concepts for image improvement are digital signal transfer, array coil design, strong gradients, and new sequence techniques. These concepts are only partially adapted for low-field MRI systems until now

**Table 2.1** MR imaging criteria for social-insured patients in Germany. The Siemens Magnetom C! fulfills all conditions, except the homogeneity measurement: the 40 cm phantom does not fit in the magnet opening of 36 cm

| No. | Requirement | Magnetom C! .35 T |
|---|---|---|
| 1 | Special RF coils | Yes |
| 2 | Minimal slice thickness < 1 mm 3D Spinecho<br><3 mm 2D Spinecho | Yes |
| 3 | Cardiac triggering | Yes |
| 4 | Presaturation, fat saturation, motion compensation, flow rephasing | Yes |
| 5 | No 2–4 in 1 acquisition | Yes |
| 6 | Gradient echo with variable flip angles<br>or | Yes |
| | Single slice with < 10 s acq. Time | Yes |
| 7 | Inhomogeneity < 5 ppm over 40 cm sphere phantom (impossible for low-field scanners) | No |
| 8 | For vascular or musculoskeletal imaging<br>3D acquisition with a matrix of 256 × 256 × 64<br>or | Yes |
| | Voxel volume < 1 $mm^3$, double-angulated scan | Yes |
| 9 | Cine gradient echo for cardiac exam | Yes |
| 10 | Double breast coil | Yes |
| 11 | TOF-, PC-, and CE MR Angio | Yes |
| 12 | Contrast injector triggering with bolus tracking or timing | Yes |

## References


Bigwood WD Jr, Horii SC, Pior WL (1997) Understanding and using DICOM, the data interchange standard for biomedical imaging. J Am Med Inform Assoc 4:199–212

Blasche M, Dale BM (2005) MRI hot topics. Vertical and horizontal fields for MRI. Siemens medical solutions USA, Inc. www.usa.siemens.com/medical

Bracewell R (1965) The Fourier transform and its applications. McGraw-Hill, New York

Carlson JW, Deby KA, Hawryszko KC et al (1992) Design and evaluation of shielded gradient coils. Magn Reson Med 26:191–206

Edelstein WA, Hayes CE, Souza SP, Müller O (1990) The NMR phased array. Magn Reson Med 16:192–225

Engelhardt K, Kuth R. Lokalspulenanordnung für eine Magnetresonanzanlage. Offenlegungsschrift DE 102 21 644 A1 11.12.2003

Kaufman L, Arakawa M, Hale J et al (1989) Accessible MR imaging. Magn Reson Q 5:283–297

Klein HM (2008) Whole body RF coil for MRI. German patent application DE 10 2008 061 938 A1

Mansfield P, Morris PG (1982) NMR in biomedicine. Academic, New York. ISBN 012-025562-6

Rinck P (2009) Magnetic resonance in medicine. Blackwell scientific publications, Oxford. ISBN 0-632-03789-4

Shellock FG, O'Neil M, Ivans V et al (1999) Cardiac pacemakers and implantable cardiac defibrillators are unaffected by operation of an extremity MR system. AJR Am J Roentgenol 72:165–170

Shellock FG, Stone KR, Resnik D et al (2000) Subjective perceptions of MRI examinations performed using an extremity MR system. Signals 32:16

Stark D, Bradley WG (1992) Magnetic resonance imaging. Mosby Year Book, St. Louis. ISBN 0-8016-4930-7

Vlaardingerbroek MT, den Boer JA (2002) Magnetresonanzbildgebung. Klinik und Praxis. Springer, Berlin, pp 22–25

Zijlstra H (1985) Permanent magnetic systems for MR tomography. Philips J Res 40:259–288

# 3 Site Planning

For the installation of low-field MR systems, particularly with permanent magnets, certain special requirements have to be considered. The specific advantages of these systems influence the concept of the scan site and enable to realize MR imaging units in locations that are impossible to service with high-field systems. However, there are certain prerequisites that must be taken into account.

## 3.1 MRI System Components

A typical magnetic resonance system consists of a number of components. The components, their weight, and power consumption values for a Siemens Magnetom C! with a field strength of 0.35 T are given in Table 3.1.

## 3.2 Room Size and Conditions

Spatial requirements for most low-field systems are limited. A minimum room size of 30 m$^2$ (325 sq. ft) would be sufficient (www.siemens.com/medical) (Fig. 3.1).

This enables installation in small buildings or, if a larger room is available, improves access to the patient, emphasizing the openness of the MR, which is important for claustrophobic or handicapped patients. The creation of an attractive and aesthetic design for the scan room (Fig. 3.2) is eased by permanent magnet systems.

Open design improves access to the patient for interventional or surgical MR-guided procedures (Petersilge et al. 1997; Yamada et al. 2015). Access to the patient is easier; positioning of instruments and medical equipment is facilitated. Additionally, anesthesiologists appreciate the reduced missile effects of ferromagnetic instruments (see below).



H.-M. Klein, *Clinical Low Field Strength Magnetic Resonance Imaging: A Practical Guide to Accessible MRI*, DOI 10.1007/978-3-319-16516-5_3

**Table 3.1** System dimensions Siemens Magnetom C!, 0.35 T. Source: Siemens Healthcare planning Dept., Erlangen/ Germany

| Component | Weight [kg] | Power consumption [W] |
|---|---|---|
| Magnet | 16,308 | 2000 |
| Patient table | 200 | |
| RF cabin | | |
| RF door | | |
| RF window | | |
| RF filter plate | 80 | 150 |
| EFI pickup coil | | |
| Electronics cabinet | 600 | 2000 |
| Heat exchanger (gradient) | 310 | 9400 |
| Power supply | 35 | |
| User console | 20 | 200 |
| Host PC | 22 | 700 |
| Intercom | | |
| Switch on box | 1 | |
| Air conditioned | | |

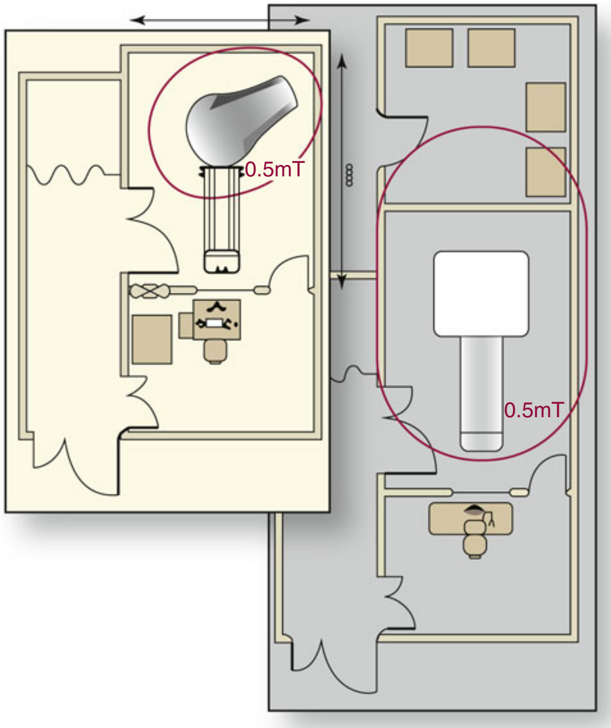


**Fig. 3.1** Space requirements of a typical low-field MR setting (20–30 m$^2$) compared to a high-field system (40–60 m$^2$) (Courtesy: Esaote Inc.)

**Fig. 3.2** Patient-oriented scan room design for open low-field MRI (Photography: Ulrich von Born)

Since the need for air ventilation and cooling is limited, the room height can be reduced. The size of gradient amplifiers is smaller, and there are no cryogenic components (Helium compressor). Therefore, the technical components can be installed in a smaller cabinet, giving additional flexibility. Minimum height is typically only > 225 cm.

The examination room temperature is required to be between 21 and 27 °C, at a humidity of 40–80 %.

The technical room temperature is required to be between 18 and 24 °C, at a relative humidity of 40–80 %.

The operator room temperature has to be between 15 and 30 °C at a relative humidity of 40–80 %.

Heat production of the MR components is about 2 KW in the examination room, about 2 KW in the operator area, and maximally 11.4 KW in the tech room.

The scan room needs an antistatic floor.

To enable remote control and maintenance, a high-speed connection has to be provided. Ideally, an Ethernet connection with a data transfer rate of more than 100 MBit/s should be available.

## 3.3 Transport and Installation

For unloading of the system, particularly the magnet, sufficient space for truck and cranes has to be provided. The door openings have to be of adequate size. The magnet weight of 16 tons requires strong and stable transport ways (Fig. 3.3).

**Fig. 3.3** Installation of a 0.35 T magnet (Siemens Magnetom C!, Siemens Healthcare, Germany). Important: protection of the floor by steel plates

## 3.4 Static Requirements

A drawback of low-field systems is the weight of the permanent magnet. This magnet consists of a solid iron block, in the form of a horseshoe, with a size of typically about 190 × 190 x 130 cm (length × height × depth). This results in a volume of more than 2 m$^3$ and a weight of >16,000 kg.

Therefore, a weight-bearing capacity of >70 N/cm$^2$ has to be provided. The weight of the magnet can be distributed over a larger area using a steel plate. The floor surface irregularity has to be less than ±2 mm.

## 3.5 Power Supply and Cooling

For power supply of the system, a three-phase connection is needed with a voltage between 380 and 480 V. Electric stability requires voltage changes +/−10 %. Alternating current frequency has to be 50 or 60 Hz +/−1 Hz. The maximum net asymmetry is 2 %. The maximum power consumption is 23 kVA during scan operation.

## 3.6 Sound and Vibration

The mean acoustic noise value generated by a low-field MRI is < 115 dB(A) in the scan room and <60 dB(A) in the evaluation room. Therefore, additional acoustic shielding is not necessary.

Vibrations of the building can distort the image. The vibration intensity should not exceed 85 dB(g) for frequencies < 100 Hz (Siemens Inc./ Germany).

## 3.7 Static Magnetic Field

The static magnetic field is very difficult to shield. It reduces with the distance to the magnet. For planning of the imaging suite, all procedures of scan personal should be placed outside the 0.5 mT line. This area is much wider for a high-field system (Fig. 3.4).

## 3.8 Distortion of the Magnetic Field

Another problem is represented by the increased sensitivity for external electromagnetic fields. The effect of ferromagnetic bodies, particularly if they are moving, on magnetic field homogeneity is high. This is true for all open-design MR systems (compared with closed-bore machines), but it is particularly important for systems with lower field strength.

We had considerable problems with ambulance cars passing by the magnet room. The solution was an electric field inhomogeneity-reduction system (called EFI), provided by the manufacturer of the MRI system. It produced a compensatory field avoiding the "ambulance artifacts."

Sources of field distortion:

- Static: Steel components of the building (reinforcements, steel beams)
- Dynamic: Cars, electric cables, transformers, other MR systems (Tables 3.2 and 3.3)

## 3.9 Distortion of Equipment by the MRI Magnetic Fringe Field

All instruments and electronic devices, which can be influenced by magnetic fields, have to be taken into consideration. The maximum acceptable magnetic flux density and the resulting minimum distances depend on individual sensitivity and have to be given by the manufacturer (Table 3.4).

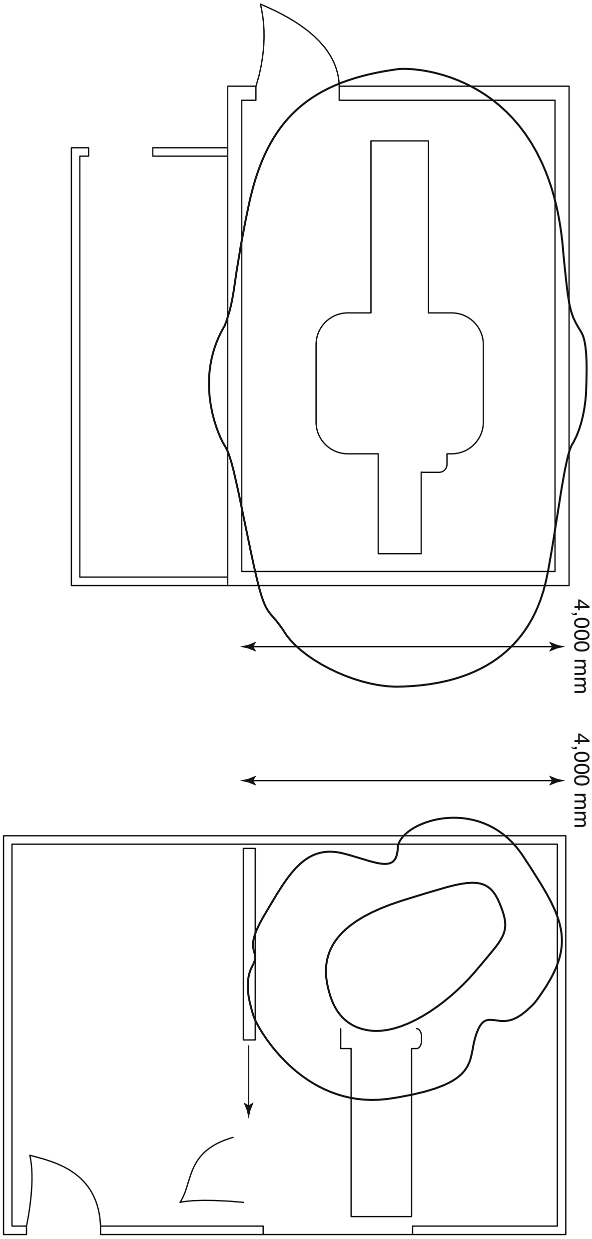


**Fig. 3.4** 0.5 mT line for a 0.4 T and a 1.5 T MRI system (Courtesy Hitachi Medical Imaging Inc.)

**Table 3.2** Minimal distance to ferromagnetic objects

| Object | Min. distance, radial | Min. distance axial | Max. weight |
|---|---|---|---|
| Cooling aggregate | >4 m | >4 m | |
| Wheelchair (<50 kg) | >4 m | >4 m | |
| Transport vehicles (<200 kg) | >5 m | >5 m | |
| Transformer | >9 m | >9 m | |
| High-power cable | >9 m | >9 m | |
| Cars < 900 kg | >5.5 m | >5.5 m | |
| Trucks < 4500 kg, elevator | >9 m | >9 m | |
| Zyklotron | >20 m | >20 m | |
| Trains | >200 m | >200 m | |
| Steel beams, steel reinforcements | >1.2 m below magnet center | >1.2 m below magnet center | <100 kg/m$^2$ |

Source: Siemens Healthcare planning Dept., Erlangen/Germany

**Table 3.3** Minimal distance MRI to MRI

| [m] | 0.2 T | 0.35 T | 1.0 T | 1.5 T | 3.0 T |
|---|---|---|---|---|---|
| 0.2 T | 10 | 10 | 5 | 6 | 10 |
| 0.35 T | 10 | 10 | 5 | 6 | 10 |
| 1.0 T | 5 | 5 | 4,5 | 5 | 6 |
| 1.5 T | 6 | 6 | 5 | 5 | 6 |
| 3.0 T | 10 | 10 | 6 | 6 | 6 |
| 7 T | 10 | 10 | 10 | 10 | 10 |

Source: Siemens Healthcare planning Dept., Erlangen/Germany

**Table 3.4** Maximum acceptable magnetic field (mT). Source: Siemens Healthcare planning Dept., Erlangen/Germany

| | |
|---|---|
| Servo ventilator | 20 mT |
| RF filter plate | 10 mT |
| Electronics cabinet | 5 mT |
| Small motors, watches, camera, data carrier | 3 mT |
| Personal computer | 1 mT |
| B/W monitor, insulin pump, cardiac pacemaker | 0.5 mT |
| Color monitor | 0.2 mT |
| CT | 0.2 mT |

## 3.10 RF Shielding

For the MRI examination room, an RF shielding (faraday cabin) is needed, to protect the MRI system against surrounding magnetic field distortions. The required attenuation is >90 dB 15–130 MHz which has to be measured before installation of the magnet.

Every MR room should have, if possible in any way, a daylight window. Daylight reduces claustrophobia and gives an additional open feeling to the patient. The improvement of comfort cannot be overrated.

The costs for this RF-shielded window are limited, and the effect is a very good compensation. Ideally, the transport access to the room can be closed by a daylight window, giving the additional advantage of easier access to the room in case of necessary magnet exchange.

## 3.11 Room Light, Reporting Stations

Ambient light conditions in rooms, where reviewing and reporting is performed, have to fulfill the following requirements (Klein et al. 1994):

- Reproducible intensity of light
- No reflection of windows or light box
- The ambient light should be ideally < 50 lm

## 3.12 Warning Signs

All areas, with a potential maximum magnetic flux density of more than 0.5 T, have to be signed and access to these areas has to be controlled.

- Low-field MRIs with permanent magnet are 3× heavier than high-field MRIs
- Low-field MRIs are highly sensitive for external influences on the magnetic field
- Patient-oriented room design is important for patient comfort and facilitated by open MRI systems
- Cars, elevators, or any other moving metallic objects should be kept at a distance
- One or more daylight windows have an important effect on room atmosphere

## References

Klein HM, Stargardt A, Grehl T, Glaser KH, Günther RW (1994) Einfluss der Raumbeleuchtung auf die diagnostische Leistung an Bildschirmarbeitsplätzen. Fortschr Rontgenstr 160:168–172

Petersilge CA, Lewin JS, Duerk JL, Haem SF (1997) MR Arthrography of the shoulder: rethinking traditional imaging procedures to meet the technical requirements of MR image guidance. Am J Roentgenol 169:1453–1457

Siemens Healthcare (2004) Installation requirements Magnetom C! 0.35T

Yamada S, Muragaki Y, Maruyama T, Komori T, Okada Y (2015) Role of neurochemical navigation with 5-aminolevulinic acid during intraoperative MRI-guided resection of intracranial malignant gliomas. Clin Neurol Neurosurg 130:134–139

# 4 Safety Considerations

Dangerous bioeffects of magnetic resonance imaging can arise from:

1. Static magnetic fields
2. Gradient magnetic fields
3. Radiofrequency fields
4. Acoustic noise

Potential dangers are:

1. Magnetic attraction of ferromagnetic objects (missile artifacts)
2. Magnetic force on body implants (aneurysm clips, pacemaker, intraoperative devices, prosthesis, cardiac valve prosthesis, otologic implants, etc.)
3. Interaction with cardiac pacemakers, insulin pumps, cerebrospinal fluid valves, etc.
4. Body heating by gradient field and radiofrequency fields
5. Exposure to acoustic noise, particularly for psychiatric patients, sedated patients, and neonate patients, which can demonstrate reactions to acoustic noise

Nearly all of the potential dangers mentioned above correlate overproportionally with magnetic field strength of the MR imaging system.

With increasing numbers of diagnostic and interventional MR procedures, there is a critical need for careful investigations concerning acute and cumulative effects of magnetic field exposure on patients and healthcare professionals, to help in establishing guidelines for occupational and patient exposures to static magnetic fields and radiofrequency (Fuentes 2008, DIN EN 60601-2-33).

For X-ray diagnostic imaging, radiation exposure for patients and healthcare professionals has to be reduced to the absolute necessary minimum – it has to be as low as reasonably achievable ("ALARA" principle). A similar principle could be demanded for magnetic resonance imaging (Table 4.1).


H.-M. Klein, *Clinical Low Field Strength Magnetic Resonance Imaging: A Practical Guide to Accessible MRI*, DOI 10.1007/978-3-319-16516-5_4

**Table 4.1** Typical sources of electromagnetic fields

| Frequency range | Frequencies | Examples of exposure sources |
|---|---|---|
| Static | 0 Hz | Video display units; MRI; industrial electrolysis; welding devices |
| ELF (extremely low frequencies) | 0–300 Hz | Power lines; domestic distribution lines; domestic appliances; electric engines in cars, trains, and tramways; welding devices |
| IF (intermediate frequencies) | 300 Hz–100 kHz | Video display units; antitheft devices and shops; free access control systems, card readers, and metal detectors; MRI; welding devices |
| RF (radio frequency) | 100 kHz–300 GHz | Mobile telephones; broadcasting and TV; microwave oven; radar and radio transceivers; portable radios; MRI |

Scientific Committee on Emerging and Newly Identified Health Risks, European Commission 2009

## 4.1 Static Magnetic Fields

Contemporary MR imaging systems operate at a field strength ranging from 0.2 to 3 T.

For short-term exposure to RF energy, multiple investigations are available including studies on cell alteration and reproduction, teratogenicity, DNA structure and gene expression, blood–brain barrier permeability, nerve activity, cognitive function and behavior, cardiovascular and hematological dynamics, temperature regulation, circadian rhythms, immune responsiveness, visual and auditory functions of the brain, and other biological processes (FDA 2003, Weintraub et al. 2007). Most, but not all, of these studies demonstrated no substantial harm caused by exposure to static magnetic fields (Shellock 2004, 2009; Schwenzer and Bantleon 2007; Von Klitzing 1986, Hong 1989).

Until 2002, MR imaging at field strength larger than 2.5 T was considered to be potentially dangerous (Kuhl et al. 2008).

According to the American Food and Drug Administration (FDA), clinical MRI systems up to 8 T are considered a "nonsignificant risk" for adult patients (Zaremba 2001, Hoult 2011).

Atkinson and coworkers examined the biological effects of strong magnetic at the field strength of 9.4 T (Atkinson et al. 2007).

The increased risk for medical staff exposed to static magnetic fields in MRI units was addressed in 2009 by the Scientific Committee on Emerging and Newly Identified Health Risks (SCENIHR) of the European Commission. A limited use of MRI was discussed. Only by consequent and immediate reaction of the medical scientific societies could this initiative be stopped (European Commission 2009). The present opinion of the SCENIHR is that exposure to electromagnetic fields may increase the risk of adverse health effects. Exposure of patients and medical staff could exceed safety limits for the general public.

Most documented severe injuries and some even fatal accidents occurred in using MR imaging systems when ferromagnetic objects like oxygen tanks, wheelchairs, or medical equipment were brought under the influence of the strong static magnetic field. Even more critical can be ferromagnetic biomedical implants like aneurysm clips. Dislocation of aneurysm clips has already resulted in fatal injuries.

Influence on ferromagnetic objects is called “missile effect” and represents the most important danger for patients in magnetic resonance imaging units. The underlying electric force is proportional to the square of the magnetic field strength. This means a 3 T magnet has a 100 times stronger magnetic attraction force compared to a 0.3 T magnet (Clark 2006).

A big advantage of open low-field MRI is better access to the patient, particularly for traumatized, unconscious, or pediatric patients. Anesthesiologists appreciate the reduced “missile effects” on ferromagnetic objects, which led to hazardous accidents in the past (Capelastegui et al. 2006) (Fig. 4.1).

## 4.2 Gradient Magnetic Fields

Gradient- or time-varying magnetic fields may induce neuromuscular stimulation by inducing local electric fields (Abart 1997, Cavin 2007). The bioeffects of gradient magnetic fields depend on a variety of factors, including field frequency, magnetic flux density, presence of harmonic frequencies, waveform characteristics


**Fig. 4.1** Head examination of a trauma patient. No interaction between anesthesiologist equipment and MRI (Siemens Magnetom C!, 0.35 T)

and polarity of the signal distribution in the body, electric properties, and sensitivity of the cell membranes (Mansfield 1993).

The US Food and Drug Administration has defined threshold levels for the strength of gradient magnetic fields. These safety standards, combined with contemporary MR technique, are considered adequate for patient protection.

Gradient magnetic fields may stimulate peripheral nerves, producing sensory events experienced as "tingling" or "tapping" (Cohen 1990, De Vocht 2006).

At substantially increased gradient energy level, lying above the perception thresholds, the patient may experience pain. At extremely high levels, cardiac stimulation can be produced; the gradient magnetic field energy necessary for cardiac simulation exceeds the commercially available MR system performance by about one order of magnitude.

Present-day low-field MR systems are equipped with gradient systems, nearly equivalent to high-field installations. The gradient amplitude lies above 23 mT, the rise time is about 400 ms, and the resulting slew rate is about 55 T/m/s (Siemens Healthcare). With increasing gradient performance, neuromuscular stimulation is theoretically possible also in low-field MR systems.

## 4.3 Radiofrequency Fields

Radiofrequency exposure of the patient is strongly dependent on field strength. Remember our comparison at the beginning: the string tension of a guitar becomes stronger with increasing frequency.

Whereas the SNR increases nearly with field strength, SAR increases exponentially (as a function of the square of field strength) (Bottomley 2008, Quick 2011).

This limits the use of SAR intense imaging sequences, particularly in ultrahigh-field systems (>3T) (Chen 1986, Atalar 2005). If field strength is increased two times, the resulting RF frequency exposure is increased by $2^2$.

That means, if you increase the field strength from 0.3 to 3 T, the resulting radiofrequency exposure of the patient is increased by $10^2$, or 100 times higher. Most of the radiofrequency power transmitted in MR imaging is transformed into heat within the patient's body as a result of resistive losses (Bottomley 1981, Shellock 1988, 2000, 2009).

Before 1985, when the systems were mostly equipped with permanent magnets with low field strength, there were no reports concerning thermal physiologic problems in MR imaging. With increasing number of clinical high-field systems (equal or larger than 1.5 T), a dosimetric term was defined: the specific absorption rate (SAR). The unit is Watts per kilogram body weight (W/kg). Usually the whole-body averaged SAR is measured by RF energy dosimetry. An RF energy dose of more than 4 W/kg is considered to expose the patient to significant hazard (US Food and Drug Administration, Table 4.2) (Hoult 2000, Schaefer 2001).

Particularly for pregnant women, a whole-body averaged RF exposure >2 W/kg for more than 6 min can result in a heating of the fetus >38 °C (Hand et al. 2010).

**Table 4.2** Specific absorption rate (SAR) (Shellock 2009)

| Site | Dose | Time (>min) | SAR (W/kg) |
|---|---|---|---|
| Whole body | Averaged | 15 | 4 |
| Head | Averaged | 10 | 3 |
| Head or torso | /g of tissue | 5 | 8 |
| Extremities | /g of tissue | 5 | 12 |

Thermoregulatory response of the patient to radiofrequency energy exposition is dependent on several physiologic factors and surrounding conditions, like underlying health condition (cardiovascular disease, hypertensive, diabetes, fever, old age, and obesity), the individual thermoregulatory system, duration of exposure, and rate of energy deposition.

Furthermore, several drugs can influence thermophysiologic response, including beta-blockers, diuretics, Ca antagonists, and amphetamines.

In an experimental study, 26 pigs were exposed to different amounts of RF energy in a whole-body birdcage coil at 3T. SAR (specific absorption rate) was below 6 W/kg and exposure time is between 30 and 60 min. Severe thermal damage of body tissues was found, depending on exposure time and applied energy levels. The SAR was found to be unreliable, concerning grade end extension of tissue damage. As an explanation for the surprisingly high RF damage, it was assumed that porcine thermal regulation is different from human physiology (Kobelt 2011).

The potential genotoxicity (DNA damage) of RF radiation is subject of an ongoing discussion (Duan et al. 2015).

All these potential hazardous effects of exposure can be avoided or at least minimized using low-field magnetic resonance imaging.

## 4.4 Acoustic Noise

Why is MR imaging so loud? We can come back to our initial comparison of magnetic and musical resonance.

Principally, the MR system behaves like a loudspeaker (Counter 1997). The gradient coils and gradient housing of the MRI represent the speaker coil and membrane. Each gradient field-switching procedure in the presence of a strong static magnetic field induces a force in the coil (Lorentz force). The switching frequency represents the frequency of the resulting MR noise (Bowtell and Mansfield 1995).

The intensity of the gradient output influences the level of acoustic noise. Enhancement is achieved by decreasing section thickness, field of view, repetition, and echo time. Presence and size of the patient himself can also affect the level of acoustic noise.

Therefore, one way to reduce acoustic noise is reduced magnetic field strength and gradient power (Brummet 1988).

Usually, low-field systems produce less noise. However, an open system with a gradient amplitude of up to 25 mT and a slew rate of 55 T/m/s can produce a significant sound level (<115 dB in the scan room; see Chap. 6).

Another way to reduce acoustic noise is to attenuate the gradient coils, for example, to enclose them into a vacuum. This way has been pursued by Toshiba (pianissimo system, Fig. 4.2).

The most innovative way to reduce noise in MRI has been introduced in 2013 to the medical community. The so-called "silent MR" technique (GE Healthcare Inc.) uses gradually increasing gradient field amplitudes to perform MR imaging at 1.5 T without any acoustic noise (Alibek et al. 2014).

## 4.5 Claustrophobia

Every patient visiting the doctor for a diagnostic procedure experiences a certain amount of psychological stress. The MRI environment increases the stress level. A mild dysphoric psychological reaction has been reported by about 65 % of all patients examined with MR imaging. In extreme cases, claustrophobia can lead to severe anxiety and panic attacks (Shellock 1996, Murphy 1997).

Symptoms of panic attack and emotional distress are conducted by catecholamine output which can result in cardiac arrhythmia or ischemia in susceptible patients.

According to contemporary literature, as many as 20 % of individuals trying to undergo an MRI examination cannot complete the procedure due to serious distress like claustrophobia or unwanted sensations (Dewey 2007).

The most important factors contributing to emotional distress are the physical environment of the MR system, combined with acoustic noise, as well as temperature variations inside of the MR system. Furthermore, the restriction of motion causes distress (Eshed 2007). The feeling of sensory deprivation, particularly in

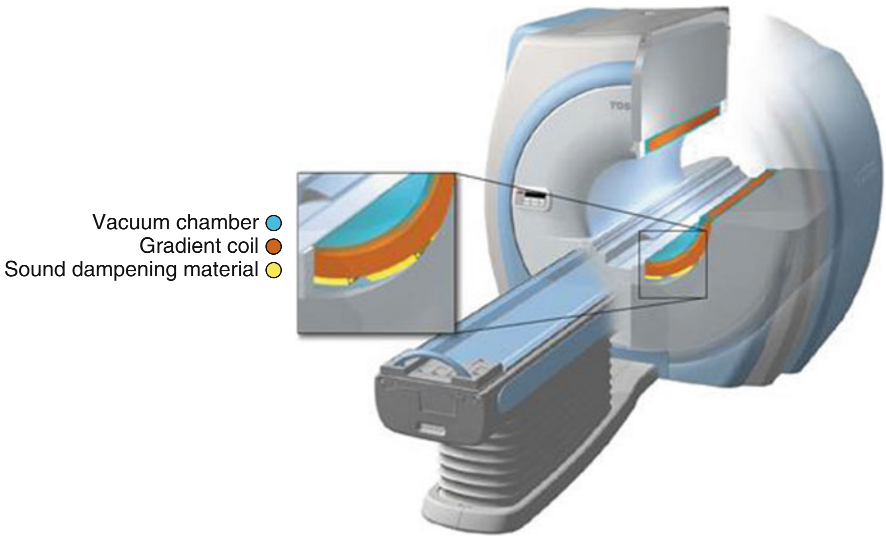


**Fig. 4.2** 3T MR system with acoustic noise reduction using a vacuum chamber (Pianissimo, Vantage Titan 3T, Toshiba Inc.)

narrow-bore magnets, is experienced negatively by the patient. The duration of the examination plays another important role.

MR systems, using vertical magnetic field, enable to design more open MR units, reducing the frequency of claustrophobic reactions during MR procedures.

Furthermore, the new so-called wide bore provides larger gantry opening, also reducing spatial restriction.

In 1993, a specially designed 0.2 T MRI was made available for MR imaging of the musculoskeletal system. Image quality for diagnosis of the extremities was reported to be comparable to mid- or high-field-strength MR systems and is therefore acceptable as an alternative to whole-body MR systems for musculoskeletal diagnostic imaging.

ONI Inc. developed a one Tesla dedicated extremity MR system which is designed for optimal imaging of the ankle and knee joint as well as the elbow and hand. The system was acquired by GE Healthcare. The plan was to improve magnet and coil performance, as well as image- and signal-processing devices. However, production was stopped recently, since the market acceptance was too low to justify the development costs.

An effective way to avoid psychological distress in MR imaging is to include a large daylight window in the examination room wall. This procedure is far less complicated than should be expected. If possible, the patient should be enabled by positioning or by use of a mirror system to watch through the daylight window, giving the examination situation a much more open and unobtrusive character.

The following list can give some recommendations for the responsible medical staff, to reduce emotional distress for patients in MR imaging:

1. Educate the patient concerning problematic aspects of MR imaging (size, noise, intercom system, duration of examination).
2. Keep verbal, visual, or physical contact with the patient.
3. Provide music or video to the patient.
4. Place patient prone for the examination.
5. Position the patient feet-first instead of head-first.
6. Use mirrors of prism glasses to direct the patient's line of sight outside the MR magnet.
7. Provide bright lights inside the MR system.
8. Provide fan inside the system.
9. Provide scented oils (vanilla, etheric oils) for aromatherapy.
10. Provide relaxation techniques like controlled breathing.
11. Administer sedative drugs.

## 4.6 Pacemaker

If a patient carrying a cardiac pacemaker is positioned in the MRI system, principally three possible events could take place (Bonnet 1990):

1. There is no effect on the pacemaker.
2. The pacemaker function is modified, causing the pacemaker generator to adapt to a fixed frequency.
3. The pacemaker function is compromised when the generator is switched off.

In case 1 or 2, nothing serious will happen to the patient. In case 3, if the patient is permanently depending on pacemaker function, there may be potential hazardous complications.

Therefore, cardiac pacemakers or implantable cardioverter defibrillators (ICDs) were considered to be a relative contraindication for magnetic resonance imaging. Additionally, individuals carrying pacemakers or ICDs should be prevented from entering the MR environment to avoid potential risks.

Various mechanisms could cause potential problems:

1. Mechanical movement of the pacemaker generator
2. Modification of the device function
3. Effect on appropriate sensing of the device
4. Excessive heating of the wires; induced currents in the lead (Shellock 2005)

All these effects, mechanical movement, effect and sensing of the devices, as well as eddy current induction or heating of the devices, depend proportional or overproportionally on the magnetic field strength of the MRI system (Erlebacher 1986).

Modification of the device function could take place by accidental reprogramming of the generator. Reprogramming can occur, particularly if the resonance frequency of the MR system is close to the programming frequency of the device.

To our personal experience with a low-field permanent magnet system (0.35 T, 14.9 MHz frequency), most examined patients required reprogramming of the pacemaker generator after the MRI.

Implantable cardioverter defibrillators (ICDs) are designed to detect and treat episodes of cardiac fibrillation, ventricular tachycardia, bradycardia, and other cardiac conditions. As soon as a problem occurs, the ICD can deliver defibrillation, cardioversion, antitachycardiac pacing, or other therapies. ICDs are considered to have similar effects as pacemakers since most of the basic components are comparable.

ICDs have electrodes placed in the myocardium, which increases risks. Furthermore they possess certain additional features which can expose the patient to additional risk.

Most reports in the literature referred to these devices dated before 1996. Meanwhile, new pacemakers have been developed, enabling to perform MRI procedures with low risk for the patient.

Torsten Sommer performed a study including 115 patients. He found that extrathoracic MRI of non-pacemaker-dependent patients can be performed with an acceptable risk–benefit ratio under controlled conditions and by taking both MR- and pacemaker-related precautions (Sommer et al. 2006 Sep 19). Using low-field MRI, pacemaker patients including high-risk patients and scan regions can be examined with an acceptable risk–benefit ratio (Strach et al. 2010).

The American College of Cardiology/American Heart Association has published guidelines for performing MRI in non-pacemaker-dependent patients (Loewy et al. 2004). The following precautions should be considered:

1. Establish a risk–benefit ratio for the patient.
2. Obtain written and verbal informed consent.
3. Pretest pacemaker functions using appropriate equipment outside of the MR environment.
4. The cardiologist should decide whether it is necessary to program the pacemaker prior to the MR examination.
5. A cardiologist with cardiac life support training must be in attendance for the entire examination.
6. The patient should be monitored continuously during the MR examination.
7. Appropriate personnel, crash cart, and defibrillator must be available throughout the procedure to address adverse event; visual and voice contact should be maintained throughout the procedure.
8. The patient should be instructed to inform the MR system operator of any unusual sensations or problems during the examination process.
9. After the completion of the MR examination, a cardiologist should inspect the pacemaker to confirm that the function is consistent with the preexamination state.

As recommended by the American Society for Testing and Materials (ASTM), an important measure for the magnetic force on the pacemaker generator is the deflection angle for implant or device measured at the point of the "highest spatial gradient" for the specific MR system used for testing. The critical angle is 45° deflection (ASTM 2014).

The deflection angle was found to be dependent on the length of the magnet ("short bore" versus "long bore"), a short-bore magnet having a stronger spatial gradient than a long-bore magnet.

Furthermore, the field strength is an important parameter. Shellock and coworkers performed a study on 14 pacemakers and four ICD devices (Shellock et al. 2003). They found that:

1. At 1.5 T, three cardiac pacemakers exhibit deflection angles greater than 45° on both long- and short-bore systems.
2. At 3 T, 7 of 14 devices showed deflection angles of greater than 45° on the long-bore system, while 13 of 14 devices exhibited deflection angles greater than 45° on the short-bore system.

## 4.7 Other Devices

All implanted biomechanical or bioelectronic devices represent potential dangers for carriers undergoing an MR examination.

In every case, the exact type and function of the device has to be cleared, considering the device manual and manufacturer guidelines. For further information, the standard textbook of Frank G. Shellock (Shellock 2009) is recommended.

### 4.7.1 Cerebrospinal Fluid Valves

Cerebrospinal drainage systems with mechanical valves are used to treat circulation and resorption defects in the cerebrospinal fluid system.

These systems are widely known to be influenced by MRI procedures, especially if they contain adjustable or programmable valves (Akbar 2010).

The larger the field strength, the higher the probability of an impairment of functionality.

According to the literature, most systems are safe at field strengths up to 1.5 T.

Some systems contain magnetic components which can be subject to permanent magnetization, if exposed to strong magnetic fields. For all patients with cerebrospinal fluid valve systems, strict conditions have to be followed:

1. MR systems with a static magnetic field of 3 T or less
2. MR system with a spatial gradient of 720 gauss/cm or less
3. Specific absorption rate limited to 3 W/kg for 15 min
4. Verifying the valve setting after the MRI procedure

### 4.7.2 Cochlear Implants

Cochlear implants are electronically activated devices. Generally, all patients carrying these devices should be prevented from entering the MR room (Teissl 1998).

However, if specific guidelines given by the manufacturer are followed, MR may be possible in certain cases.

There are some cochlear implants which can only be examined using low-field systems with the subject field strength of less than 0.4 T.

### 4.7.3 Bullets, Pellets, Shrapnel

The question whether there is a danger resulting from bullets or pellets depends on the composition of the material (Teitelbaum 1990). In several countries all over the world, steel shotgun and rifle bullets are replacing lead ammunition for hunting. If they are ferromagnetic, there is a dangerous potential for surrounding structures. If they are not ferromagnetic, there should be no danger for patients. In the MRI procedure, a distortion of the local magnetic field homogeneity can be expected.

- Magnetic resonance imaging is a very safe diagnostic procedure
- However, certain highly specific risks have to be considered. All of these risks increase, sometimes more than proportional, with magnetic field strength
- Body heating by radiofrequency and gradient field energy at 3 T can be reduced by a factor of 100, if a 0.3 T system is used
- Missile effects, which can be fatal for the patient, represent no severe problem at 0.3 T. The same is true for deflection forces on metallic implants
- All electronic implants, particularly if magnetic components are used, can be influenced or possibly damaged by magnetic fields. This risk can be minimized using low field strength
- Claustrophobia is considerably reduced, using open-design magnets, facilitated at lower field strength
- It could be discussed that the “ALARA principle” of X-ray imaging should be adapted to magnetic resonance imaging, meaning that the field strength and hence the field strength-induced risks should be “as low as reasonably achievable”

## References


Abart J, Eberhardt K, Fisher H et al (1997) Peripheral nerve stimulation by time varying magnetic fields. J Comput Assist Tomogr 21:532–538

Akbar M, Aschoff A, Georgi JC et al (2010) Adjustable cerebrospinal fluid shunt valves in 3.0-Tesla MRI: a phantom study using explanted devices. RöFo 182(7):594–602

Alibek S, Vogel M, Sun W et al (2014) Acoustic noise reduction in MRI using Silent Scan: an initial experience. Diagn Interv Radiol 20(4):360–3

ASTM F2052-14 (2014) Standard Test Method for Measurement of Magnetically Induced Displacement Force on Medical Devices in the Magnetic Resonance Environment, ASTM International, West Conshohocken, PA. www.astm.org

Atalar E (2005) Radiofrequency safety for interventional MRI procedures. Acad Radiol 12:1149–1157

Atkinson JC, Renteria L, Burd H, Pliskin NH, Thulhorn KR (2007) Safety of human MRI at static fields above the FDA 8 Tesla guideline: sodium imaging at 9.4 Tesla does not affect vital signs of cognitive ability. J Magn Reson Imaging 26:1222–7

Bonnet CA, Elson JJ, Fogoros RN (1990) Accidental deactivation of the automatic implantable cardioverter defibrillator. Am Heart J 3:696–697

Bottomley PA (2008) Turning up the heat on MRI. J Am Coll Radiol 5:853

Bottomley PA, Edelstein WA (1981) Power deposition whole body then MR imaging. Med Phys 8:510–512

Bowtell RW, Mansfield PM (1995) Quiet transverse gradient coils: Lorentz force balancing designs using geometric similitude. Magn Reson Med 34:494–497

Brummet R, Talbot JM, Caruhas P (1988) Potential hearing loss resulting from MR imaging. Radiology 169:539–540

Capelastegui A, Fernández-Canton G, Fernández-Ruanova B (2006) The safety of magnetic resonance imaging: an analysis based on a review of incidents at the Osatek Center. Radiologia 48(4):225–34
Cavin DW, Glover PM, Bowtell RW, Gowland PA (2007) Thresholds for proceeding metallic taste high magnetic fields. J Magn Reson Imaging 26:1357–61
Chen DJ, Snk VJ, Cohen SM, Hoult DI (1986) The field dependence of NMR imaging. I: laboratory assessment of signal-to-noise ratio and power deposition. Mag Reson Med 3:722
Clark R (2006) http://info.ee.surrey.ac.uk/Workshop/advice/coils/force.html
Cohen MS, Weiskopf R, Kantor H (1990) Sensory stimulation by time varying magnetic fields. Magn Reson 14:409–414
Counter SA, Olofsson A et al (1997) MRI acoustic noise: sound pressure frequency analysis. J Magn Reson Imaging 7:606–611
De Vocht F, Stevens T, van Wendel-de-Joode B, Engels H, Kromhout H (2006) Acute neurobehavior effects of exposure to static magnetic fields: analysis of exposure-response relations. J Magn Reson Imaging 23:291–297
Dewey M, Schink T, Dewey CF (2007) Claustrophobia during magnetic resonance imaging: Cohort study in over 55,000 patients. J Magn Reson Imaging 26:1322–7
Duan W, Liu C, Zhang L et al (2015) Comparison of the genotoxic effects induced by 50 Hz extremely low-frequency electromagnetic fields and 1800 MHz radiofrequency electromagnetic fields in GC-2 cells. Radiat Res 183:305–14
Erlebacher JA, Cahill PT, Pannizzo F, Knowles RJR (1986) Effect of magnetic resonance imaging on DDD pacemakers. Am J Cardiol 57:437–440
Eshed I, Althoff CE, Hamm B, Hermann KG (2007) Claustrophobia and premature termination of magnetic resonance imaging examinations. J Magn Reson Imaging 10(6):401–404
European Commission (2009) http://ec.europa.eu/health/scientific_committees/opinions_layman/en/electromagnetic-fields/
Fuentes MA, Trakic A, Wilson SJ, Crozier S (2008) Analysis and measurements of magnetic field exposures for health workers in selective MR environments. IEEE Trans Biomed Eng 55:1355–64
Gimbel JR (2008) Magnetic resonance imaging of implantable cardiac written devices at three Tesla. Pacing Clin Electrophysiol 31:795–801
Glover PM, Eldeghaidy S, Mistry TR, Gowland PA (2007) Measurement of visual evoked potential during and after periods of pulsed magnetic field exposure. J Magn Reson Imaging 26:1353–6
Hand JW, Li Y, Hajnal JV (2010) Numerical study of RF exposure and the resulting temperature rise in the foetus during a magnetic resonance procedure. Phys Med Biol 55(4):913–30
Hong CZ, Shellock FG (1989) Short-term exposure to a 1.5 T static magnetic field does not effect somatosensory evoked potentials in man. Magn Res Imaging 8:65–69
Hoult DI, Phil D (2000) Sensitivity and power deposition in a high field imaging experiment. J Magn Reson Imaging 12:46–67, Review
International commission on non-ionizing radiation protection (ICNIRP) statement, medical magnetic resonance procedures: protection of patients (2004) Health Phys 87:197–216
International Electrotechnical Commission (IEC) (2002) Medical electrical equipment, particular requirements for the safety of magnetic resonance equipment for medical diagnosis. International standard IEC. DIN EN 60601-2-33
Kobelt F (2011) Untersuchung von Hochfrequenz (HF) basierten thermischen Effekten bei der 3-Tesla-Magnetresonanz (MR) – Tomographie in einer Hochfrequenz-Spule im Schweinemodell mit besonderer Betrachtung der histologischen Muskelveränderungen. Inaugural-Dissertation zur Erlangung des Grades eines Doktors der Veterinärmedizin an der Freien Universität Berlin Journal-Nr.: 353
Kuhl CK et al (2008) Whole body high-field strength (3.0-T) MR imaging in Clinical practice. Radiology 246:675–696
Loewy J, Loewy A, Kendall DJ (2004) Reconsideration of pacemakers and MR imaging. Radiographics 24:1257–1268

Mansfield P, Harvey PR (1993) Limits to neural stimulation in echo-planar imaging. Magn Reson Med 29:746–758

Murphy KJ, Brunberg JA (1997) Adult claustrophobia, anxiety and sedation in MRI. Magn Reson Imaging 15:51

Quick HH (2011) Seven Tesla MRI: from technical developments to imaging applications. Diagn Imaging Eur 10–12

Schaefer DJ (2001) Health effects and safety of radiofrequency power deposition associated with magnetic resonance procedures. In: Shellock FG (ed) Magnetic resonance procedures: health effects and safety. CRC Press, Boca Raton, pp 55–74

Schwenzer NF, Bantleon R (2007) Do static or time varying magnetic fields in magnetic resonance imaging (3.0 T) alter protein gene expression? A study on human embryonic lung fibroblasts. J Magn Reson Imaging 26:1210–5

Shellock FG (1996) Claustrophobia, anxiety, and panic disorders associated with MR procedures. In: Shellock FG, Kanal E (eds) Magnetic resonance: bioeffects, safety, and patient management. Lippincott-Raven Press, New York, p 65

Shellock FG (2000) Radiofrequency energy induced heating during the MR procedures: a review. J Magn Reson Imaging 12:30–36

Shellock FG (2004) MR safety and cerebrospinal fluid shunt (CSF) valves. Signals 51(4):10

Shellock FG (2009) Reference manual for magnetic resonance safety, implants and devices: 2009 edition. Biomedical research publishing group and Shellock R&D services Inc. Los Angeles CA

Shellock FG, Crues JV (1988) Temperature changes caused by clinical MR imaging of the brain and 1.5 Tesla using a head coil. AJNR Am J Neuroradiol 9:287–291

Shellock FG, O'Neil M, Ivans V et al (1999) Cardiac pacemakers and implantable cardiac defibrillators are unaffected by operation of an extremity MR system. AJR Am J Roentgenol 72:165–170

Shellock FG, Stone KR, Resnik D et al (2000) Subjective perceptions of MRI examinations performed using an extremity MR system. Signals 32:16

Shellock FG, Tkach JA, Ruggieri PM et al (2003) cardiac pacemakers, ICPs, and loop recorder: evaluation of translation attraction using conventional (longboard) and short for 1.50 and three Tesla MR systems. J Cardiovascul Magn Reson 5:387–397

Shellock FG, Valencerina S, Fischer L (2005) MRI related heating of pacemaker at 1.5- and 3 Tesla: evaluation with and without pulse generator attached to leads. Circulation 112(Suppl II):561

Sommer T, Naehle CP, Yang A et al (2006) Strategy for safe performance of extrathoracic magnetic resonance imaging at 1.5 tesla in the presence of cardiac pacemakers in non-pacemaker-dependent patients: a prospective study with 115 examinations. Circulation 114(12):1285–92

Strach K, Naehle CP, Mühlsteffen A et al (2010) Low-field magnetic resonance imaging: increased safety for pacemaker patients? Europace 12(7):952–60

Teissl C, Kremser C, Hochmair ES et al (1998) Cochlear implants: in vitro investigation of electromagnetic interference at MR imaging-compatibility and safety. Radiology 208:700–708

Teitelbaum GE, Yee CA, Van Horn DD et al (1990) Metallic fragments: MR imaging safety and artifacts. Radiology 175:855–859

U.S. Department of Health and Human Services, Food and Drug Administration, Center for Devices and Radiological Health, Guidance for Industry and FDA Staff (2003) Criteria for significant RISC investigations of magnetic resonance diagnostic devices, July 14, 2003

Von Klitzing L (1986) Do static magnetic fields in MR influence biological signals? Clin Phsy Physiol Meas 7:157–160

Weintraub MI, Khoury A, Cole SP (2007) Biological effects of 3T MR imaging comparing traditional 1.5-T and 0.6-T in 1023 consecutive outpatients. J Neuroimaging 17:241–5

Zaremba LA (2001) FDA guidance for magnetic resonance system safety and patient exposures: current status and future considerations. In: Shellock FG (ed) Magnetic resonance procedures: health effects and safety. CRC Press, Boca Raton

# Low-Field-Specific Physical Aspects

# 5

In low-field MR scanners, some imaging parameters are different from high-field systems. These different characteristics can be of advantage or disadvantage, depending on the imaging situation (Kuhl et al. 2008; Hoult et al. 1986).

## 5.1 Larmor Frequency and Chemical Shift

The resonance frequency of molecules in a strong external magnetic field is called Larmor frequency $\omega$. The relation between field strength $B_o$ and the resonance frequency is given by the Larmor equation:

$$\omega = \gamma \times B_o$$

The gyromagnetic ratio for protons is 42.6 MHz/T.

The lower the field strength, the slower the spins rotate around the $z$-axis. The spin cycle time is therefore increased from 4.6 ms at 1.5 T to 19.7 ms at 0.35 T.

This means that fat-suppressed sequences with opposed-phase technique, where the spins of fat and water have to be in 180° opposite direction, take a longer acquisition time (Schild 2005). The same is true for time-of-flight angiographic sequences (Pavone 1992, Keller and Saloner 1993).

For time-critical sequences with exact phase setting, like MR mammograms, where small time deviations lead to severe signal changes, longer spin cycle time can be advantageous.

Another consequence of lower field strength is that the resulting lower frequent RF signal shows better tissue penetration (Kuhl et al. 2008). Therefore, the homogeneity of the RF magnetic field, the so-called $B_1$ field, is improved, giving better inherent field homogeneity. In high-field MRI > 1.5 T, $B_1$ inhomogeneity is a big issue, which can be compensated only by expensive multi-transmit technology, helpful, but still a compromise.



H.-M. Klein, *Clinical Low Field Strength Magnetic Resonance Imaging: A Practical Guide to Accessible MRI*, DOI 10.1007/978-3-319-16516-5_5

Furthermore, higher RF increases RF deposition and in consequence tissue heating dramatically (see below), influencing clinical use.

Another consequence of lower field strength is a slightly different resonance frequency between tissues (Peh and Chan 2001). At 1.5 T, fat and water resonance peaks are shifted by 220 Hz. At 0.4 T, the chemical shift is only 66 Hz. With decreased chemical shift, the black bands at fat–water interfaces become smaller (another way would be to increase frequency bandwidth, thus reducing SNR).

Chemical shift, however, is the basic principle for spectroscopic differentiation of substances. MR spectroscopy is inferior in lower-field systems.

Another disadvantage resulting from reduced chemical shift is the insufficient effect of spectral fat saturation (see below).

## 5.2 Homogeneity

Homogeneity is a decisive parameter for image quality.

Homogeneity of the magnetic field depends on the primary structure of the magnet, in case of low field strength mostly a permanent magnet, and equalization of inhomogeneities, the shimming process.

Optimizing the shimming procedure is of crucial importance to provide optimal imaging results. In any way, it is difficult to achieve the values of a high-field system, particularly using an open design permanent magnet.

Why is homogeneity so important? Spatial encoding is done by superimposing a gradient field and thereby modulating the local field strength. This results in a locally defined resonance frequency. Using a Fourier analysis of the resonance spectrum, each spatial point is represented by a certain resonance frequency. Inhomogeneous magnetic field strength therefore directly influences spatial resolution (Edelstein et al. 1983).

The quantification of homogeneity is regularly measured in parts per million (ppm). A homogeneous field strength for the whole field of view (40 cm) with a deviance of less than 5 ppm measured peak to peak is mandatory for acceptance of an MR system by the public health insurances in Germany (see Chap. 2).

Since lower field strength goes along with a better background homogeneity (Kaufman et al. 1989), it may be more adequate to measure this parameter in absolute values. Absolute homogeneity is given by ppm × field strength (gauss). A homogeneity value of 5 ppm on a 0.35 T (3500 G) system is better than 5 ppm at 1.5 T (15,000 G):

$$0.35\text{T} : 5 \times 3500\ \text{gauss} \times 10^{-6} = 0.0175\ \text{gauss}$$
$$1.5\text{T} : 5 \times 15{,}000\ \text{gauss} \times 10^{-6} = 0.075\ \text{gauss}$$

An argument in favor of a relative homogeneity measurement is the fact that spectral fat saturation depends on field strength homogeneity. As said above, at 0.4 T the frequency offset between fat and water is only 66 Hz and at 1.5 T 220 Hz. Spectral saturation of fat protons is an important tool for clinical imaging. The small frequency difference makes spectral fat saturation difficult in low-field imaging and requires even more homogeneity. To ensure reliable fat saturation, the absolute homogeneity needs to be proportional to field strength. The same is true for spectroscopic analysis.

Modern low-field systems are capable to fulfill every criterion of the German MR commission (see Chap. 2), except a relative field strength homogeneity of less than 5 ppm measured peak to peak in a 40 cm sphere phantom – not because they are inhomogeneous, but because the permanent magnet opening is smaller than 40 cm. The phantom simply doesn't fit.

The homogeneity is higher at the center of the magnetic field. Since a more flexible positioning of the body is possible in an open system, this can partly compensate for peripheral field inhomogeneity. Shoulder imaging, for example, is performed in the peripheral part of the field in a conventional closed-bore magnet system. In an open magnet, the shoulder can easily be positioned in the field center and therefore in a sufficiently homogeneous area.

## 5.3 T1 Relaxation

T1 and, to a smaller degree, T2 relaxation depends on field strength. With decreasing magnetic field, the T1 time (longitudinal or spin–lattice relaxation) is shortened, and T2 time (transversal or spin–spin relaxation) is prolonged.

How does this influence tissue contrast?

The most simple MR sequence is a partial saturation (sequence). Signal intensity (SI) in this sequence is given by

$$\mathrm{SI} = K \times \rho \times \left(1 - \exp\left[-\mathrm{TR} / \mathrm{T1}\right]\right)$$

where $K$ is a constant, combining the effects of flow, diffusion, perfusion, and other parameters, $\rho$ is proton density, TR is the repetition time (time between 2 RF excitation pulses), and T1 is the time.

This means that with shorter T1 time, signal increases. This refers to T1-weighted spin echo and gradient echo technique.

Furthermore, TR has to be less than 5 × T1 to ensure sufficient recovery of longitudinal relaxation (and hence enough spins in z-axis direction for the next 90° pulse). Therefore, with decreasing T1, TR could be shortened, increasing scan speed and partially compensating the reduced signal at lower field strength (Fischer et al. 1990).

For T2-weighted sequences, the effect of short T1 time is less important. T2 contrast increases with the echo time TE, the time interval between excitation pulse and spin echo.

Signal intensity is (SI) given by

$$\mathrm{SI} = K \times \rho \times \left(1 - \exp\left[-\left(\mathrm{TR} - \mathrm{TE}\right) / \mathrm{T1}\right] \times \exp\left[-\mathrm{TE} / \mathrm{T2}\right]\right)$$

where $K$ is a constant, combining the effects of flow, diffusion, perfusion, and other parameters, $\rho$ is proton density, TE is the echo time, TR is the repetition time, and T1 and T2 are the time.

The contrast between body tissues is reduced, if the field strength is increased.

The same is true for the contrast between lesions and healthy tissue. Pathological changes go along with a prolongation of T1 and T2 time.

As the relaxation times converge with increasing field strength, the lesion-tissue-contrast decreases (Kaufman et al. 1989; Hayashi et al. 2004) (Fig. 5.1).

For radiologists, this is comparable to the effect of a converging mass absorption coefficient of different tissues (fat, water, bone) at increasing tube voltage in X-ray imaging.

The resulting increase in contrast-to-noise ratio can be used to partially compensate for the smaller signal-to-noise ratio in low-field systems.

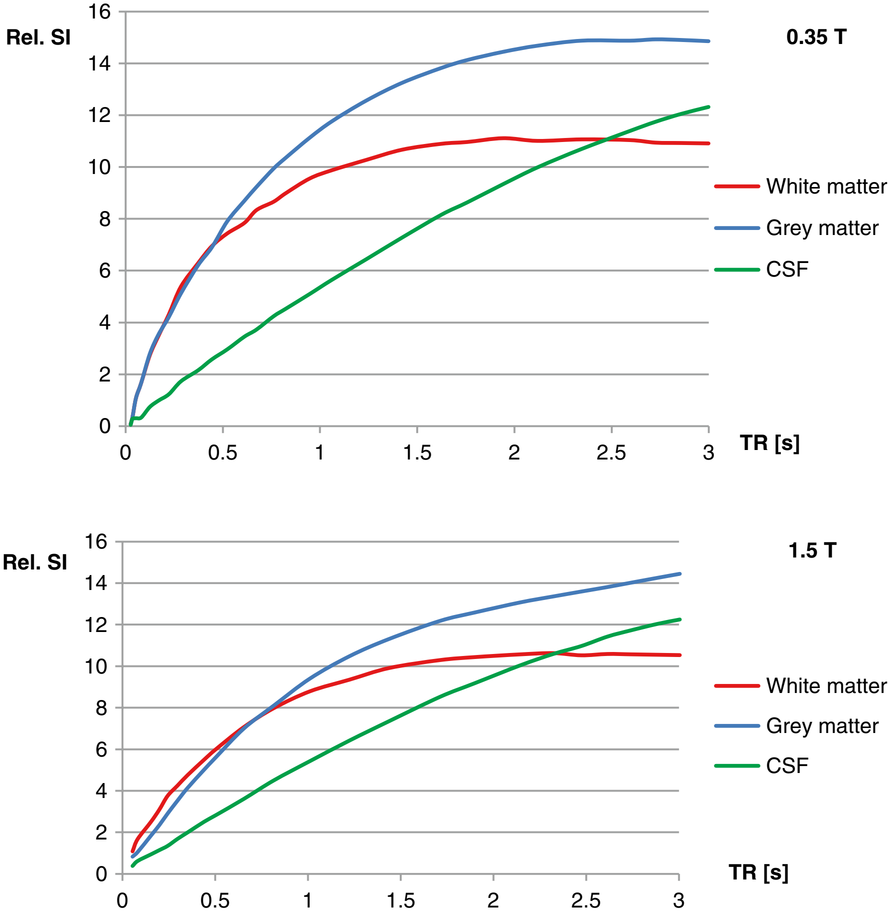


**Fig. 5.1** At lower field strength, solid tissues have shorter T1 values. This gives more signal at every TR and yields better lesion-tissue-contrast

In conclusion, it can be said that shorter T1 time in low-field systems improves signal intensity for T1-weighted SE, GE, and inversion recovery (STIR) sequences. Here, it partially compensates the lower signal strength.

In T2-weighted sequences, the T1-shortening effect is of less importance.

Taking all factors into consideration, there is a gain in tissue contrast at lower field strength.

## 5.4 Contrast-Enhanced Imaging

The effect of Gd-containing contrast agents is reduction of T1 time. If T1 is shortened in low-field imaging, this means that the contrast effect of T1 agents is reduced. While the potential of such agents to reduce T1 time is stable between 1 and 5 T, at lower field strengths, this effect becomes relevant.

With inflammatory cerebral disease, where a subtle evaluation of enhancement in demyelinated lesions is of therapy-influencing relevance, the dosage of contrast agent has to be increased. Brekenfeld and coauthors recommend a doubling of the contrast agent for diagnosis of cerebral lesions at 0.2 T compared with 1.5 T (Brekenfeld et al. 2001).

For body imaging, the good RF penetration at lower frequency improves the tissue contrast and also the demonstration of contrast-agent-induced T1 shortening.

There are only very few reports on contrast-enhanced MR angiography in low-field MR imaging, since most installed systems are not capable to perform these short TE gradient echo sequences with a high spatial resolution in an adequate acquisition time (Anzalone et al. 2005; Barbier et al. 2001; Fellner et al. 2005).

To our own experiences, there is only a marginal difference of image quality in CE angiographies performed on low-field MRI compared to high-field MRI if a high-performance low-field system is used (Klein et al. 2008).

## 5.5 Bandwidth

The readout field gradient has a given magnetic field amplitude. This amplitude defines a local resonance frequency. Readout gradient strength and field of view define the bandwidth:

$$\text{Readoud gradient}\left[\text{Hz / cm}\right]\times\text{FOV}\left[\text{cm}\right]=\text{bandwidth}\left[\text{Hz}\right]$$

The bandwidth is apportioned to the number of pixels along the frequency-encoding gradient. It is equivalent to the digital sampling rate (Vlaardingerbroek and den Boer 2002).

For example, if 256 points are sampled in 8 ms, the sampling rate is 32,000/s or 32 kHz. If the FOV is 12 cm,

$$32,000\,\text{Hz} / 12\,\text{cm} = 2667\,\text{Hz} / \text{cm or } 6\,\text{mT} / \text{m}$$

Each frequency contains noise. Therefore, widening the frequency bandwidth increases noise and reduces SNR.

The sampling rate (bandwidth) is proportional to the gradient amplitude. SNR is proportional to the square root of bandwidth (Wehrli 1992). Therefore, gradient performance is an important contributor to image quality.

## 5.6 RF Deposition

One potential harmful factor in MR imaging is RF energy deposition. The maximum RF energy is limited to a value that causes less than 1° Celsius tissue heating. The specific absorption rate (SAR) must not exceed 4 W/kg body weight in a 15 min period.

The SAR increases approximately with the square of field strength. The exact increase is influenced by the number of RF pulses/time (echo spacing), increasing flip angles, shorter TR, coil design, position of the patient relative to the isocenter, etc.

In low-field imaging, the RF problem is far smaller (see Chap. 4). Using the same sequence on a 0.3 T system compared with a 3 T system results in applying only 1 % of the RF energy. For high-field imaging, this means that a lot of advantages provided, mainly higher spatial and temporal resolution, cannot be used due to exceeding SAR limit. Low-field imaging, on the other hand, has a great potential to compensate for the missing field strength by optimizing other image-relevant factors.

What consequence has this on imaging? Let's address the chemical shift artifact:

- To reduce it, the bandwidth has to be increased.
- Increasing bandwidth by a factor of 2 reduces SNR by the square root of 2 to about 70 %.
- Doubling field strength from 1.5 to 3 T doubles SNR.
- So, practically 3 T MRI has (0.7 * 2 or) about 40 % more signal, compared with 1.5 T. But the deposited RF energy is four times higher.

## 5.7 Susceptibility

The term "susceptibility" describes the ability of a material to be magnetized, meaning that it will develop its own magnetic field if positioned in an external magnetic field. This tissue field influences the external field with an intensity determined by the tissue or material susceptibility. Most body tissues are diamagnetic, meaning that they reduce the local magnetic field strength.

Paramagnetic agents, like Gd-containing contrast material, increase the local magnetic field and thereby the local magnetic inhomogeneity. This leads to an increased T1 signal decay and increased T1 signal intensity (contrast effect).

Superparamagnetic agents like hemosiderine or ferrite (iron oxide)-containing contrast agents increase the net magnetic field more intensely. Ferromagnetic agents like iron or steel alloys result in a very strong field intensification and strong artifacts.

These susceptibility effects can be used to detect small hemorrhage or hemosiderine deposits after bleeding, for example, in cerebral tissue or in the diagnosis of endometriosis. Susceptibility effects are reduced at lower field strength.

For imaging of metal implants like hip or knee prostheses (Grebmeier et al. 1991), low-field MR provides the chance to provide diagnostic images (Sugimoto et al. 2003). Important are a minimized TE, maximum bandwidth, orientation of the readout gradient along the long axis of the prosthesis (maximum metal diameter), and maximum possible number of refocusing 180° RF pulses (turbo factor) (Klemm et al. 2000).

## 5.8 Sensitivity to Motion

For reasons not completely understood, motion artifacts are increasing with field strength (Kaufman et al. 1989). Part of the explanation may be a more convenient patient positioning and therefore less motion. Care has to be taken to improve patient comfort in every possible way. Convenience decreases motion and improves image quality.

Only a well-comforted patient tolerates the examination well and manages to avoid moving.

## 5.9 Dielectric Effects

The wavelength of an electromagnetic wave (e.g., RF radiation) is defined by light speed and frequency. At 3.0 T the frequency is 128 MHz; therefore, the resulting wavelength in a vacuum is approximately 2.4 m, while in water it is reduced to about 26 cm. This has an effect on absorption and reflection of RF radiation in the body and hereby for homogeneity of the magnetic conditions (Kuhl et al. 2008).

It can lead to field-focusing effects with higher energy deposition in deep body parts or reflection at structures with high conductivity gradients like the body wall, chest wall, or biomedical implants (dielectric intracorporeal resonance).

Furthermore, as explained above, the RF exposure is proportional to the square of field strength. In consequence, compared with 0.3 T, at 3 T the patient is exposed to about 100 times higher RF energy with a much shorter wavelength and the resulting dielectric intracorporeal effects (Fig. 5.2).

Due to these facts, safety considerations are much less problematic in low-field imaging.

The image deterioration at higher field strength, caused by these dielectric effects, can be partially compensated by multiple transmitters. The resulting different B1 fields (RF fields) allow to adjust the overall field homogeneity in the body.

At lower field strength and therefore lower Larmor frequency, transmission, reflection, and absorption of RF energy are by far smaller. Dielectric effects do not

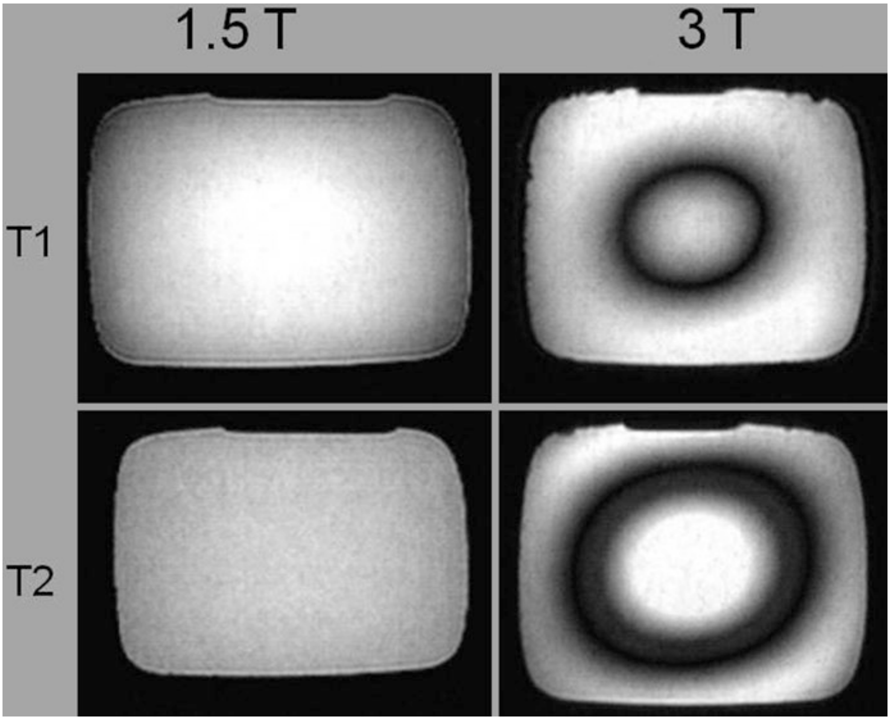


**Fig. 5.2** Dielectric effects causing concentric artifacts at high field strength. Phantom study at 1.5 and 3 T. *Left*: no image deterioration at 1.5 T. *Right*: dielectric artifacts at 3 T (Reprinted with modification, permission from C. Kuhl, RWTH Aachen)

play an important role. This results in a higher B1 homogeneity, less body heating, and far higher SNR at a given RF input (Hoult et al. 1986).

## 5.10 Signal-to-Noise Ratio

The relation between signal strength and noise level is the key parameter for image quality.

It is important to reduce noise as far as possible. Shielding has to be optimized and RF noise sources should be carefully avoided. Coils must be optimized to acquire the highest possible signal. Signal decrease by long transmit ways or insufficient electronic components has to be minimized. Going back to our initial comparison, we need absolute HiFi quality.

Since the resonance signal increases with field strength, a 1.5 T system has about four times the signal level compared to a 0.35 T unit. In fact, the real signal strength is even a little higher (about five times), since the relation is slightly overproportional. To some extent this is caused by the Zeeman effect (Loretz and Rosskopf 2014).

Signal-to-noise ratio and the resulting image noise level are influenced not only by field strength (Edelstein et al. 1983). A variety of other parameters are important: receiver bandwidth, echo spacing, voxel size (matrix, spatial resolution), coil design, and parallel imaging.

Body volume is important too, since low resonance frequency provides better RF penetration, which is advantageous, for example, in abdominal imaging.

Furthermore, the T1 tissue contrast is superior at lower field strength, with a maximum around 0.3 T. In fact, the difference of 1/T1 between the gray and white matter of the brain has an optimum at a Larmor frequency of 10 MHz (Fischer et al. 1990). This allows to partly compensate for the lower basic signal level.

However, several imaging techniques with low resulting signal, like functional imaging (BOLD sequences) or spectral fat saturation, are difficult to perform at low-field systems.

Spectroscopy is limited to high-field systems, since (frequency) spectral separation of the molecular composition of body tissue is strongly dependent on field strength and therefore improved at 3 T.

*Lower field strength leads to*
- Increased T1 contrast
- Decreased RF exposure
- Decreased metal (susceptibility) artifacts
- Decreased missile effects
- Decreased effect of Gd contrast agents
- Decreased chemical shift
- Inferior fat saturation and spectroscopy
- Inferior signal-to-noise ratio

## References

Anzalone N, Scomazzoni F, Castellano R, Strada L, Righi C, Politi LS, Kirchin MA, Chiesa R, Scotti G (2005) Carotid artery stenosis: intraindividual correlations of 3D time-of-flight MR angiography, contrast-enhanced MR angiography, conventional DSA, and rotational angiography for detection and grading. Radiology 236(1):204–213

Barbier C, Lefevre F, Bui P, Denny P, Aiouaz C, Becher S (2001) Contrast-enhanced MRA of the carotid arteries using 0,5 tesla: comparison with selective digital angiography. J Radiol 82:245–249

Brekenfeld C, Foert E, Hundt W, Kenn W, Lodemann KP, Gehl HB (2001) Enhancement of cerebral disease: how much contrast agent is enough? Comparison of 0.1, 0.2, and 0.3 mmol/kg gadoteridol t 0.2 T with 0.1 mmol/kg gadoteridol at 1.5 T. Invest Radiol 36:266–275

Edelstein WA, Bottomley PA, Hart HR, Smith LS (1983) Signal, noise, and contrast in nuclear magnetic resonance (NMR) imaging. J Comput Assist Tomogr 7:391–401

Fellner C, Lang W, Janka R, Wuttke R, Bautz W, Fellner FA (2005) Magnetic resonance angiography of the carotid arteries using three different techniques: accuracy compared with intraarterial x-ray angiography and endarterectomy specimens. J Magn Reson Imaging 21(4):424–431

Fischer HW, Rinck PA, van Haverbecke Y, Muller RN (1990) Nuclear relaxation of human brain gray and white matter: analysis of field dependence and implications for MRI. Magn Reson Med 16:317–334

Hayashi N, Watanabe Y, Masumoto T, Mori H, Aoki S, Ohtomo K, Okitsu O, Takahashi T (2004) Utilization of low-field MR scanners. Magn Reson Med Sci 3(1):27–38

Hoult DI, Chen CN, Sank VJ (1986) The field dependence of NMR imaging. II. Arguments concerning an optimal field strength. Magn Reson Med 3(5):730–746

Kaufman L, Arakawa M, Hale J, Rothschild P, Carlson J, Hake K, Kramer D, Lu W, Van Heteren J (1989) Accessible magnetic resonance imaging. Magn Reson Q 5(4):283–297

Keller PJ, Saloner D (1993) Time-of-flight flow imaging. In: Potchen EJ, Haacke EM, Siebert JE, Gottschalk A (eds) Magnetic resonance angiography, concepts and applications. Mosby, St. Louis, pp 146–159

Klein HM, Buchal R, Achenbach U, Domalski S (2008) CE-MRA of carotid and vertebral artery: open 0.35T vs. 1.5 T MRI. Clin Neuroradiol 18(2):107–112

Klemm T, Duda S, Machann J et al (2000) MR imaging in the presence of vascular stents: a systematic assessment of artifacts for various stent orientations, sequence types and field strengths. Magn Reson Imaging 12:606–615

Kuhl CK, Träber F, Schild HH (2008) Whole body high-field-strength MR imaging in clinical practice. Part 1. Technical considerations and clinical applications. Radiology 246(3): 675–696

Loretz M, Rosskopf T, Boss JM et al (2014) Single-proton spin detection by diamond magnetometry. Science pii:1259464

Pavone P, Marsili L, Catalano C, Petroni GA, Aytan E, Cardone GP, Passariello R (1992) Carotid arteries: evaluation with low-field-strength MR angiography. Radiology 184(2):401–404

Peh WC, Chan JH (2001) Artifacts musculoskeletal magnetic resonance imaging: identification and correction. Skeletal Radiol 30:179–191

Schild H (2005) Clinical highfield MR. Rofo 177(5):621–631

Sugimoto H, Hirose I, Miyaoka E et al (2003) Low field strength MR imaging of failed hip arthroplasty: association of femoral periprosthetic signal intensity with radiographic, surgical, and pathologic findings. Radiology 229:718–723

Vlaardingerbroek MT, den Boer JA (2002) Magnetresonanz-Bildgebung: Theorie und Praxis. Springer, Berlin

von Grebmeier J et al (1991) In-vitro-und Patientenuntersuchung mittels MRT: Bedeutung metallischer Implantate. Fortschr Rontgenstr 154(5):484–487

Wehrli F (1992) Principles of magnetic resonance. In: Stark D, Bradley WG (eds) Magnetic resonance imaging. Mosby, St. Louis, pp 3–20

# 6 Low-Field Imaging Technique

We have taken a look at the construction of MRI systems, how they work, and which low-field-specific aspects of physics have to be considered. Now, before we consider clinical imaging, we will think about ways to optimize low-field scanning, which advantages we can use and which drawbacks we have to be aware of.

## 6.1 Positioning

Let us start with the patient itself. The patient is one important source of artifacts: body movement, breathing, heartbeat, vessel movement, and bowel peristalsis.

The best patient is one who feels comfortable and relaxed, experiences no pain, and maybe has something to hear (music) or look (pictures) at.

Very important is the effect of a large daylight window, visible from the patient table (see Sect. 3.9).

Permanent magnets allow an open design, providing good access to the patient, reduce claustrophobia, and ease positioning. This improves comfort for patient as well as healthcare professionals. Comfort means better compliance of the patient, better imaging results by reduced motion, and better tolerance, even if the patient suffers from claustrophobia (Rothschild et al. 1992; Heuck et al. 1997; Hayashi et al. 2004).

In certain clinical situations, it may also mean increased safety. This is regularly the case in patients who need intensive care. Positioning is far more easy. The anesthesiologist has nearly free access to the patient. Possible missile effects of ferromagnetic medical devices are significantly reduced (Kaufmann 1989; Bohinski et al. 2001).

Comfortable patient positioning is a crucial prerequisite for successful imaging. Furthermore, it is important that the patient understands the examination procedure. It is good practice to explain to the patient what will happen and how long the examination takes. We tell the patient that this machine is very careful with his body



H.-M. Klein, *Clinical Low Field Strength Magnetic Resonance Imaging: A Practical Guide to Accessible MRI*, DOI 10.1007/978-3-319-16516-5_6

and that we therefore have to invest some more time in the examination. If ever possible, we talk to the patient during the procedure – talking makes it easier for the patient and gives us a kind of "interactive biomonitoring."

## 6.2 Sequences

In this section, we will briefly address the sequence technique and consider low-field-specific changes of the scan procedure.

### 6.2.1 Spin Echo

Spin echo sequences are the classical "working horses" of MRI.

1. The sequence starts with a 90° RF excitation pulse. The gradient in z-direction is switched on.
2. The phase encoding gradient is switched on.
3. After a time TE/2, a 180° inversion pulse is transmitted.
4. The readout gradient is switched on. The spin phase is different for each phase encoding step.
5. After a time, TE the spins are in phase again, giving the maximum spin echo.
6. After recovery of the z-magnetization, the next sequence is started (Fig. 6.1).

Sequences with a short echo time TE (minimal TE, about 15 ms) and a short TR (400–600 ms) are influenced mainly by T1 relaxation. Short TE, long TR gives a proton-density image. Long TE, long TR results in images influenced more by T2 relaxation.

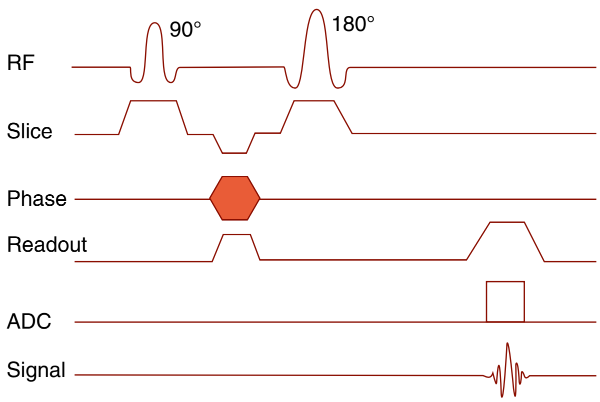


**Fig. 6.1** Spin echo sequence pulse sequence timing diagram

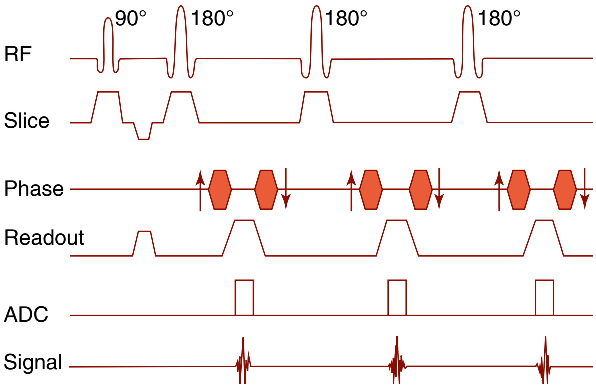


**Fig. 6.2** Fast spin echo pulse sequence timing diagram

The shorter T1 time at lower-field strength provides higher signal at short TE and a better T1 contrast.

Minimum TE is depending on the gradient performance in terms of gradient amplitude and, more importantly, gradient slope (or rise time). The combination of these two parameters is called "slew rate."

Some younger low-field scanners have improved gradient performance.

A good example is gradients with 24 mT/m amplitude and a rise time of 450 ms. The slow rate is therefore 55 T/m/s, enabling sufficiently short echo time.

Since T1 relaxation is faster, the time until recovery of longitudinal relaxation is completed is shorter: TR can be reduced to <500 ms, providing some gain in scan time, at equal signal-to-noise and contrast-to-noise ratio (SNR and CNR).

T2-weighted sequences do not take profit from lower field strength, contrast-enhanced T1 sequences likewise, due to the reduced contrast effect of Gd (see below).

### 6.2.2 Multi-Spin Echo

To increase scan speed, one excitation pulse can be followed by multiple inversion pulses (multi-echo). The higher the number of echoes/TR, the faster is the sequence. Since TR is short in T1 sequences, they take only limited profit. For T2 sequences with long TR, the number of echoes can go up to 100/TR and above. The late echoes, however, have lost most of their signal (Fig. 6.2).

To increase signal strength for sequences with long echo trains, a trick is played: The early echoes fill the central part of the signal space (k-space) defining image contrast. The late echoes fill the peripheral part of the k-space, giving mainly contour information (Fig. 6.3).

Peter Rinck gives a beautiful example for the k-space function (Rinck 2009) (Fig. 6.4)

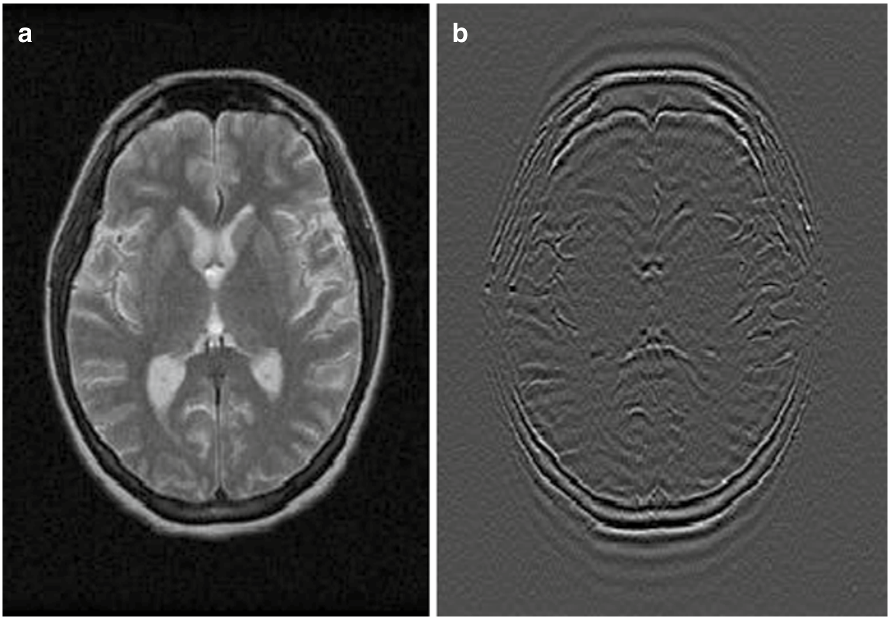


**Fig. 6.3** (**a**) Central k-space contains contrast information. (**b**) Peripheral k-space contains contour information

**Fig. 6.4** A cat by day, and a cat by night. In bright daylight, the pupil is small, the central parts of the retina give excellent resolution. At night, the pupil widens, since the peripheral parts of the retina are needed to gain as much of the weak light (signal) as possible

### 6.2.3 Gradient Echo

In a gradient echo sequence, spin rephasing is not achieved using an inversion 180° RF pulse, but by inverting the frequency encoding gradient. Keep it simple! (Fig. 6.5)

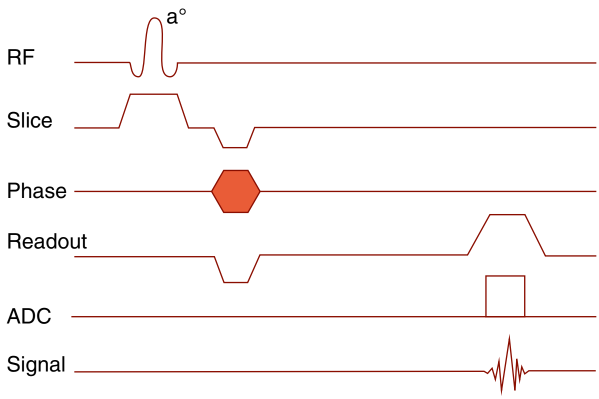


**Fig. 6.5** Gradient echo pulse sequence timing diagram

Since there is no time needed for an echo refocusing pulse, TE can be shorter, and therefore, gradient echo sequences are better suited for shorter T1 times in low-field imaging.

A big drawback of gradient echo is the strong influence of gradient field inhomogeneities, particularly in T2 images. These are compensated, if the spins "go back the same way they came" after a refocusing RF pulse. Therefore, T2-weighted images in gradient echo sequences are addressed to as T2* images.

Further inhomogeneities occur through susceptibility effects, causing areas of rapid dephasing, black ribbons, on bone–fat or bone–air borders (paranasal sinus). To reduce this additional T2* effect, short T1 times are preferred, again supporting the advantages of low-field scanners.

Susceptibility effects are used to detect small iron deposits in areas of micro-hemorrhage (sequence names: GE, SWAN; Siemens, HEMO).

### 6.2.4 Rapid Gradient Echo Imaging

One way to increase the scan speed of gradient echo sequences is to reduce the proton flip angle. The excitation pulse is selected <90°. Therefore, only a part of the protons is flipped. Since TR is short, the residual z-magnetization increases the signal for the next excitation pulse. Haase and coworkers invented this technique in 1986 and called it FLASH (fast low-angle shot) (Haase et al. 1986). The optimal "flip angle," yielding maximum signal, is called the Ernst–Winkel.

$$\text{Ernst} - \text{Winkel} = \cos^{-1}\left[\exp\left(-\text{TR}/\text{T1}\right)\right]$$

Therefore, with shortened T1 times in low-field imaging, larger flip angles are possible (Fig. 6.6).

In the late 1970s, Peter Mansfield had a brilliant idea (Mansfield and Maudsley 1977). A single excitation pulse, followed by a series of strong gradients, resulting in a series of gradient echoes (echo train) (Fig. 6.7).

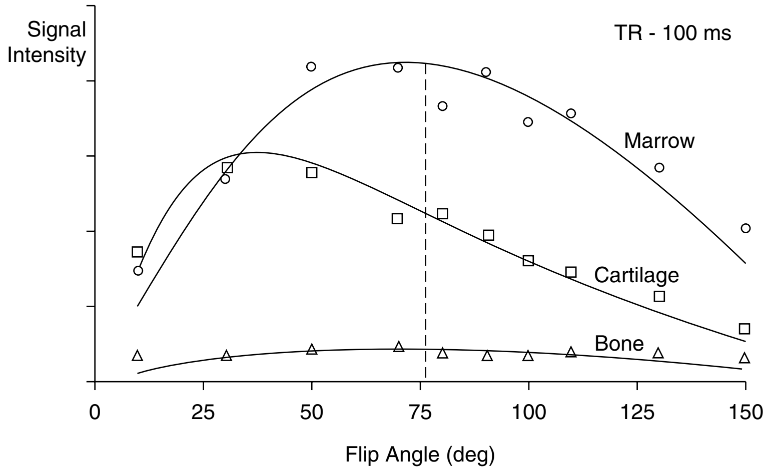


**Fig 6.6** In gradient echo sequences, the flip angle (α) is important for T1-weighted images. GE sequences generally use small flip angles (<90°) and very short TRs (typically 150 ms). The optimal flip angle depends on the T1 value of the tissue being imaged. A short T1 results in a larger optimal flip angle. *Dotted line*: best contrast-to-noise ratio for a TR of 100 ms

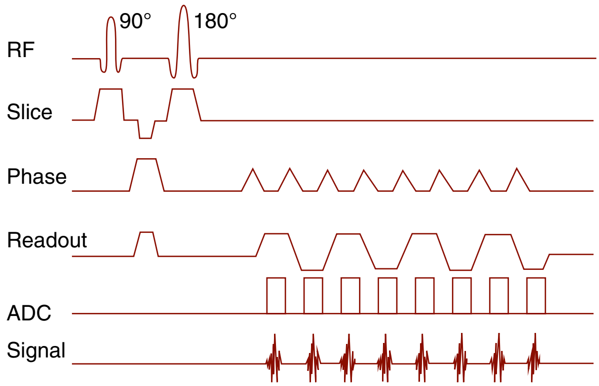


**Fig. 6.7** Echo planar imaging pulse sequence timing diagram

This extremely fast imaging is strongly influenced by susceptibility effects. Today, it is mainly used for diffusion-weighted imaging (Fig. 6.7).

EPI imaging takes advantage from higher field strength and gradient performance. Therefore, on low-field scanners, it is possible, but less frequently used. There are concerns about safety of EPI imaging: The rapid gradients can cause eddy currents, potentially leading to neuromuscular stimulation.

If multiple gradient echoes are acquired (fast gradient echo), a further increase of speed is possible. The problem is incomplete recovery of magnetization. Different approaches are realized:

- Refocusing the magnetization with an RF pulse (FISP, FFE).
- Spoiling the residual magnetization with a spoiler gradient at the end of the read out (FLASH, GFE).

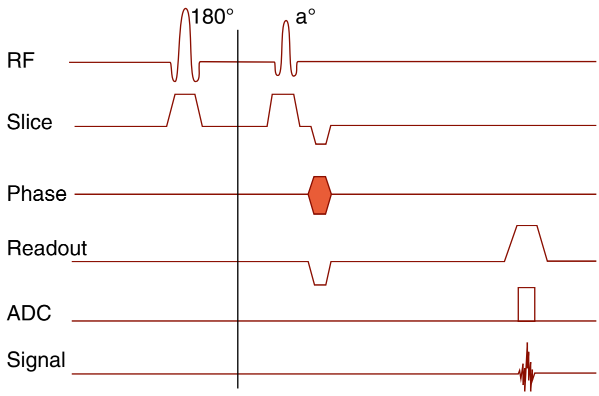


**Fig. 6.8** Ultrafast gradient echo pulse sequence timing diagram

- Balanced scanning: The sequence contains two RF excitation pulses. Before the second pulse, the gradients are balanced, so their net value is zero; all spins are excited by the second RF pulse (True-FISP, FIESTA).

Ultrafast gradient echo uses extremely short TE (2 ms) and TR (3–5 ms); the flip angle is about 5°, giving poor tissue signal. Acquisition time is <1 s.

A 180° inversion pulse starts the sequence, giving the option to use the zero passing and selectively suppress fat or water or silicone (breast imaging).

The readout module may use a single shot (excitation) with variable flip angle or multiple segments (multi-shot). If multiple lines are acquired after a single pulse, the pulse sequence is a type of gradient echo planar imaging (EPI) pulse sequence (Fig. 6.8).

### 6.2.5 3D Imaging

The first MRI examinations in the late 1970s and early 1980s were three-dimensional sequences. The larger the excited volume, the smaller the noise component. Therefore, 3D imaging has a much better SNR than 2D imaging. A 3D sequence is produced by applying an RF excitation pulse without slice selection gradient to a regular 2D sequence, exciting the whole imaging volume.

The disadvantage is the long examination time, which made gradient echo sequences the typical 3D technique.

In 2007, Erik Schweitzer made a far seeing statement during David Stoller's course on musculoskeletal MRI. He said that in maybe 10 years, an MRI could be performed with only one 3D turbo spin echo sequence. It didn't take 10 years, but it was a close guess.

A regular fast (turbo) spin echo sequence with an echo train (turbo factor) of 20 and 256×256 matrix and 128 slices (the interlacing slice is interpolated to get an isometric volume) takes at a TR of 2.5 s 68 min. Using parallel imaging, this can be shortened to 34 min. Still too long for clinical routine.

The newest 3D TSE sequences (Dr. Schweitzer was right) are called SHAPE in the Siemens world, VISTA on Philips, and CUBE on GE machines. They have an echo train length of >100. With such a long ETL, there is usually only very few signal left for the late echoes. This signal has to be increased.

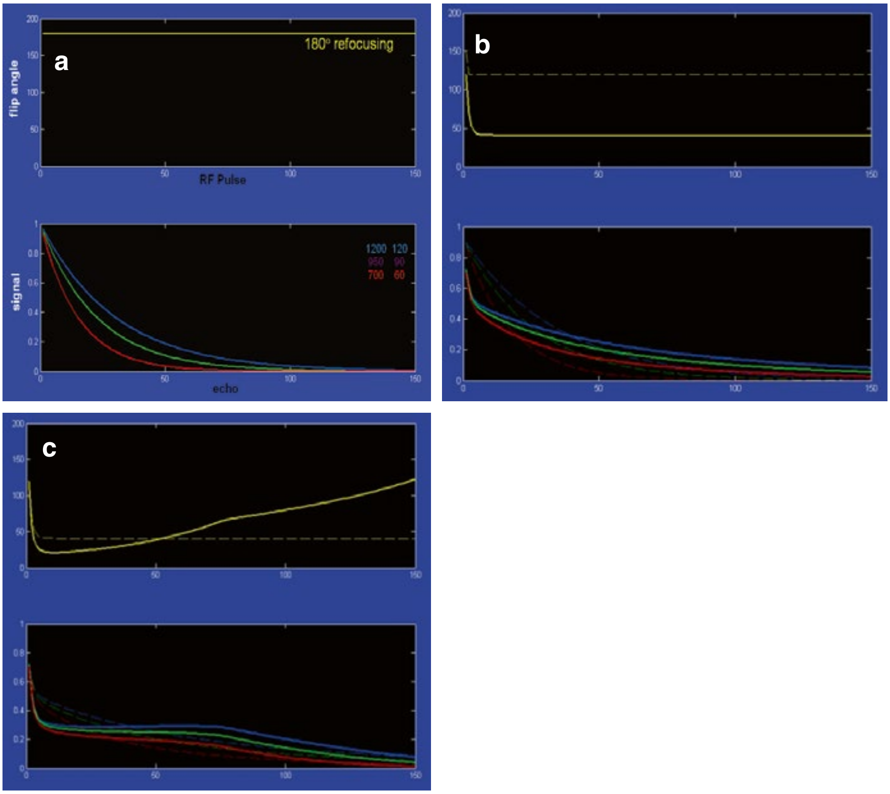


**Fig. 6.9** (**a**) Refocussing with a 180° pulse results in weak late echoes. (**b**) Reduced angle preserves more signal. (**c**) Modulated angle can result in even stronger late signal

A possible trick is a refocussing pulse with variable reduced flip angle. Flip angles below 180° lead to reduced early echo intensities but conserve more signal for the late echoes. The original name was FSE-XETA (fast spin echo with extended echo train acquisition) (Fig. 6.9).

Another trick is a three-dimensional reconstruction kernel for parallel imaging using self-calibration and a three-dimensional interpolation of missing data. The algorithm is called ARC (Autocalibrating Reconstruction for Cartesian imaging) (Fig. 6.10).

The resulting 3D TSE sequence is able to scan a T2-weighted sequence with a TR of 2.5 s, an ETL of 100, and a 256×256×256 volume in 4:30 min. The RF power is low, with metal artifacts reduced. SNR and tissue contrast are spin echo like.

These sequences can be performed on low-field scanners with a to some extent longer scan time (due to less SNR).

### 6.2.6 Fat Saturation

Fat is bright in T1, T2, and proton-density imaging. Contrast enhancement results in signal increase in pathologic (inflammatoric, neoplastic, hyperperfused) areas.

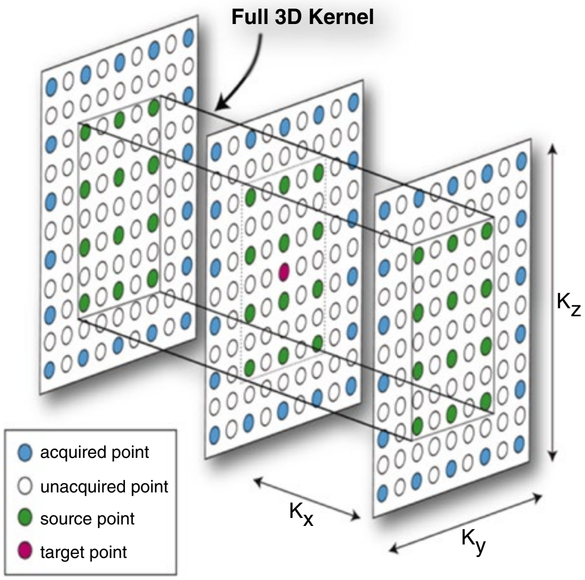


**Fig. 6.10** ARC. A three-dimensional data space is partially filled with measured data. The missing data are computed by 3D interpolation, reducing the needed scan information

Edema is bright in T2-weighted sequences. To increase detectability of these pathological findings, the suppression of bright fat signal is mandatory.

Different concepts and techniques exist for fat suppression. Since field strength has an important effect on fat suppression effects, they have to be briefly addressed.

There are two principles for fat suppression: relaxation dependent (STIR) and chemical shift dependent (Dixon, spectral saturation, water excitation, and SPAIR) (Horger and Kiefer 2011).

#### 6.2.6.1 Dixon Technique

In 1984 W.T. Dixon proposed a novel technique for fat saturation in MRI (Dixon 1984).

This technique makes use of different resonance frequencies (chemical shift) of fat and water-bound protons. Basically, two images are acquired: an image where the fat and water protons are "in-phase" and an image where fat and water protons are "opposed-phase." Four contrasts can be provided: fat image, water image, "in-phase" image, and "opposed-phase" image.

Since a long TR is required to obtain these scan data, the scan time is relatively long, which can be partially compensated by parallel imaging (Wohlgemuth et al. 2002).

The Dixon technique is well suited for low-field systems and can represent an alternative to spectral fat saturation techniques in high-field settings.

#### 6.2.6.2 Spectral Fat Saturation

For the chemical shift between fat and water protons, the difference in resonance frequency is 3.4 ppm. Spectral fat saturation uses this frequency difference by emitting a narrow band pulse at the fat frequency, switching fat protons off the *z*-axis direction (and deleting the resulting transverse magnetization by spoiler gradients).

Since the frequency offset is proportional to field strength, it is markedly reduced in low-field MRI (66 Hz at 0.4 T, see above).

Two modes of fat saturation intensity can be selected (strong/weak), defining how much signal the fat-bound protons contribute to the image.

Spectral fat saturation does not affect tissue contrast and is therefore frequently used. It is depending on homogeneity of the $B_0$ and $B_1$ field. The additional preparation pulses increase scan time.

Therefore, to achieve sufficient image quality in spectral saturated sequences on a low-field MRI is challenging.

#### 6.2.6.3 Water Excitation

Fat suppression by spectral saturation costs signal. An alternative is to selectively excite the water-bound protons.

This means, no additional pulses are needed, but the minimum TE is longer. The sequence is less dependent from $B_1$-field inhomogenieties, which is more important for 3 T scanners.

#### 6.2.6.4 STIR

The acronym means "short TI inversion recovery". Fat has a shorter T1 relaxation time than other body tissues. Before the scan sequence, a 180° inversion pulse is applied, which flips all spins in the $-z$-direction. This is followed by T1 relaxation. After a time $TI_{fat}$, the fat protons are in transverse orientation. If the 90° excitation pulse is emitted at this time, the fat protons cannot contribute to the resonance signal. This process is called "zero passing."

STIR images have an inverted T1 contrast (not T2 contrast).

In principle, the fat zero passing is reached when

$$\mathrm{TI} = \mathrm{T1}_{\mathrm{fat}} \times \ln 2 = (260\,\mathrm{ms}) \times 0.693 = 180\,\mathrm{ms}\ \text{at}\ 1.5\,\mathrm{T}$$

In practice, the optimal value will also depend on other sequence parameter settings (e.g., TR); the typical TI at 1.5 T is chosen to be 150 ms. TI will also depend on field strength since $T1_{fat}$ increases with field strength. If the TI value is selected <150 ms, more fat signal is received, reducing fat suppression, but improving image signal to noise.

The major advantage of STIR imaging is the complete insensitivity to $B_0$ inhomogeneities. Furthermore, it doesn't depend on chemical shift. This predestines this technique for fat suppression in areas with signal and field inhomogeneity, like shoulder or foot.

One major disadvantage is that it cannot be used after intravenous contrast injection. Gd shortens the T1 time of all tissues, which can then have the same "zero-passing" time as fat. The other disadvantage is the reduced SNR compared with spectral saturated spin echo sequences (see above).

#### 6.2.6.5 SPAIR

The acronym stands for "spectral adiabatic inversion recovery." Different from STIR, only the fat protons are inverted by a 180° pulse. With gradient spoiling, the

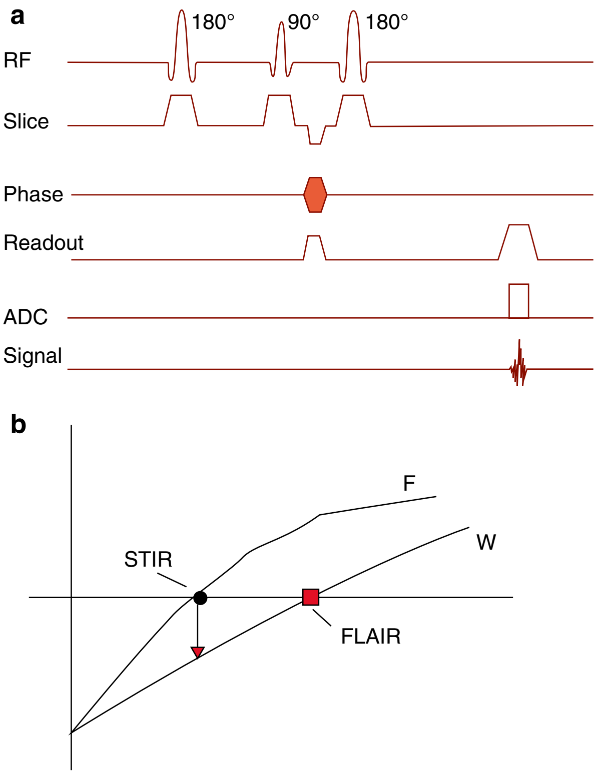


**Fig. 6.11** (**a**) STIR pulse sequence timing diagram. A 180° preparation pulse skips the spins in $-z$-direction. (**b**) At a time TI of 150 ms (1.5 T) fat protons and at a time TI of 2200 ms (1.5 T), free water protons are in the transverse plane and do not contribute to signal. This allows a reliable suppression of fat or water

transverse magnetization is deleted. The inversion time TI is selected at the time, when the contribution of fat-bound protons to the signal is nulled.

Since this sequence uses a frequency selective inversion, it is not well suited for low-field scanners (Horger and Kiefer 2011).

For musculoskeletal imaging, spectral fat saturation in proton-density images is optimal for evaluation of cartilage lesions. For MR arthrography, regular T1-SE sequences with spectral fat saturation are used. For the latter application, a contrast-enhanced MR angiography sequence or a DIXON fat saturation technique is a possible alternative (ultrafast short TE 3D gradient echo).

What works best and most reliable for fat suppression is STIR imaging. Since STIR is strongly T1-dependent, high-resolution images are provided, sensitive for bone marrow edema and even for cartilage surface evaluation (Fig. 6.11).

### 6.2.7 Diffusion Imaging

Diffusion imaging uses the movement of water molecules as contrast-giving principle. Different sequence types are used.

Basically, it is a T2-weighted spin echo, gradient echo, or EPI sequence, using a 180° – rephasing pulse surrounded by a bipolar gradient pair of equal strength.

This means that movements between this gradient pair are not completely rephased, which leads to a signal loss. The signal loss is proportional to the spin movement, which in turn depends on the presence of diffusion barriers, like cell membranes. In case of disease (tumor, ischemia), the cell membranes can be damaged, which leads to increased diffusion.

Sensitivity of measurement concerning diffusion is based on strength and duration of the gradient pair, as well as the time interval between the gradient activation. These conditions are summarized in a "sensitivity coefficient" *b*, given by

$$b = \gamma^2 \times G^2 \times \delta^2 \times \left(\Delta - \delta / 3\right)$$

with $\gamma$ = gyromagnetic constant of hydrogen, $G$ = strength of diffusion gradient, $\delta$ = duration of the gradient, and $\Delta$ = time interval between the gradient. The higher the value, the higher the signal loss by diffusion of water molecules.

Diffusion imaging is mainly used in brain imaging. Recently, new concepts for whole-body diffusion imaging have been proposed, opening new diagnostic, particularly for tumor diagnosis (e.g., prostate gland).

Diffusion imaging is working with very low-signal amplitudes and therefore takes profit from improved SNR. However, acceptable results for low-field cerebral diffusion MR imaging have been reported (Mehdizade et al. 2003).

We have proposed a combination of a diffusion-weighted HASTE sequence for diffusion contrast with a T1-weighted fast gradient echo sequence for anatomical detail (Domalski and Klein 2006). The sequence worked well for diagnosing tissue viability in metastatic liver disease (see Chap. 7).

### 6.2.8 Angiographic Techniques

Basically, there are four concepts for vascular imaging in MRI (Bosmans et al. 2001):

- Time of flight
- Phase contrast
- Contrast-enhanced (CE) angiography
- Black blood angiography

#### 6.2.8.1 Time of Flight (Inflow Angiography)

TOF MR angiography is a bright blood technique, meaning that flowing blood gives a bright signal. It consists of a gradient echo sequence with short TR and minimum TE. The surrounding stationary tissue is saturated (Anzalone et al. 2005; Keller and Saloner 1993; Muhs et al. 2005).

Flowing blood is not influenced by the saturation and provides a maximum longitudinal magnetization, leading to a high signal, and a bright presentation of the vessel.

The resulting data points undergo three-dimensional image processing with multiplanar reconstruction (MPR), volume rendering (VRT), and maximum intensity projection (MIP).

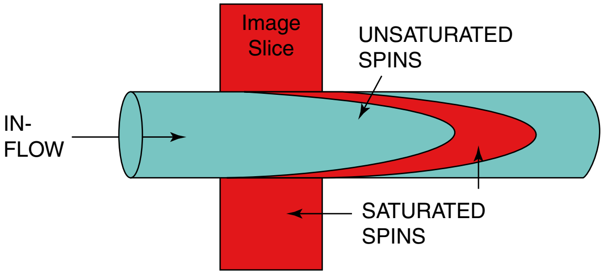


**Fig. 6.12** Time-of-flight MR angiography. The more voxel volume is filled with inflowing blood, the brighter the signal

A problem is turbulent flow, which destroys the signal of flowing blood. Therefore, the vascular images are optimal, when the plane of signal acquisition is perpendicular to the direction of the blood flow.

A combination with contrast agents is possible and advocated by several authors.

There is no limitation for time-of-flight MR angiography in low-field scanners (Fig. 6.12).

#### 6.2.8.2 Phase-Contrast MR Angiography

This method is based on the fact that spins flowing between a bipolar gradient experience a phase shift, compared with stationary spins (Dumoulin et al. 1993; Isoda et al. 1998).

Since the bipolar gradient pair has opposite direction, the net value of phase change is zero in the stationary tissue.

The strength of the gradient pair depends on the expected flow velocity. If the spins in the flowing blood move so fast that the phase change is more than 180°, the computer can misinterpret the phase value and hence give incorrect flow values. By correct selection of the velocity encoding parameter (VENC), these artifacts can be avoided.

The VENC determines strength of the gradient and the relation between flow velocity and phase change. Given these informations, a flow velocity measurement is possible, useful for defining the hemodynamic effect of a stenosis. The selection of the VENC is based on a correct a priori knowledge on what velocity is expected (how fast is flowing arterial or venous blood in that area). This is a frequent cause of errors.

#### 6.2.8.3 Contrast-Enhanced MR Angiography (CE-MRA)

This concept uses a spoiled gradient echo sequence with short TR and very short TE. Stationary tissue is separated, while the flowing blood, containing contrast media with a T1-shortening effect, gives a very bright signal (Jager et al. 2000; Herold et al. 2004; Leiner et al. 2003; Nederkoorn et al. 2003; Remonda et al. 2002).

Additionally, subtraction of contrast-enhanced and non-contrast-enhanced image can lead to further improvement of the image by suppression of the background noise.

Most important is the adequate timing between contrast inflow and start of the scan sequence.

Decisive for this sequence is gradient performance. The stronger the gradients, the shorter is the minimum possible TE.

CE-MR angiography can be performed with low-field scanners with image quality comparable to high-field system (Klein et al. 2008).

#### 6.2.8.4 Black Blood MR Angiography

If a usual spin echo sequence is performed, inflowing or outflowing blood does not contribute to signal. This is called "flow void." An additional suppression of flowing blood can be achieved by using a double-inversion recovery pulse. This concept is only adequate for large vessels and yields good information about the vessel wall and surrounding tissues.

## 6.3 Spatial Resolution

In all computerized diagnostic imaging procedures, the images are composed from picture elements, so-called pixels, representing physical properties of discrete body volume elements, so-called voxels.

The volume elements can be deliberately small. The size of the volume elements depends on the spatial resolution of the imaging system.

In a cross-sectional imaging modality like CT or MRI, the sections of the object are divided, for example, in $256 \times 256 \times 1$ voxel, and transferred into pixels, which are displayed on two-dimensional screen.

### 6.3.1 Matrix

These $256 \times 256$ pixels are called the image matrix. The matrix is characterized by the number of pixels in $x$- and $y$-direction. The number of pixels multiplied by the side length gives the size of the measurement field, the "field of view" (FOV).

The smaller the field of view at a given matrix size, the higher the spatial resolution.

If the side length of the voxel is equal in all directions, the resolution is called isotropic. If the in-plane voxel size is smaller than the voxel thickness (or slice thickness), the resolution is called anisotropic.

The smaller the voxel size, and therewith the resolution, the finer details of body tissue can be imaged.

If different tissues are acquired in one voxel, the voxel signal is partially influenced by both. This so-called "partial volume" effect is reduced by using smaller voxels (larger matrix).

Matrix resolution is a decisive parameter for image quality.

The coarser the matrix resolution, larger is the voxel size. The larger the voxel, the higher the signal in the voxel is, improving the signal-to-noise ratio.

Doubling the matrix size from hundred 128 to 256 pixels decreases signal-to-noise ratio by the factor of four.

Therefore, the SNR directly influences the spatial resolution.

For a long time, depending not only on SNR but also on the available computing speed, low-field MR systems used a low spatial resolution and low matrix size.

Modern low-field MR systems regularly use a standard matrix size of 512 × 512 to 2048 × 2048 and provide excellent image resolution (see Chap. 7).

### 6.3.2 Interpolation

Increasing the slope of the frequency encoding gradient causes higher RF deposition (SAR). Increasing the phase encoding gradient increases scan time (and RF deposition too). If a 1024 × 768 matrix is used, one way to optimize resolution and scan time is to use a rectangular field of view, the shorter axis representing the phase encoding gradient.

A further acceleration is possible by measuring only half the phase encoding steps and generating the interlacing image lines by interpolation. Several procedures are implemented, mostly using linear or complex interpolation concepts. Despite the image information is a little artificial, "guessed," and reduced compared with a full resolution scan, the image impression is improved.

An example of a complex three-dimensional autocalibrating interpolation for fast 3D TSE sequences is mentioned above (Fig. 6.9).

## 6.4 Contrast

Contrast is defined as the relative difference of signal intensity between adjacent object areas on an intensity scale.

Digital imaging in nuclear medicine X-ray, CT, and MRI enables direct quantitative access to the contrast expression.

The signal intensity on the grayscale can be given in a numeric value. The numeric difference between two intensities allows the quantitative definition of contrast (Rinck 2009).

The higher the difference of intensity between two pixels (Ia and Ib), the larger the contrast $C$ is.

$$C = \left(\mathrm{Ia} - \mathrm{Ib}\right) / \left(\mathrm{Ia} + \mathrm{Ib}\right)$$

$C$ = contrast and Ia and Ib = signal intensities of two adjacent pixel or voxel.

### 6.4.1 Contrast to Noise

It is important to understand that the signal intensity in MRI is not standardized. There is no signal intensity parameter for MRI like the Hounsfield units (HU) in CT.

Signal intensity in MRI can be influenced by T1, T2, proton density, flow, diffusion, perfusion, and other complex factors.

**Fig. 6.13** Patient with a contrast standard (bottle of iodine X-ray contrast agent) in a contrast comparison study

As we said at the university clinic of the RWTH Aachen: "CT is a measurement, MRI is an experiment" (Bohndorf 1990).

Therefore, comparison between signal intensities from different MR systems is of no clinical significance. Only image correction, based on reference data purchased by a contrast standard, for example, a bottle of contrast agent outside the body in the scan volume, can enable to compute relative signal intensities (Fig. 6.13).

We already learned that the relation between signal and noise (SNR) is an important parameter of image quality.

SNR increases with field strength. With increasing field strength, the gradient strength has to be increased. Doubling gradient strength, as explained above, doubles bandwidth, leading to an increase of noise by $\sqrt{2}$.

Therefore, the effect of doubling the field strength does increase signal to noise by $\sqrt{2}$. Body heating and other potentially dangerous effects of RF energy are increased at the same time by a factor of 4. To increase the field strength from 0.3 to 3 T theoretically increases SNR by $\sqrt{10}$ (factor 3.16), but increases SAR by $10^2$!

Another descriptor for image quality can be derived from the contrast expression.

If the image contrast between two adjacent tissues is divided by the image noise, we get the contrast-to-noise level (CNR).

Since tissue T1 contrast is higher at lower field strength (see Sect. 5.3), this can partially compensate for the lower signal intensity, at least in T1 imaging.

### 6.4.2 Number of Excitations

Another way to reduce the influence of noise is to increase the number of acquisitions NA (number of excitations, NEX). This is analogous to the procedure of multiplexing acoustic signals for noise reduction in audio components.

Doubling the number of excitations doubles the scan time and increases S/N by $\sqrt{2}$. At the same time, it increases the RF exposure (SAR) linearly (factor of 2). Therefore, theoretically the SNR of a 3 T scanner could be reached on a 0.35 T machine by increasing the NEX to 8, resulting in an 8 times longer scan time, but at less than 10 % of the SAR for the patient.

### 6.4.3 Postprocessing

There is a variety of ways to improve image presentation.

The most simple ones are windowing and center adjustment.

The more isotropic the voxels become, the more impressive 3D reformatting is. The abovementioned 3D TSE sequences enable true three-dimensional image analysis. The surgeon can interactively reproduce the optimal image plane, imaging the structure of his interest, for example, the politeo-fibular ligament before reconstruction of the posterolateral complex in knee surgery.

This may open a totally new access to image production and viewing in the next years.

Noise can be reduced by postprocessing with complex filter algorithms, improving tissue homogeneity or better edge delineation. The application of filter algorithms requires that we are always critically aware of the manipulation.

## 6.5 Temporal Resolution

If we talk about temporal resolution, we have to consider the "k-space." We have already mentioned this in Sect. 6.2.2 in connection with multi-echo sequences.

The k-space can be described as a "space" (data matrix), where the raw data are stored.

Every excitation pulse can create a new line in k-space. The length of the line depends on the amplitude of the frequency encoding gradient and the number of lines on the amplitude of the phase encoding gradient (phase encoding steps).

The time $T$ for a scan sequence is therefore given by

$$T = N_{Gy} \times \mathrm{TR} \times \mathrm{NEX}$$

where $N_{Gy}$ is the number of phase encoding steps, TR the repetition time, and NEX the number of excitations.

Now the raw data matrix undergoes the first Fourier transformation in x-direction, producing a new matrix, in which every line contains data on one frequency (and different phases).

Then follows the second Fourier transformation in y-direction, creating a new matrix in which every point contains signal information on one voxel (a “modulus” or magnitude image).

Manipulation of the k-space can result in changes of:

- Speed
- Spatial resolution (interpolation)
- Field of view (rectangular FOV)
- Contrast (see Sect. 6.2.2)
- Artifacts

### 6.5.1 Partial Scan

The easiest way to reduce scan time by k-room manipulation is simply leaving away some of the measurements. This is acceptable since most of the data is concentrated in the center of the k-space.

Leaving away data of the peripheral parts and filling the matrix with zero in these areas reduces resolution, scan time, and noise (since the exterior k-room area contains noise too). This concept is applied up to 30 % reduction of k-space data.

Another concept uses the fact, that there is a certain symmetry in the k-room data. The magnetization of two points lying symmetrical to the zero point of k-space behave complex conjugated with each other (Vlaardingerbroek and den Boer 2002).

If only half of the profile is measured, the missing half can be estimated by mirroring the measured data around the origin of k-space (half-scan, half-Fourier). This procedure leads to a loss of SNR, but preserves spatial resolution (Chandra et al. 1996).

The so-called “keyhole” technique is used for dynamic contrast-enhanced studies, for example, in dynamic liver or brain imaging.

At first, a complete scan is carried out, followed by subsequent scans acquiring only the central k-space data (contrast information). The higher k-space data (contour information) are taken from the original scan. This enables to perform very fast scans detecting contrast changes in the tissue (perfusion imaging).

### 6.5.2 Parallel Imaging

If a set of simultaneously working coils is used, the k-space can be filled with signal from several parallel sources. Due to a number of reasons (field inhomogeneity, dielectric effects), the spatial encoding of different matrix coil elements can be incorrect. To control and compensate this effect, the scan data have to contain reference lines to adjust the spatial localization of the image voxel.

As mentioned in Chap. 2, parallel imaging with multi-element coils can markedly increase scan speed, as well as spatial resolution.

The classical saddle or birdcage coils are well suited for construction of coil arrays.

However, the geometry of vertical fields in low-field scanners can also facilitate this technique, but is not fully developed today. There is only one system in the market with a multichannel coil array for clinical routine (see Fig. 2.9).

## 6.6 Contrast Agents

One major advantage of MRI is its high intrinsic tissue contrast. The aim in using a contrast agent is to further improve tissue contrast and provide additional information on tissue characterization concerning inflammatory or neoplastic diseases, perfusion, and cellular function.

### 6.6.1 Positive Contrast Agents

The magnetic field induced by an electron is far stronger than that of a proton. Since the electrons mostly occur in pairs, the electron particle fields compensate each other and only a weak netto magnetic field results.

The more unpaired electrons a molecule possesses, the stronger is its effect on local magnetic field (paramagnetic effect).

Gadolinium (Gd) has seven unpaired electrons and therefore a strong local paramagnetic effect. The relaxation rate (the relaxivity) of adjacent tissue molecules is increased, T1 time is shortened, and signal intensity in T1-weighted scans is increased.

Other MR contrast agents like mangane (Mn) or iron (Fe) have less free electrons and therefore a weaker T1 effect. They are mainly used for liver imaging. Limanond investigated Gd-containing and ferumoxide contrast agents in low- and high-field MRI of the liver. He found that lesion detection is facilitated by iron oxide agents, while lesion characterization is improved by Gd contrast agents (Limanond et al. 2004).

### 6.6.2 Negative Contrast Agents

Substances, which shorten T2 or T2* time, reduce T2 signal intensity. Typical substances are iron (Fe) or magnetite ($Fe_3O_4$), which possess a ferromagnetic influence (Reimer et al. 1998).

With reduced molecular size, they become so-called superparamagnetic particles, showing additional T1 effects.

Magnetite, coated with an inert polymer, is taken up by the Kupffer cells of the liver parenchyma and can lead to better detection of small metastatic lesions.

### 6.6.3 Gadolinium

The contrast effect of Gd is based mainly on its local susceptibility effect (influencing relaxivity). Since susceptibility effects are reduced at lower field strength, the resulting T1-contrast effect of Gd is smaller. To achieve a comparable contrast effect, the dosage of Gd has to be increased (see Sect. 5.4).

Desai concludes in his review paper that for MR systems with a field strength below 0.5 T, a dosage of 0.2 mmol/kg body weight is comparable to a dosage of 0.1 mmol/kg in high-field systems (Desai and Runge 2003).

In recent years, the application of Gd-containing contrast agents has been connected with the presentation of a rare and severe disease, the nephrogenic systemic fibrosis (NSF). It is recommended to use as few contrast agent as possible and prefer the more stable substances.

We regularly used gadobutrol (Gadovist$^R$, Bayer, Germany), which has twice the relaxivity of Gd-DTPA, at a dosage of 0.1 mmol/kg body weight.

### 6.6.4 Ventilation Imaging

Magnetic resonance imaging is definitely not the method of first choice for diagnosis of pulmonary diseases.

However, with the use of lower field strength, lung parenchyma becomes visible.

Furthermore, there have been attempts at lung imaging with xenon ($^{129}Xe$), helium-3, hydrogen ($^{1}H$), or fluoride ($^{19}F$) (Triphan et al. 2015). Gadolinium-containing aerosols, as well as hyperpolarized gases or oxygen, have been proposed as possible ventilation contrast agents (Rinck et al. 1984). These partially complicated and expensive methods remain not completely investigated.

### 6.6.5 Enteral Contrast Agents

The best enteral contrast agent is water. It has low signal in T1 images, improving detection of contrast enhancement, and high signal in T2 imaging, delineating the bowel wall (Hohl et al. 2005). If administered with methyl cellulose over a naso-duodenal probe, an MR enteroclysis can be performed. If mannitol as osmotic agent and some flavor substance (to improve the taste) is added, the patient can drink the agent to improve bowel distension.

There have been attempts with oral magnetite particles, but susceptibility artifacts at 1.5 T were a problem. This could be a smaller problem at lower field strength. However, there are no reports in the literature on bowel MRI at low field strength.

## 6.7 Artifacts

The knowledge of artifacts and methods to avoid them are of great importance for clinical imaging. In the following, they should be only briefly discussed considering the effect of low field strength on imaging artifacts.

### 6.7.1 Distortion of the Magnetic Field

Distortion of the main magnetic field can be caused by multiple factors outside the magnet, mainly by big stationary or moving iron-containing objects like cars or escalators.

These field inhomogeneities have to be avoided during the construction process by installation of a sufficient shielding and by shimming of the magnet (Fig. 6.14).

#### 6.7.1.1 Inhomogeneity

Internal effects on the magnetic field cannot be avoided. Residual parts of bullets or shrapnel can cause in inhomogeneity artifacts and be potentially dangerous to the patient.

Implanted ferromagnetic objects like joint prosthesis or bioelectronic devices can also cause local ferromagnetic artifacts or be influenced by the magnetic field itself.

Metal-containing clothing, piercing, tattoos, or makeup can also disturb image quality (Figs. 6.15 and 6.16).

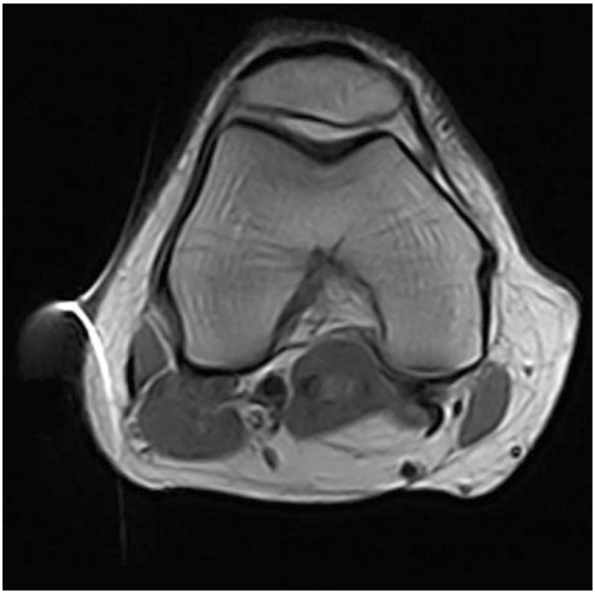

**Fig. 6.14** Object outside the FOV in the scan area of the coil. This artifact can be avoided by positioning adjacent objects at least 6 cm apart from the scanned FOV

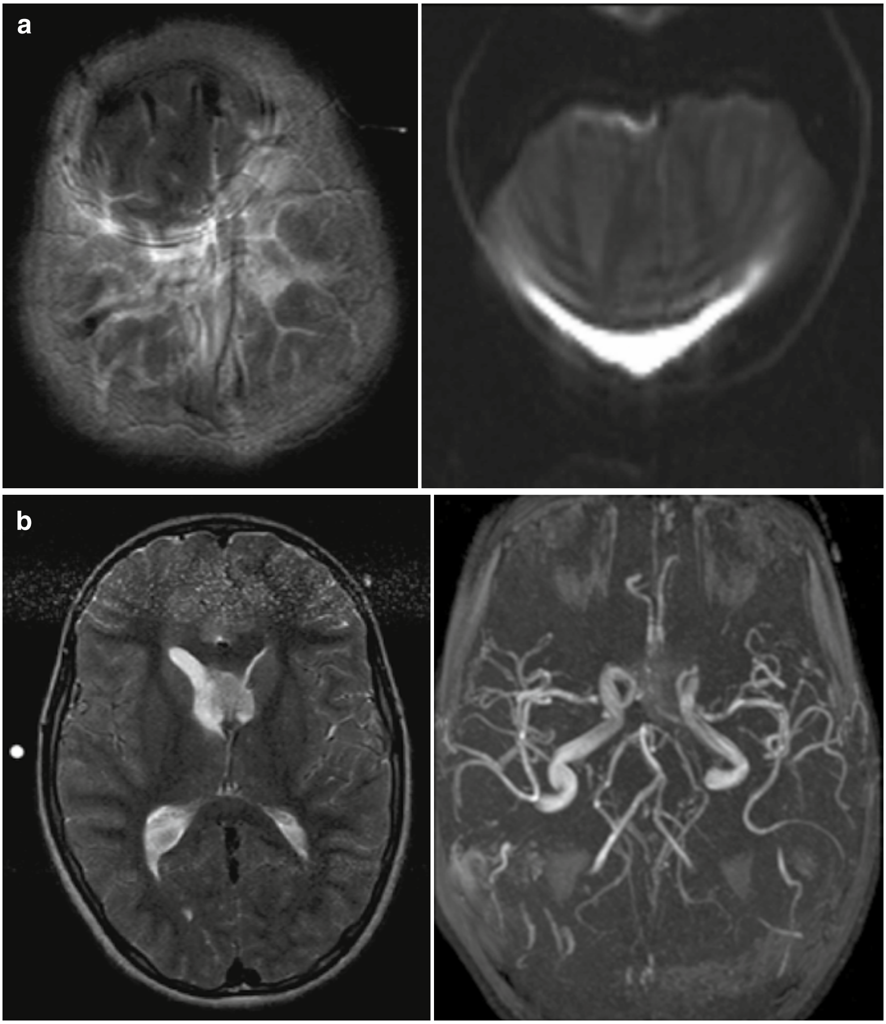


**Fig. 6.15** A 13-year-old boy with aneurysm clip in the A1 portion of the anterior cerebral artery. After insufficient scanning at 1.5 T, a low-field scan was performed. (**a**) 1.5 T (Magnetom Symphony, Siemens/Germany). T2-weighted image, TOF-MRA. (**b**) 0.35 T (Magnetom C!, Siemens/Germany), identical protocol

#### 6.7.1.2 Susceptibility

Susceptibility artifacts can be caused by remnants of hemorrhage. They can be used for detection of small hemorrhagic areas (microbleedings) with special gradient echo sequences (HEMO, SWAN, see Sect. 6.2.3). Also tissue–air interfaces, like in the paranasal sinuses or in abdominal structures, can result in susceptibility artifacts.

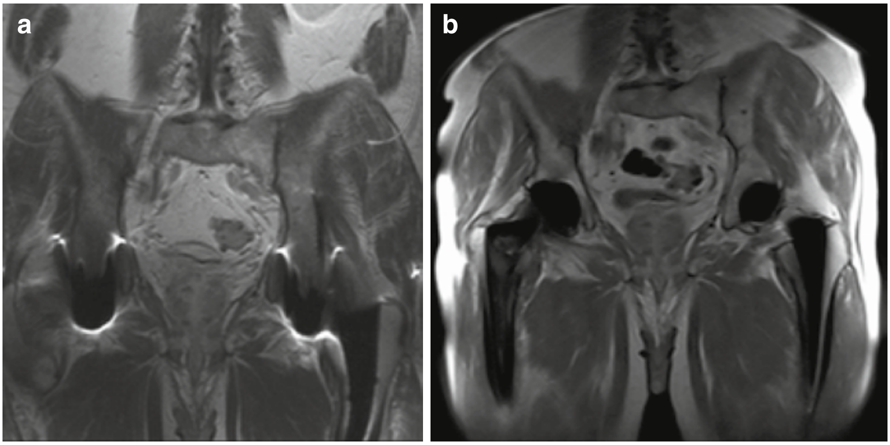


**Fig. 6.16** A 70-year-old man with bilateral hip prosthesis. (**a**) 1.5 T (Magnetom Symphony, Siemens/Germany). T1-weighted image. (**b**) 0.35 T (Magnetom C!, Siemens/Germany), identical protocol

If these artifacts occur in contrast-enhanced sequences, they can be reduced by scanning the full k-space. Partial scanning should be avoided.

## 6.7.2 RF and Gradients

### 6.7.2.1 Slice Profile Artifacts

If two slices are positioned immediately adjacent to each other, the RF pulses of one slice can influence the spins of the adjacent section. This is called the interslice crosstalk, and it changes image contrast.

By increasing the interslice distance, this effect can be reduced.

If the repetition time TR is too short, recovery of longitudinal magnetization is incomplete. This is of particular importance, if short TR values are combined with a high flip angle (Spoiled FLASH). In these cases, the desired contrast cannot be produced. The solution can be the use of a 3-D sequence.

### 6.7.2.2 Line Artifacts

High-intensity line artifacts, relatively frequent, can occur in the image center in phase encoding direction. They look like a zipper and are mostly caused by radiofrequency leaks from the transmitter to the receiver. It may be difficult to find the source of these artifacts (Fig. 6.17).

If line artifacts occur outside the magnet center in phase encoding direction, they can be caused by external radiofrequency sources like radio or cell phone transmitters (Fig. 6.17).

A broad, band-like line artifact outside the center can be caused by magnetic field inhomogeneities (Fig. 6.18).

**Fig. 6.17** Line artifact by external RF sources

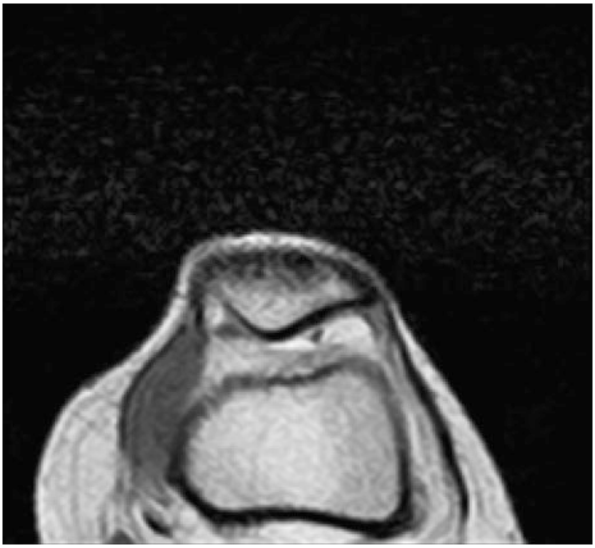

**Fig. 6.18** Line artifact caused by magnetic field inhomogeneities

### 6.7.3 Motion

Patient movement is a frequent source of image artifacts. Particularly during long examinations, convenient positioning of the patient is of decisive importance. Claustrophobic patients tend to demonstrate frequent motion artifacts, examination

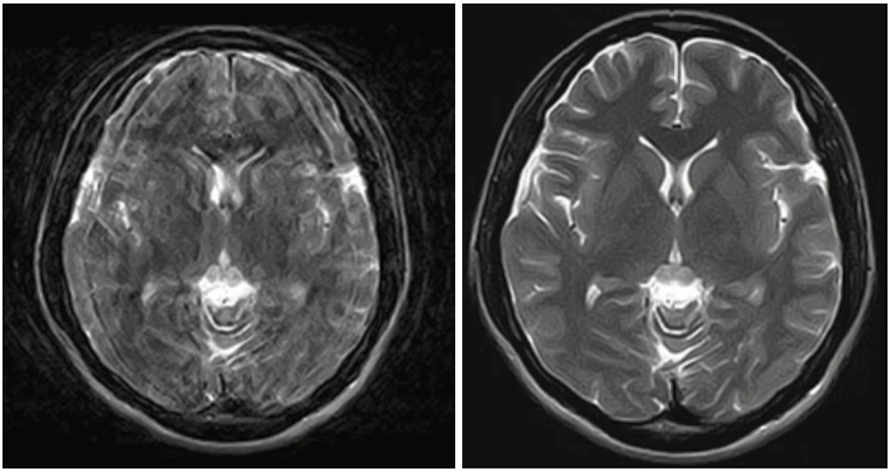

**Fig. 6.19** Modern systems possess motion-reducing scan sequences. *Left side*: motion artifact. *Right side*: motion compensation software

quality can be improved by convenient positioning. Sometimes, application of sedatives is necessary.

Motion artifacts can also be reduced by motion-tolerant imaging sequences (Siemens: BLADE, GE: PROPELLER, etc.) (Fig. 6.19).

#### 6.7.3.1 Heart and Lungs

Periodic movement of hearts, great vessels, and lung represents a difficult obstacle, particularly for cardiac imaging.

However, suppression of these artifacts is routinely possible by biomonitoring of heart activity (ECG) and respiratory activity.

Respiratory activity can be detected with so-called navigator echoes, measuring the movement of the diaphragm. Another technique uses respiratory belts to register thorax movement. Motion artifacts are more severe in phase encoding direction; therefore, makes sense to position the phase encoding gradient perpendicular to possibly expected motion, if possible.

Irregular movements between RF excitation and data acquisition are more difficult to compensate for. Suppression techniques (MAST) have been developed, using an additional phase encoding, enabling to correct the motion-induced phase shift (Pattany et al. 1987).

#### 6.7.3.2 Flow

Flow artifacts are similar to the movement of the heart or other body parts. Blood and cerebrospinal fluid pulsate. Since flow artifacts are expected in the area of great vessels, they can be avoided by spoiler pulses, saturating the spins in regions, which are not relevant for diagnostics, like the prevertebral space in spine imaging.

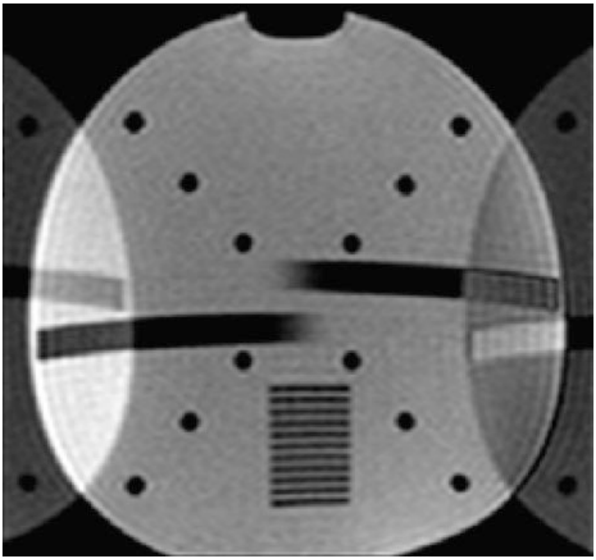

**Fig. 6.20** Phantom study. The object is larger than the scan field of view, resulting in infolding artifact ("ghosting")

### 6.7.4 Signal Processing

#### 6.7.4.1 Chemical Shift

The resonance frequency of protons in fat or water differs by about 3.4 ppm (see above). Since the spatial location of spins is encoded by frequency, the frequency shift leads to a shift in location.

Principally, these artifacts can be reduced by using stronger gradients, which, on the other hand, increases noise.

In high-field systems, these artifacts have to be suppressed by fat suppression techniques. With lower field strength, chemical shift artifacts become less important.

#### 6.7.4.2 Aliasing

If the examined body parts is larger than the field of view, signal from body parts outside the imaging volume is acquired, which leads to an infolding artifact ("ghosting," Fig. 6.20).

This problem can be solved by enlarging the field of view, which leads to an increase of scan time. On the other hand, signal-to-noise is improved. To reduce scan time, the data sampling rate (bandwidth) can be increased up to the critical frequency (Nyquist frequency) (Fig. 6.20).

#### 6.7.4.3 Truncation

The truncation artifact, also referred to as Gibbs artifact, shows parallel lines close to the interfaces of tissues with strongly different signal intensity. An example could be the interface of fat/muscle or spinal cord/cerebrospinal fluid.

They can mimic anatomic structures (like the central canal in the spinal cord) and therefore potentially lead to misdiagnosis.

The artifacts occur, if the image matrix is too coarse (the bandwidth is too high). It vanishes if a finer matrix is used.

Truncation artifacts are mostly seen in phase encoding direction, since due to reason of scan time, the phase encoding resolution is limited. This aspect should be considered in low-field imaging.

#### 6.7.4.4 Quadrature Artifact

The magnetic resonance signal is acquired with a multichannel receiver. The reference signal of each channel is phase shifted at a specific value to the reference signal of the first channel.

Each misadjustment of this phase shift causes a ghost image, which is rotated to the main image around the x- and y-axis.

- Positioning of the patient is essential for comfort and convenience, particularly in low-field imaging (slightly longer scan times)
- Shorter T1 time at lower field strength provides higher signal at short TE and a better T1 contrast
- Modern low-field scanners have improved gradient performance with shorter minimum TE, important for better T1 contrast
- With shortened T1-times in low-field imaging, larger optimal flip angles (Ernst–Winkel) are possible, resulting in better signal
- For fat suppression in low-field systems, the STIR and Dixon technique are suited. SPAIR and spectral saturation are limited due to the smaller chemical shift between fat and water
- At lower-field-strength MRI, the T1-contrast effect of contrast agents is smaller
- Susceptibility and chemical shift artifacts are reduced at lower field strength
- All angiographic techniques are possible on low-field systems with good quality

## References

Anzalone N, Scomazzoni F, Castellano R, Strada L, Righi C, Politi LS, Kirchin MA, Chiesa R, Scotti G (2005) Carotid artery stenosis: intraindividual correlations of 3D time-of-flight MR angiography, contrast-enhanced MR angiography, conventional DSA, and rotational angiography for detection and grading. Radiology 236(1):204–213

Bohinski RJ, Warnick RE, Gaskill-Shipley MF et al (2001) Intraoperative magnetic resonance imaging to determine the extent of resection of pituitary macroadenomas during transsphenoidal microsurgery. Neurosurgery 49:1133–1143

Bohndorf K (1990) Personal communication

Bosmans H, Wilms S, Dymarkowski A, Marchal G (2001) Basic principles of MRA. Eur J Radiol 38:2–9

Chandra S, Liang ZP, Webb A, Lee H, Morris HD, Lauterbur PC (1996) Application of reduced encoding imaging with generalized-series reconstruction (RIGR) in dynamic MR imaging. J Magn Res Imaging 6:783–797

Desai NK, Runge VM (2003) Contrast use at low field – a review. Top Magn Reson Imaging 14:360–364

Dixon WT (1984) Simple proton spectroscopic imaging. Radiology 153:189–194.

Domalski S, Klein M (2006) MR-diffusion imaging in liver and other body areas using HASTE and RARE technique. German patent application 2006; DE 2006E21415

Dumoulin CL, Souza SP, Pelc N (1993) Phase sensitive flow imaging. In: Potchen EJ, Haacke EM, Siebert JA, Gottschal A (eds) Magnetic resonance angiography, concepts and applications. Mosby, St. Louis, pp 173–186

Haase A, Frahm J, Matthaei KD (1986) FLASH imaging: rapid NMR using low flip angles. J Magn Reson 67:258–266

Hayashi N, Watanabe Y, Masumoto T, Mori H, Aoki S, Ohtomo K, Okitsu O, Takahashi T (2004) Utilization of low-field MR scanners. Magn Reson Med Sci 3(1):27–38

Herold T, Paetzel C, Volk M, Bachthaler M, Zorger N, Feuerbach S, Strotzer M, Lenhart M (2004) Contrast-enhanced magnetic resonance angiography of the carotid arteries: influence of injection rates and volumes on arterial-venous transit time. Invest Radiol 39:65–72

Heuck A, Bonèl H, Huber A, Müller-Lisse GU, Sittek H, Reiser M (1997) Patient acceptance of high-field whole body MR systems, open MR systems and dedicated MR systems fort he extremities. Der Radiologe 37(10):778–784. Springer

Hohl C, Haage P, Krombach GA, Schmidt T, Ahaus M, Günther RW, Staatz G (2005) Diagnostic evaluation of chronic inflammatory intestinal diseases in children and adolescents: MRI with true-FISP as new gold standard? Rofo 177:856–863

Horger W, Kiefer B (2011) Fat suppression techniques – a short overview. Magnetom FLASH 11:56–59

Isoda H, Takehara Y, Isogai H, Takeda H, Kaneko M, Nozaki A, Sun Y, Foo TK (1998) Techniques for phase contrast-enhanced three-dimensional MR angiography of the carotid and vertebral arteries. AJNR Am J Neuroradiol 19:1241–1244

Jager HR, Moore EA, Bynevelt M, Kitchen N, Taylor W (2000) Contrast-enhanced MR angiography in patients with carotid artery stenosis: comparison of two different techniques with an unenhanced 2D time-of-flight sequence. Neuroradiology 42:240–248

Kaufman L, Arakawa M, Hale J, Rothschild P, Carlson J, Hake K, Kramer D, Lu W, Van Heteren J (1989) Accessible magnetic resonance imaging. Magn Reson Q 5(4):283–297

Keller PJ, Saloner D (1993) Time-of-flight flow imaging. In: Potchen EJ, Haacke EM, Siebert JE, Gottschalk A (eds) Magnetic resonance angiography, concepts and applications. Mosby, St. Louis, pp 146–159

Klein HM, Buchal R, Achenbach U, Domalski S (2008) CE-MRA of carotid and vertebral artery: open 0.35T vs. 1.5 T MRI. Clin Neuroradiology 18(2):107–112

Leiner T, De Vries M, Hoogeveen R, Vasbinder GB, Lemaire E, Van Engelshoven JM (2003) Contrast-enhanced peripheral MR angiography at 3.0 Tesla; initial experience with a whole-body scanner in healthy volunteers. J Magn Reson Imaging 17:609–614

Limanond P, Raman SS, Sayre J et al (2004) Comparison of dynamic Gadolinium-enhanced and ferumoxides-enhanced MRI of the liver on high-low field scanners. J Magn Reson Imaging 20:640–647

Mansfield P, Maudsley AA (1977) Medical imaging by NMR. Br J Radiol 50(591):188–194

Mehdizade A, Somon T, Wetzel S et al (2003) Diffusion weighted MR imaging on a low-field open magnet. Comparison with findings at 1.5T in 18 patients with cerebral ischemia. J Neuroradiol 30(1):25–30

Muhs BE, Gagne P, Wagener J, Baker J, Ortega MR, Adelman MA, Cayne NS, Rockman CB, Maldonado T (2005) Gadolinium-enhanced versus time-of-flight magnetic resonance angiography: what us the benefit of contrast enhancement in evaluating carotid stenosis? Ann Vasc Surg 19(6):823–828

Nederkoorn P, van der Elgersma O, Graaf Y, Eikelboom B, Kapelle J, Mali W (2003) Carotid artery stenosis: accuracy of contrast-enhanced MR angiography for diagnosis. Radiology 228: 677–682

Pattany PM, Phillips JL, Chiu LC et al (1987) Motion artifacts suppression technique (MAST) for MR imaging. J Comput Assist Tomogr 11:369–377

Reimer P, Müller M, Marx C et al (1998) T1 effects of a bolus-injectable superparamagnetic iron oxide, SH U 555 A: dependence on field strength and plasma concentration – preliminary clinical experience with dynamic T1-weighted MR imaging. Radiology 209:831–836

Remonda L, Senn P, Barth A, Arnold M, Lövblad KO, Schroth G (2002) Contrast-enhanced 3D MR angiography of the carotid artery: comparison with conventional digital subtraction angiography. AJNR Am J Neuroradiol 23:213–219

Rinck P (2009) Magnetic resonance in medicine. Blackwell scientific publications, Oxford. ISBN 0-632-03789-4

Rinck PA, Petersen SB, Lauterbur PC (1984) NMR von fluorhaltigen Substanzen. 19-Fluor Ventilations- und Perfusionsdarstellungen. Röfo 140:239–243

Rothschild PA, Domesek JM, Eastham ME, Kaufman L (1992) MR imaging of excessively obese patients: the use of an open permanent magnet. Magn Reson Imaging 9:151–154

Triphan SM, Breuer FA, Gensler D, Kauczor HU, Jakob PM (2015) Oxygen enhanced lung MRI by simultaneous measurement of T1 and T2* during free breathing using ultrashort TE. J Magn Reson Imaging 41:1708–1714. doi:10.1002/jmri.24692

Vlaardingerbroek MT, den Boer JA (2002) Magnetresonanz-Bildgebung: Theorie und Praxis. Springer, Berlin

Wohlgemuth WA, Roemer FW, Bohndorf K (2002) Short tauinversion recovery and three-point Dixon water–fat separation sequences in acute traumatic bone fractures at open 0.35 tesla MRI. Skeletal Radiol 31:343–348

# 7 Clinical Application

The hypothesis of this book is, to put in a nutshell, that low-field MRI systems, with a field strength of less than 0.4 T and with a permanent magnet, are full-scale whole-body imaging machines (Marti-Bonmati and Kormano 1997).

We have spent some effort on theory, and we have found some good reasons why we even may prefer low-field scanners in some imaging settings. But, as we say in Germany, an image says more than thousand words: let us now have a look on the results.

The images demonstrated in his chapter are produced on MRI systems of different manufacturers: Esaote, GE, Hitachi, and Siemens.

Esaote images are provided by Dr. Frieder Mauch, Stuttgart, and Esaote Biomedical Imaging Deutschland GmbH.

GE images have been sent by Dr. med. Willy Loretan and his colleague Dr. med. Michael Kolbe from "Medizinische Radiologie/Radiodiagnostik" in Brig/CH. They impressed me 14 years ago with their imaging on a 0.2 T GE Signa Profile.

Hitachi images have been scanned at the institute of Dr. Brigitte Redeker-Standke from "Jade–Weser Imaging," Varel, Germany, who sent me excellent imaging examples of their 0.4 T Hitachi Aperto.

Fonar Inc., Melville/U.S.A. provided images of weight-bearing functional MRI. My images are retrieved from the Siemens reference site at Ev.-Jung-Stilling Hospital, Siegen/Germany, with a 0.35 T Siemens Magnetom C!

All images are retrieved from clinical routine imaging and represent standard, reproducible quality (Table 7.1).



H.-M. Klein, *Clinical Low Field Strength Magnetic Resonance Imaging: A Practical Guide to Accessible MRI*, DOI 10.1007/978-3-319-16516-5_7

**Table 7.1** Low-field MRI systems. The present market situation

| | Esaote G-scan | GE Signa Profile 0.2 | Hitachi Aperto Lucent 0.4 | Siemens Magnetom C! | FONAR Upright |
|---|---|---|---|---|---|
| Field strength T | 0.24 | 0.2 | 0.4 | 0.35 | 0.6 |
| Magnet type | Permanent | Permanent | Permanent | Permanent | Resistive |
| Gradient amplitude mT/m | 20 | 15 | 25 | 24 | 17 |
| Gradient slew rate T/m/s | 56 | 30 | 55 | 55 | 28 |
| Channels | 4 | 4 | 1 | 4 | 1 |
| Coil elements | 4 | 8 | 1 | 13 | Custom |

The main drawback in routine imaging is the prolonged scan time on low-field systems, which is increased by about 40 %, if a well-equipped low-field system is used. The pure scan time for four sequences was therefore between 10 and 20 min, compared to 7–15 min on a 1.5 T system. Since scan time is only about half of the regular room time of the patient and patient positioning is easier and faster in a low-field MRI, patient throughput is reduced about 20 % compared with a standard high-field scanner.

## 7.1 Cranial Imaging

Imaging of the neurocranium is one of the most frequent indications of MR imaging. To my experience, all imaging techniques can be provided by low-field scanners, except fMRI (BOLD imaging) and spectroscopy. BOLD sequences might be possible, but were not implemented on our system. These sequences, as well as cerebral MRI spectroscopy, take profit from higher field strength.

T1 imaging, including STIR technique, takes advantage of the shorter T1 time and better T1 contrast in low-field MRI. The results are throughout satisfactory (Figs. 7.1, 7.2 and 7.3).

T2-weighted and FLAIR imaging quality is comparable to high-field imaging, if imaging time is increased by about 40 % (Figs. 7.4, 7.5).

For high-resolution imaging of the posterior fossa, a balanced gradient echo sequence was added (TrueFISP, Siemens, Erlangen, Germany) (Fig. 7.6).

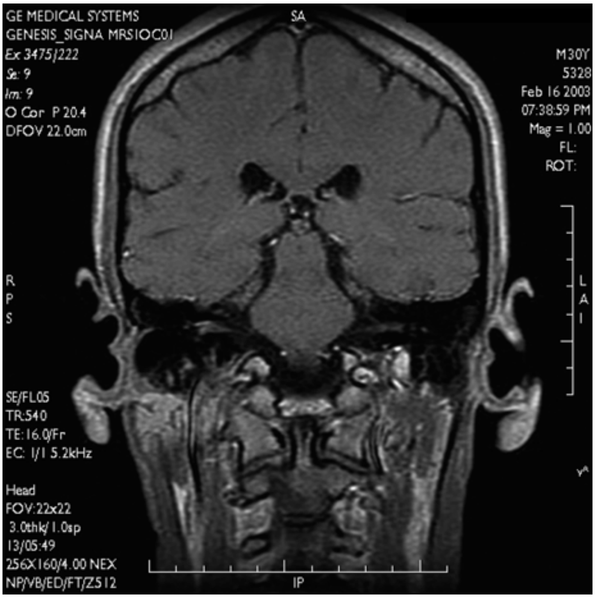


**Fig. 7.1** Coronal T1-weighted image. GE Signa Profile 0.2

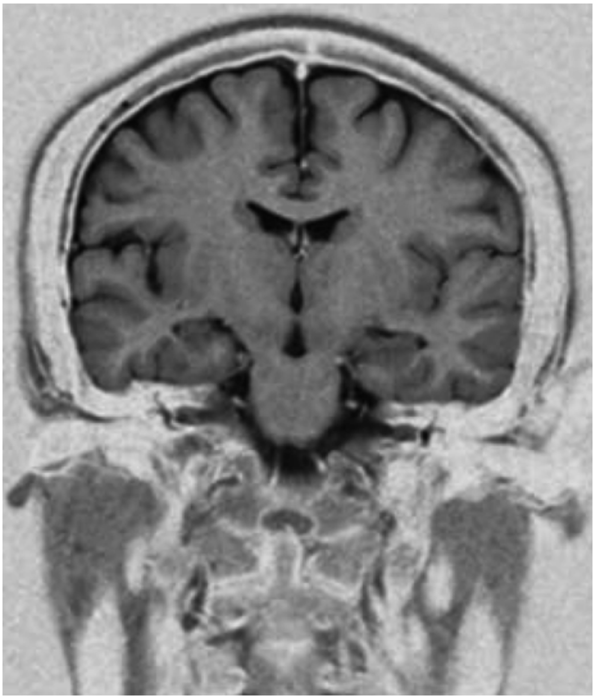

**Fig. 7.2** Coronal STIR Sequence with inverted contrast for better delineation of focal white matter lesions or cortical heterotopias. (Siemens Magnetom C!, 0.35T)

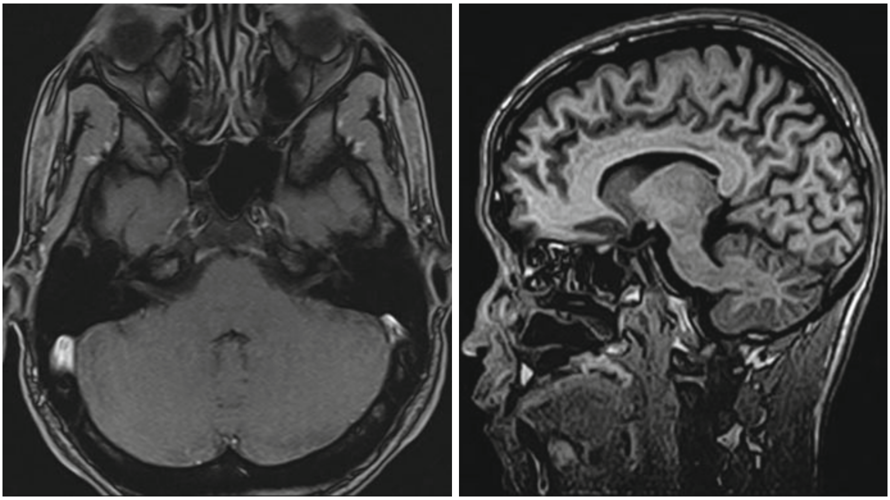

**Fig. 7.3** T1-weighted 3D gradient echo sequence. *Left*: transversal (Siemens Magnetom C!, 0.35 T), *Right*: sagittal orientation (Hitachi Aperto 0.4 T)

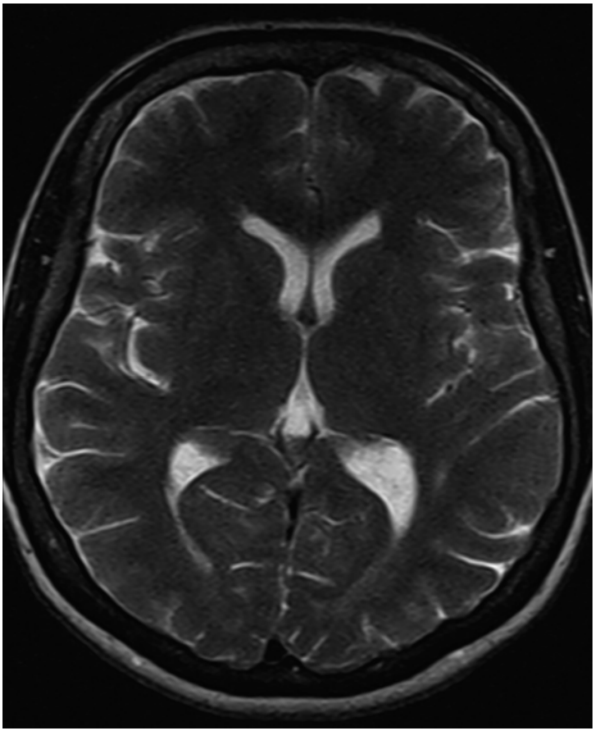

**Fig. 7.4** T2-weighted spin echo sequence. Siemens Magnetom C!

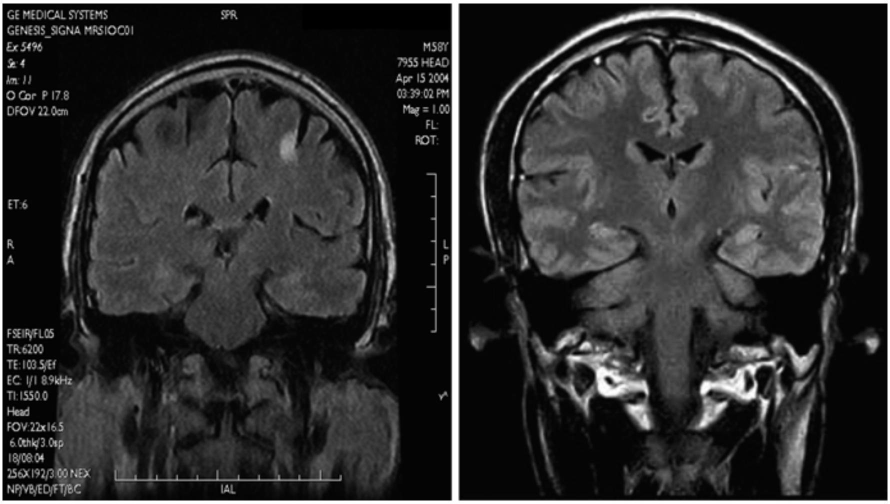


**Fig. 7.5** Coronal FLAIR sequence. *Left*: Postinflammatory scar (encephalomyelitis), GE Signa Profile 0.2. *Right*: Normal situation. Hitachi Aperto 0.4 T

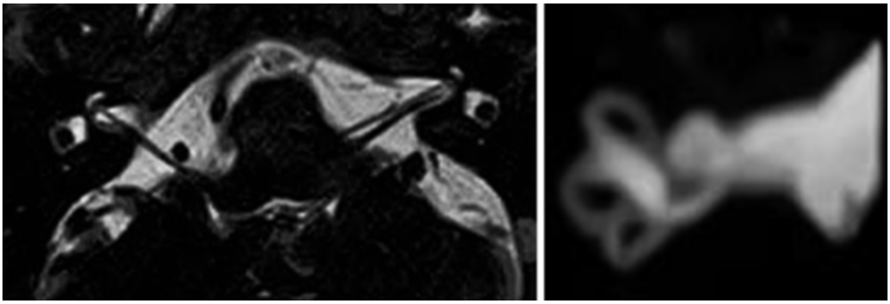

**Fig. 7.6** *Left*: High-resolution balanced 3D gradient echo sequence for imaging of the cerebello-pontine angle (TrueFISP. Siemens Magnetom C!). *Right*: 3D MIP reconstruction of the vestibulo-cochlear system from the 3D gradient echo sequence

Diffusion-weighted sequences were performed using a HASTE sequence, or EPI DWI (Fig. 7.7). Even perfusion imaging is possible (Fig. 7.8).

Cranial examinations are carried out using a solenoid (multichannel) head coil. This coil is regularly combined with another solenoid neck coil, providing coverage of the head, neck, and upper thoracic aperture.

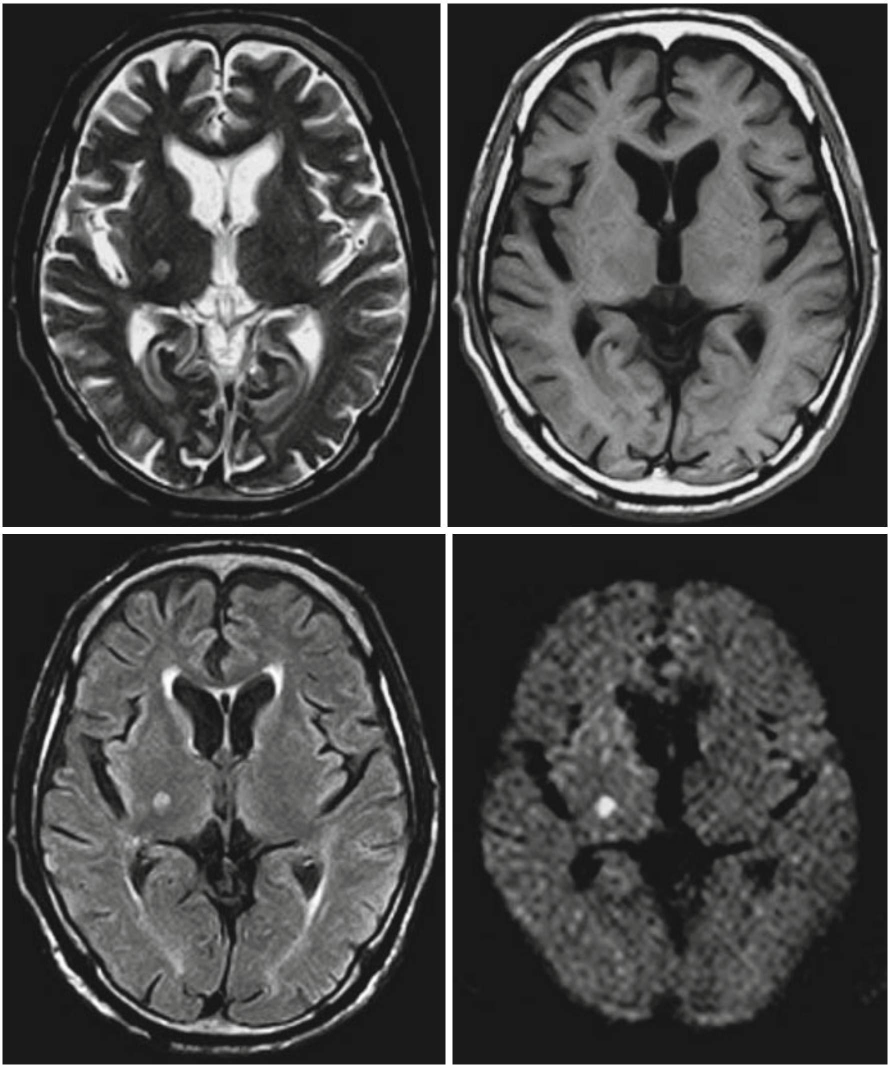

**Fig. 7.7** "One-stop shop" in MRI. T2- and T1-weighted spin echo. FLAIR and diffusion-weighted EPI sequence. Small area of acute ischemia in the right posterior capsule (Hitachi Aperto 0.4 T)

## 7.2 Neck Imaging

Imaging of the cervical neck includes the usual scan sequences, known from higher field strength: T1- and T2-weighted spin echo, STIR, T2*-weighted fast gradient echo, T1-weighted gradient echo sequences plain, and with i.v. contrast agent. On the Magnetom C!, we mostly applied the solenoid head coil combined with a solenoid neck coil, using all four system channels, to maximize signal strength (Figs. 7.9, 7.10, 7.11, and 7.12).

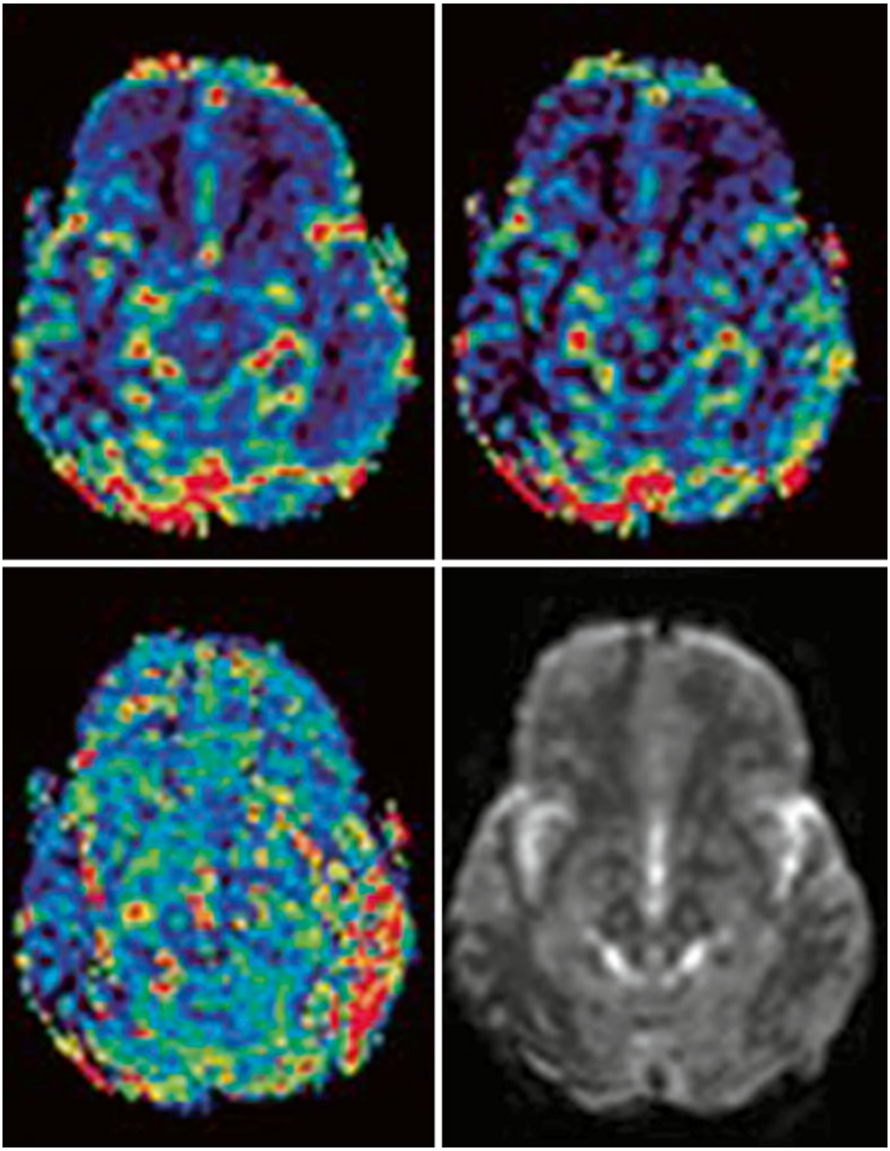

**Fig. 7.8** Cerebral perfusion imaging. Hitachi Aperto 0.4 T. Delayed mean transit time and time to peak in the right occipital cortex

## 7.3 Spine

Imaging of the vertebral spine is facilitated by multielement (saddle) coil arrays, as they are standard in closed-bore magnets with longitudinal field. In open magnets, the solenoid coils are wrapped around the body, resulting in a good coil sensitivity profile (Chap. 5), but reduced number of coil elements.

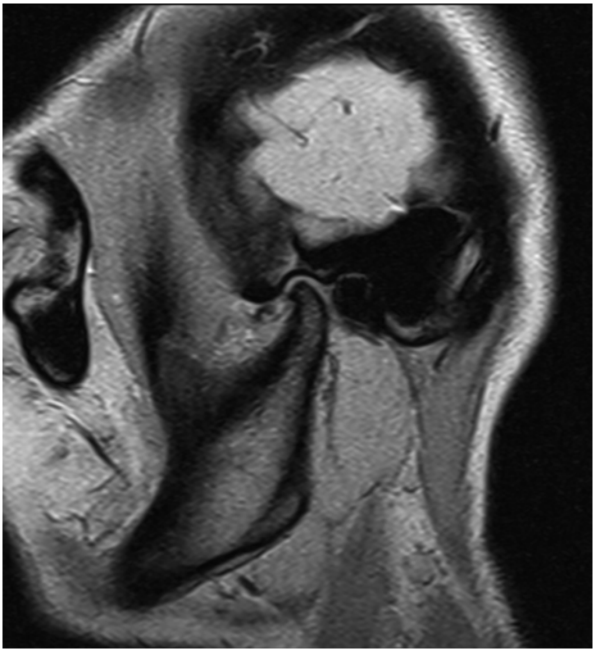

**Fig. 7.9** Imaging of the temporomandibular joint. T2*-weighted, solenoid head coil, 2D spoiled gradient echo sequence (FLASH, Siemens Magnetom C!, 0.35 T)

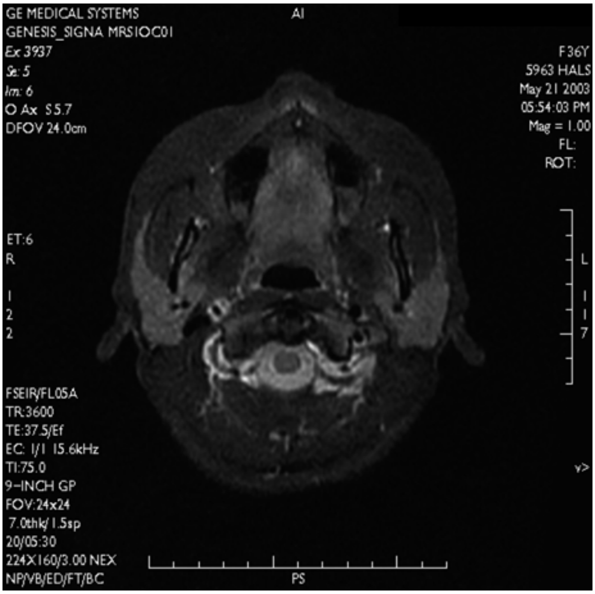


**Fig. 7.10** Transversal STIR sequence of the neck (GE Signa Profile 0.2 T)

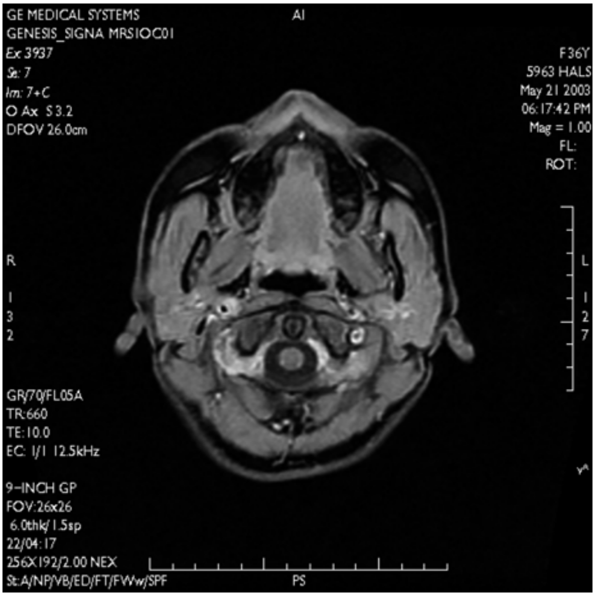


**Fig. 7.11** Transversal T1-weighted contrast-enhanced spoiled gradient echo sequence (SPGR, GE Signa Profile 0.2 T)

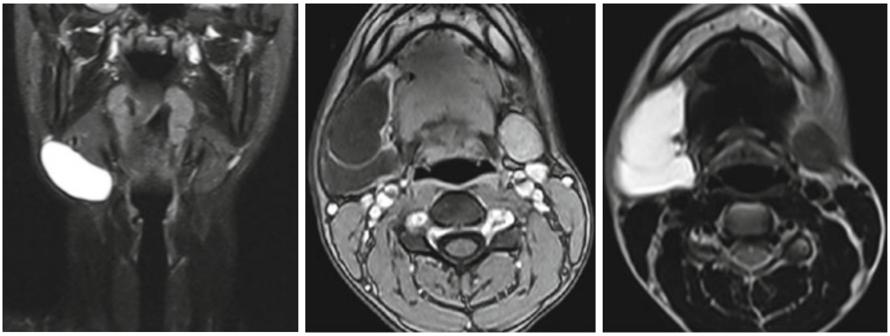

**Fig. 7.12** Lateral neck cyst. Magnetom C! 0,35 T. Coronal STIR sequence, transversal T1 gradient echo after i.v. contrast agent, and T2 spin echo sequence

The detection of small myelon lesions can represent a problem. Spatial resolution depends on gradient amplitude and slew rate (>50 T/m/s). The improved T1 contrast can only attribute to lesion detection in STIR sequences. Care has to be taken for optimized T2 images, at the cost of longer scan time (Fig. 7.13).

Lee and coworkers compared a 0.25 T with a 1.5 or 3 T scanner for diagnosis of lumbar degenerative disease. They found excellent correlation between low- and high-field systems for detection of disk herniation, central canal, lateral recess, and exit foraminal stenosis. Agreement for root compression was good (r 0.71–0.76). Low-field imaging produced more motion artifacts; the authors explained this by longer scan times (Lee et al. 2015).

**Fig. 7.13** Sagittal T2-weighted spin echo sequence. Siemens Magnetom C!

Assheuer and coworkers demonstrated that low-field MRI has no relevant quality deficits for diagnostics of the lumbar spine (Assheuer et al. 2014) (Figs. 7.14, 7.15, 7.16, 7.17, 7.18, 7.19 and 7.20).

## 7.4 Musculoskeletal Imaging

For musculoskeletal imaging, MRI has become a standard procedure of great importance.

The excellent intrinsic tissue contrast in MR imaging facilitates detection of ligamentous, fibrous and hyaline cartilage or bone marrow lesions, marrow edema, and joint effusion.

CT and MRI are complementary methods, particularly in musculoskeletal imaging. Tavernier and Cotten have discussed the impact of low field strength on musculoskeletal imaging. The literature is not equivocal. Some studies (Friedman et al. 1995) reported unsatisfactory results; others found acceptable or even advantageous results in low-field applications (Kersting-Sommerhoff et al. 1996; Cotten et al. 2000; Kreitner et al. 2003).

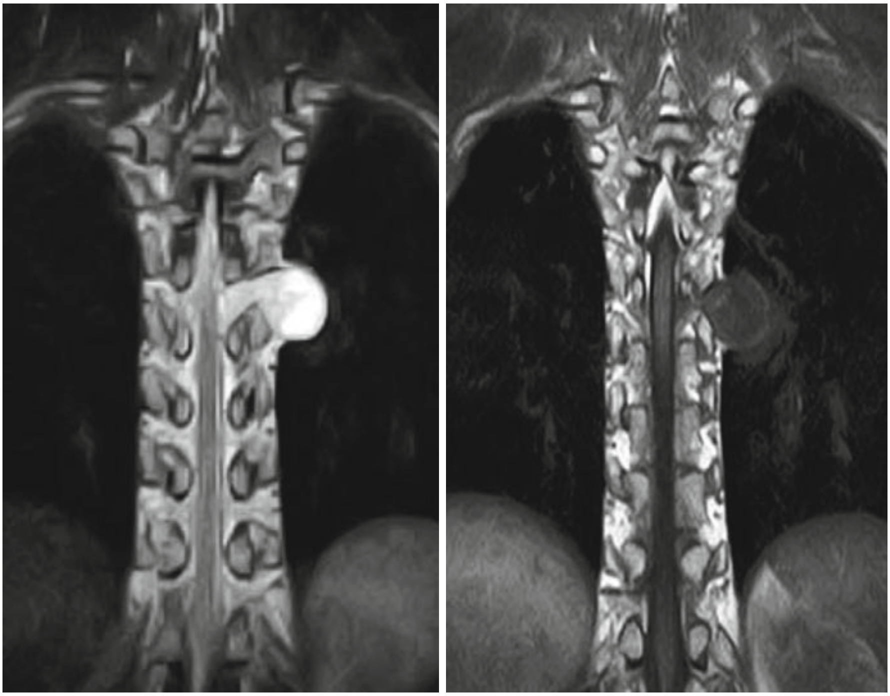

**Fig. 7.14** Thoracic neurofibroma. Coronal T2- and T1-weighted SE sequence (Hitachi Aperto 0.4 T)

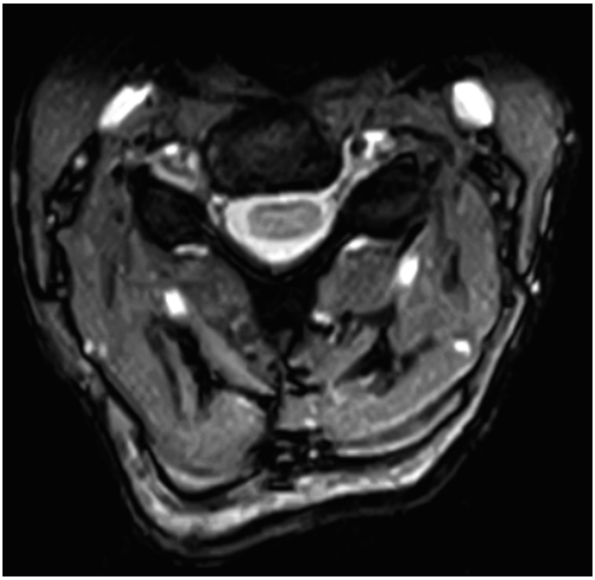

**Fig. 7.15** Transversal gradient echo sequence. Matrix 512×512 (Hitachi APERTO Lucent 0.4 T)

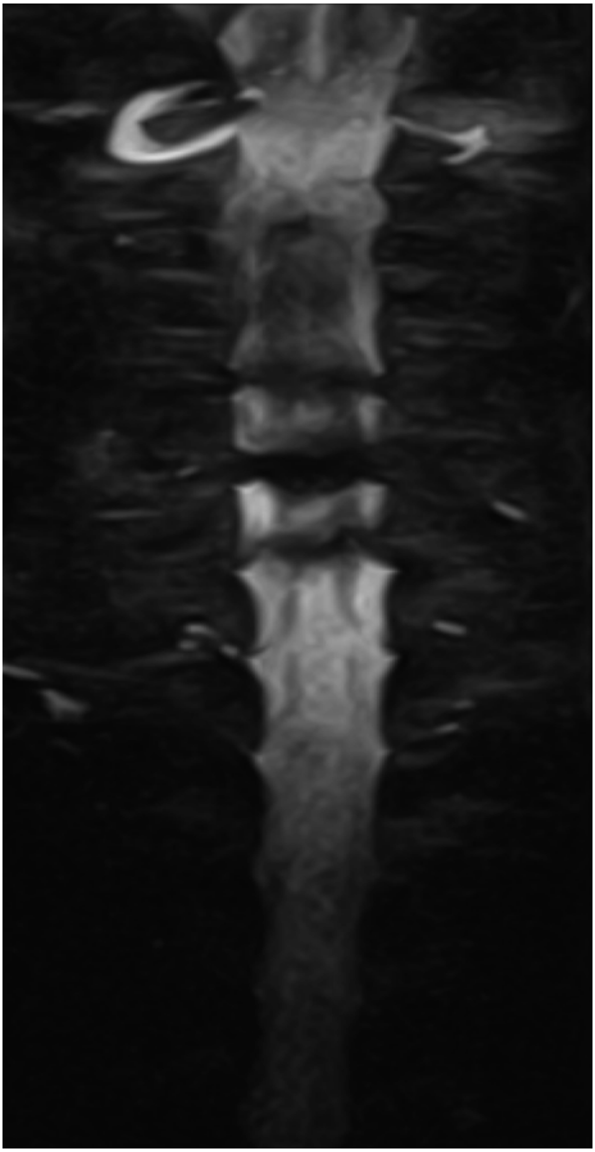

**Fig. 7.16** MR myelogram. Single-shot turbo spin echo sequence (Siemens Magnetom C!)

### 7.4.1 Trauma

The most sensitive method for detection of fracture is MRI. Particularly in critical areas, like scaphoid bone, low-field MRI can provide mandatory information for adequate clinical therapy (Raby 2001).

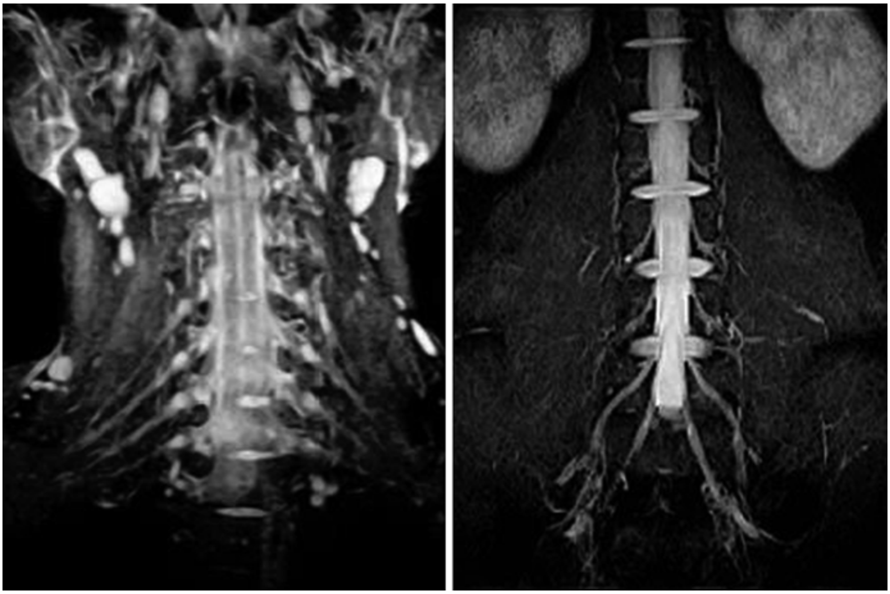

**Fig. 7.17** Plexus neurography. STIR sequence. *Left*: Cervical spine. *Right*: Lumbar spine (Hitachi APERTO Lucent 0.4 T)

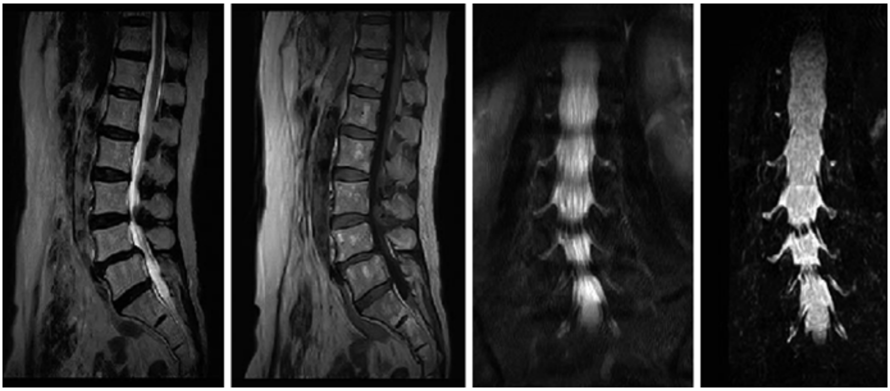

**Fig. 7.18** Spinal stenosis segment L3/4, segmental instability L4/5 (Hitachi APERTO Lucent 0.4 T). T2- and T1-weighted spin echo sequence. MR myelography

Herber and coauthors from the university of Mainz/Germany investigated low-field MRI for children with unclear chronic ankle pain and unconspicuous conventional X-ray imaging. They found ligamentous injuries in 64 % of their patients (Herber et al. 2000) (Figs. 7.21 and 7.22).

**Fig. 7.19** A case of spondylodiscitis. STIR and CE T1 images, one time performed on a 1.5 T system, the control examination 4 weeks later on a 0.35 T system (Siemens Magnetom Symphony and C!)

**Fig. 7.20** Sagittal T1- and T2-weighted SE sequence in a patient with severe hyperkyphosis of the thoracic spine (Siemens Magnetom C!). Combination of different solenoid coils enables scanning the whole cervicothoracic spine

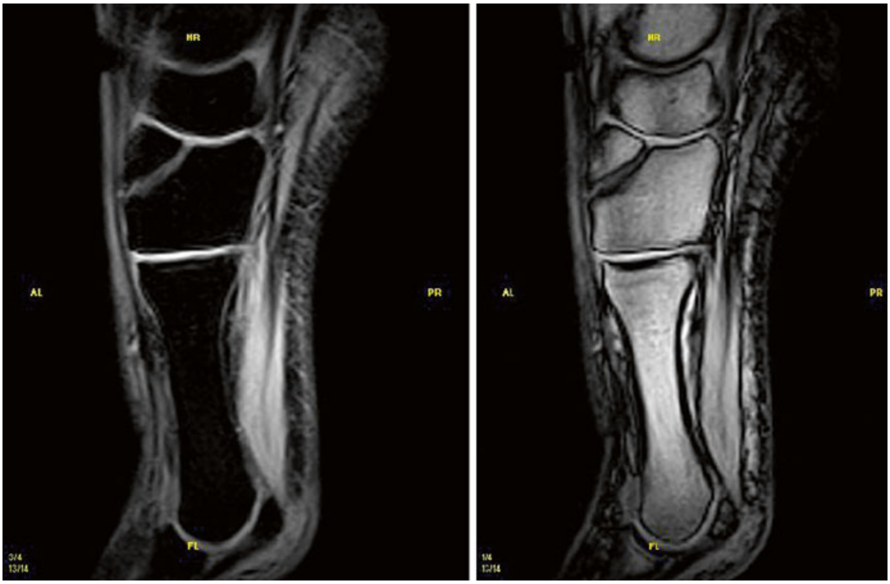


**Fig. 7.21** Fracture of the Os cuneiform med. STIR (*left*) and T2*-(*right*) weighted image (Courtesy Esaote Inc.)

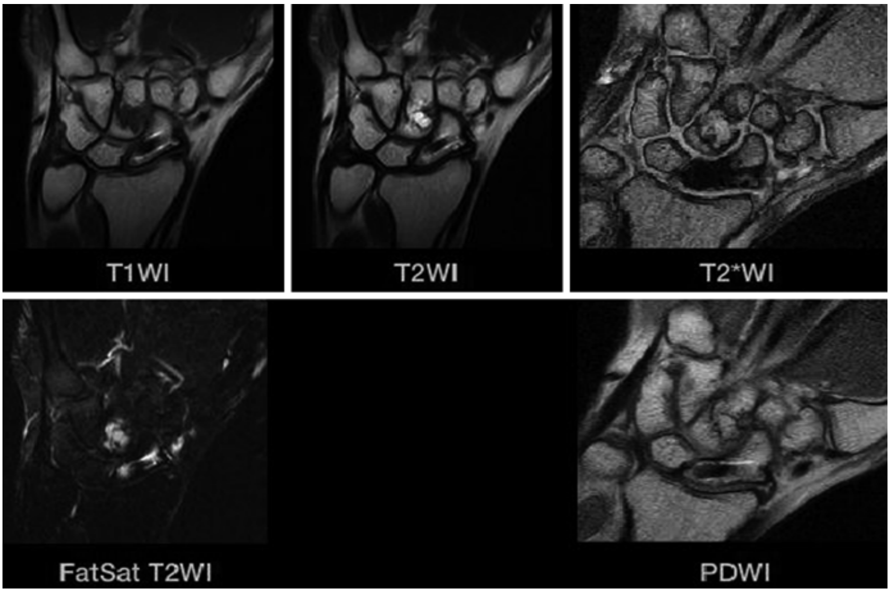


**Fig. 7.22** MR imaging after surgical repair of a scaphoid fracture using a Herbert screw (titanium). Nearly no metal artifacts (Hitachi Aperto 0.4 T)

### 7.4.2 Inflammatory Disease

The value of low-field MRI in the work-up of patients with rheumatoid arthritis has been reported (Pedersen et al. 2014). For the diagnosis of sacroiliitis and ankylosing spondylitis, particularly for assessment of the inflammatory activity, MRI is far more sensitive than X-ray imaging (Yu et al. 1998).

The recent concept of enthesitis depends on MR imaging for detection of inflammatory contrast enhancement in the fibro-osseous junction (Klang et al. 2014).

### 7.4.3 Cartilage

In recent years, cartilage lesions have attracted particular attention. Proton-density sequences with fat saturation and T1 sequences are the base of routine imaging on high-field systems.

The clue for cartilage diagnosis is spatial and contrast resolution (Bredella et al. 2001). For grade 2 lesions, a sensitivity and specificity of 25–75 % have been found on a 0.2 T system. For grade 3 lesions, the values are between 60 and 73 %, respectively (Riel et al. 1997; Ahn et al. 1998). Sensitivity and specificity were lower than in high-field MRI.

Harman compared non-contrast imaging with MR arthrography of the knee. For grade 3 cartilage lesions, he found a sensitivity for T2 sequences and MR arthrography of 0.71 and 0.85, respectively. For grade 4 lesions, sensitivity was 0.87 and 1.0 (Harman et al. 2003).

The improved T1 contrast in low-field imaging can be used for high-resolution imaging of the hyaline cartilage. Roessler and coworkers performed cartilage imaging using a single-sided, commercially available low-field MRI scanner. They achieved a vertical resolution of 20 μm (Rössler et al. 2014) (see Chap. 9) (Fig. 7.23).

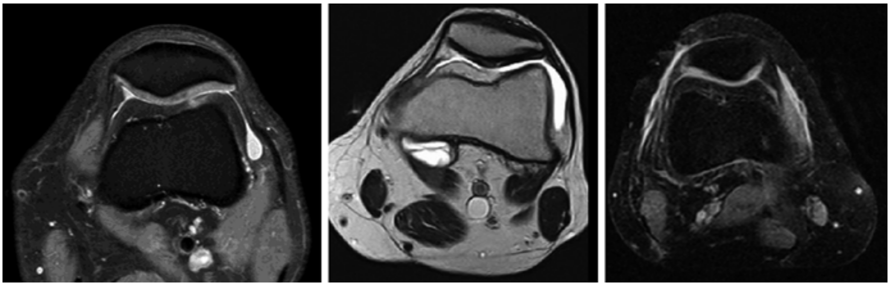

**Fig. 7.23** Retropatellar cartilage. *Left*: fat-saturated proton-density image 1.5 T, middle: T2-weighted image at 0.35 T, showing a cartilage fissure. *Right*: fat-saturated proton-density image 0.35 T

### 7.4.4 Joint Imaging

A number of publications have addressed the performance of low-field versus high-field MRI for knee diagnostic (Cotten et al. 2000). Most studies showed comparable results. Parizel compared low- and high-field MRI for diagnosis of knee disorders. He found that a low-field system represents a cost-effective alternative to high-field imaging (Parizel et al. 1995).

Kreitner and coworkers performed a prospective, arthroscopically controlled study on knee MRI. He emphasized the longer examination times (Siemens Magnetom Open 0.2 T) and the dependency on the skills of the diagnostic radiologist (Kreitner et al. 1999).

Krampla and coworkers compared three field strengths (1, 1.5, and 3 T) for diagnosis of knee disorders. They found no significant differences in interobserver variance, sensitivity, and specificity. Differences in false results depended on observer experience, not on field strength (Krampla et al. 2009) (Figs. 7.24, 7.25, 7.26, and 7.27).

**Fig. 7.24** High-resolution T1-weighted spin echo sequence. Matrix 1024 × 768 (interpolated). Scan time 2:40 min. High contrast-to-noise ratio for hyaline cartilage, menisci, and bone marrow (Siemens Magnetom C!, 0.35T)

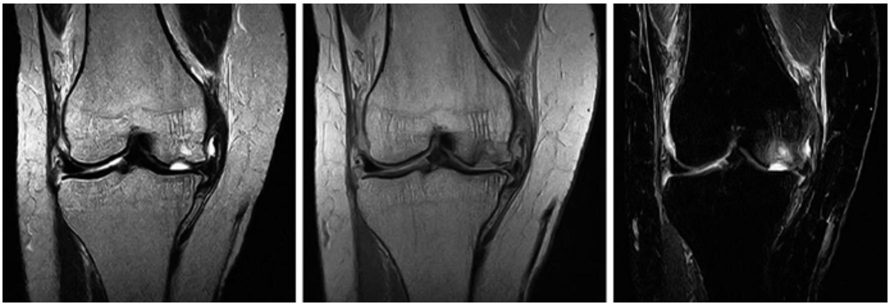

**Fig. 7.25** Patient with acute osteochondral fracture of the medial condyle. MR imaging (1024 × 1024 matrix size, Hitachi Aperto 0.4 T). *Left*: T2-weighted spin echo sequence. *Middle*: proton-density image. *Right*: STIR-sequence

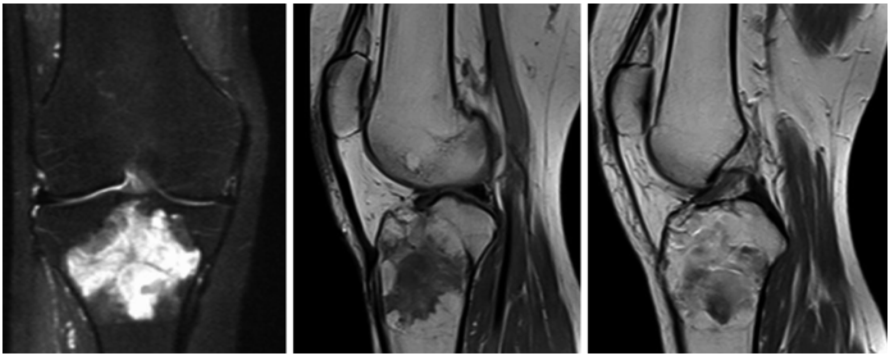

**Fig. 7.26** Giant cell tumor of the knee (Siemens Magnetom C!, 0.35 T). *Left*: STIR image. *Middle*: T1-weighted plain image. *Right*: Contrast enhanced T1-image

**Fig. 7.27** T2 relaxometry. The calculated T2 values are superimposed to the T2 image (Siemens Magnetom C!, 0.35 T)

Shoulder imaging in a closed-bore system requires off-center positioning of the joint, resulting in reduced image quality. Wide-bore MRI systems improve this situation. In open low-field MRI, the shoulder and also the elbow joint can be positioned in the magnet's center, resulting in a further increase of image quality.

Magee investigated high- versus low-field MRI of the shoulder and found the higher spatial resolution to be an important feature of high-field MRI (Magee et al. 2003).

Loew and coworkers compared MR arthrography of the shoulder between 0.2 T and 1.5 T. They found comparable imaging results, which are partly due to the fact that MR arthrography uses T1-weighted sequences with a GD contrast agent, and therefore takes profit from increased T1 contrast (Loew et al. 2000).

Rotator cuff lesions were investigated by Shellock et al. on a 0.2 T system. In 47 patients, they achieved a sensitivity and specificity of 0.89 and 1.0, respectively (Shellock et al. 2001). Kreitner et al. performed a study of 82 patients with MR arthrography on a low-field MRI. Sensitivity was 0.97 and specificity 1.00 (Kreitner et al. 2003).

Shoulder instability can be caused by rotator cuff, capsular or bony defects, and by labroligamentous lesions. Studies on unenhanced low-field imaging of the shoulder found a sensitivity and specificity for labrum pathology of 0.67 and 0.91, respectively (Merl et al. 1999). Superior labrum anteroposterior lesions (SLAP) have been reported to be more easily missed on low-field MRI (sensitivity and specificity of 0.67 and 0.8). However, 75 % of the arthroscopically found lesions, missed on MRI, were type 1 lesions with only fraying of the labrum (Tung et al. 2000). To the knowledge of the author, until now no study on low-field MR arthrography of the glenoid labrum exists (Figs. 7.28 and 7.29). Elbow imaging represents a problem in closed bore magnets. Open low field systems provide far easier access and positioning (Fig. 7.30). The same is true for the wrist (Figs. 7.31 and 7.32), and to some extent, mainly in trauma patients, for the ankle (Fig. 7.33).

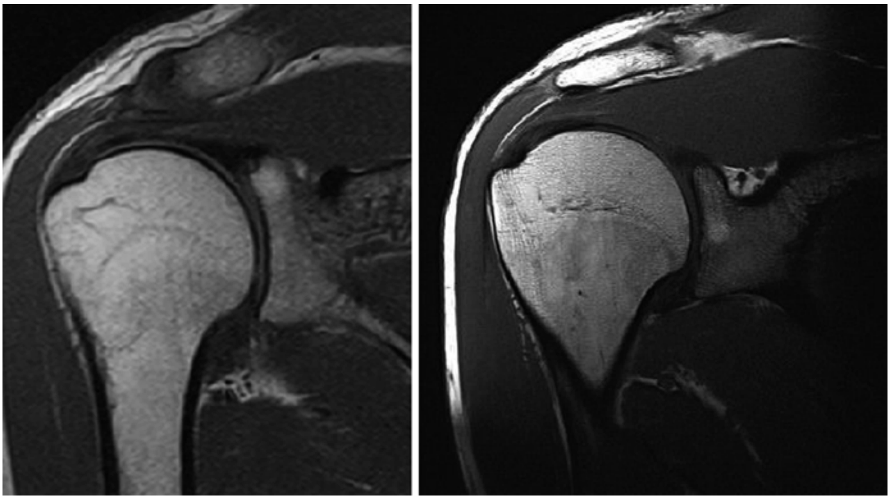

**Fig. 7.28** Shoulder imaging. T1-weighted SE sequence. *Left*: Siemens Magnetom C!, 0.35 T, *Right*: Siemens Magnetom Symphony 1.5 T. Spatial resolution is inferior on low-field imaging, but T1 contrast of cartilage is better

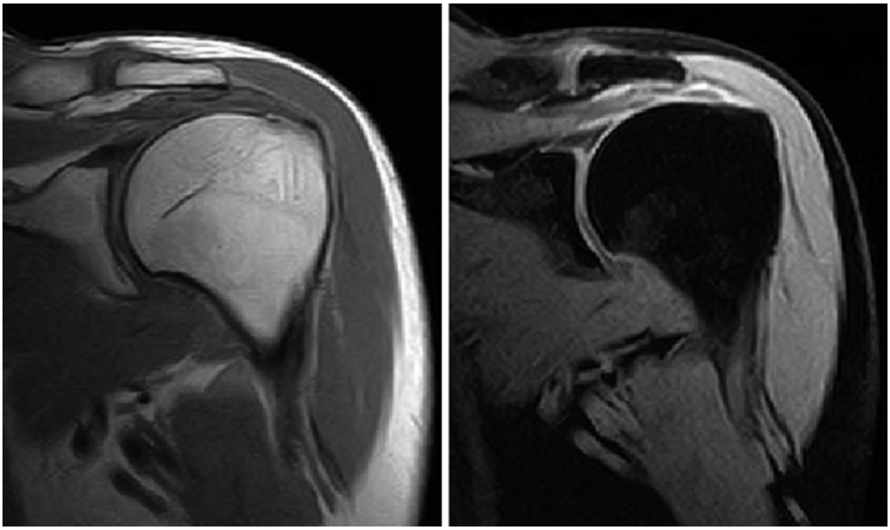

**Fig. 7.29** Shoulder imaging. *Left*: T1-weighted spin echo sequence. *Right*: fat-suppressed Dixon sequence (Hitachi Aperto 0.4 T)

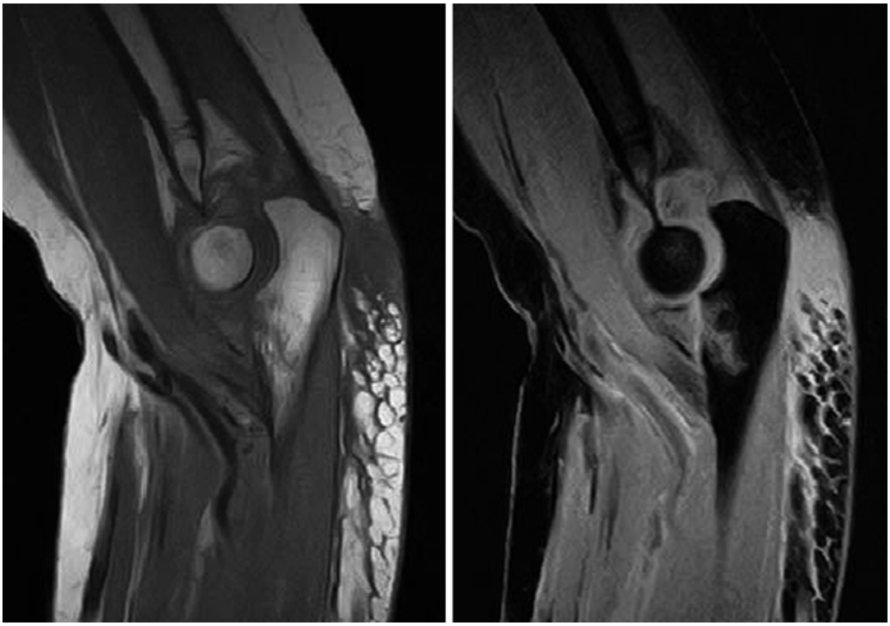

**Fig. 7.30** Elbow imaging. Coronoid process fracture type 3 (Regan–Morrey classification) involving>50 % of the process. *Left*: T1 spin echo sequence. *Right*: fat-suppressed sequence (STIR) (Hitachi Aperto 0.4 T)

**Fig. 7.31** Kienböck's disease. Gradient echo scan (Courtesy Esaote inc.)

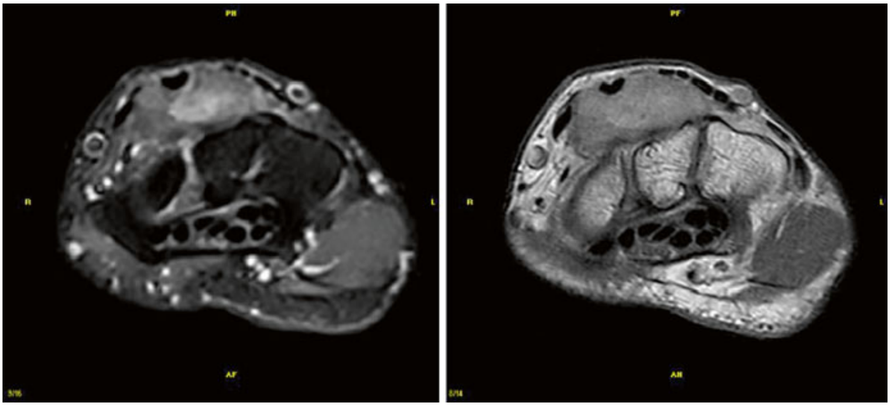

**Fig. 7.32** Giant cell tumor of the tendon sheath. *Left*: STIR technique. *Right*: contrast-enhanced T1 spin echo (Courtesy: Esaote Inc.)

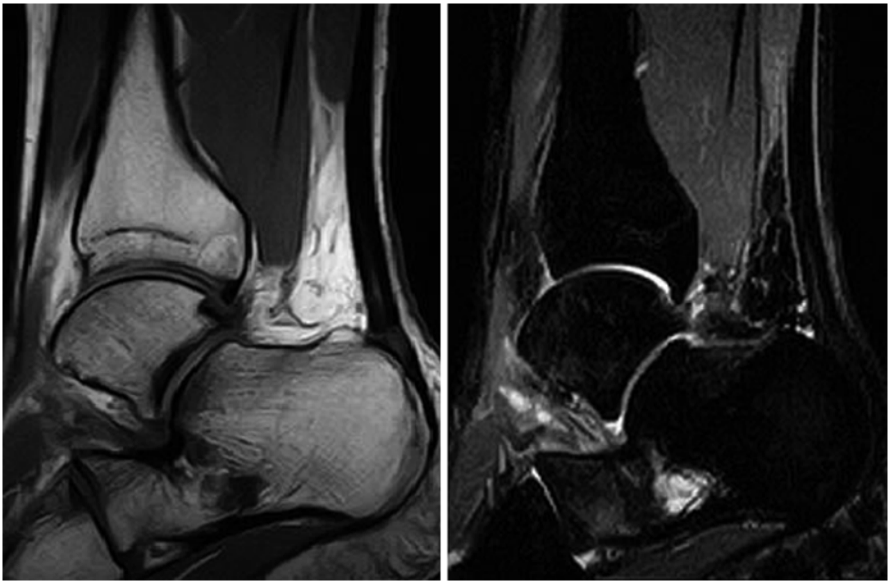

**Fig. 7.33** Ankle joint with intraosseous ganglion in the calcaneus (Hitachi Aperto 0.4 T)

## 7.5 Thoracic Imaging

There are a lot of obstacles for MR imaging of the thorax and lungs. However, at lower field strength, T1-weighted imaging with diagnostic performance is possible (Schäfer et al. 2002). Recently, a technique using hyperpolarized gas has been proposed (Mc Fain et al. 2007).

For clinical routine, thoracic imaging will remain a domain of CT (Fig. 7.34).

Breast imaging using low-field MR imaging has not been systematically evaluated. There are only very few reports, mainly in patients with severe contraindications to closed-bore high-field MR systems. Sittek and coworkers reported a study on preoperative marking of nonpalpable breast lesions, guided by a 0.2 T open MR system (Siemens Magnetom OPEN). All lesions of interest could be localized and successfully marked (Sittek et al. 1997, Reiser 1997) (Fig. 7.35).

## 7.6 Abdomen

For abdominal imaging, the reduced RF attenuation at lower frequencies becomes more relevant. Using respiratory-triggered SE sequences, high-quality images of the abdomen and pelvis are possible (Figs. 7.36, 7.37, 7.38, and 7.39).

**Fig. 7.34** Siemens Magnetom C!, 0.35 T. Lung imaging using an inverted T1 FLASH sequence. TE 4.5 ms, TR 100 ms, TA 2×20 s, Matrix 292×512 interpolated

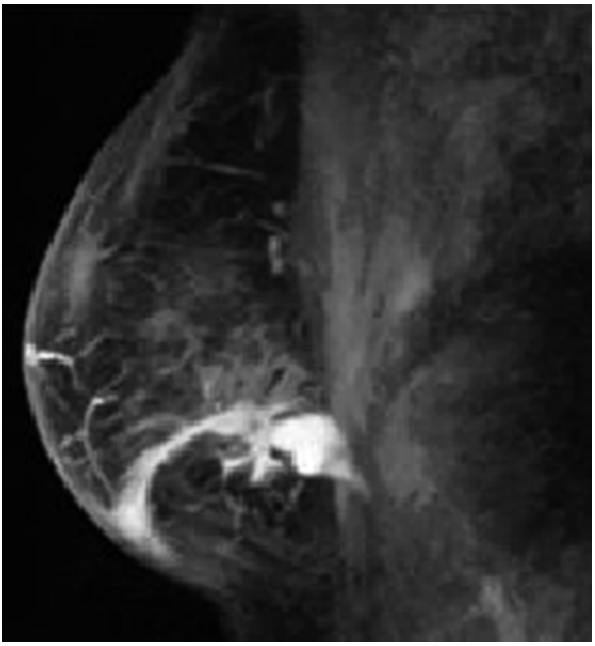

**Fig. 7.35** Fat-saturated image after i.v. contrast administration. Breast neoplasm with extension to the skin (Hitachi Aperto 0.4 T)

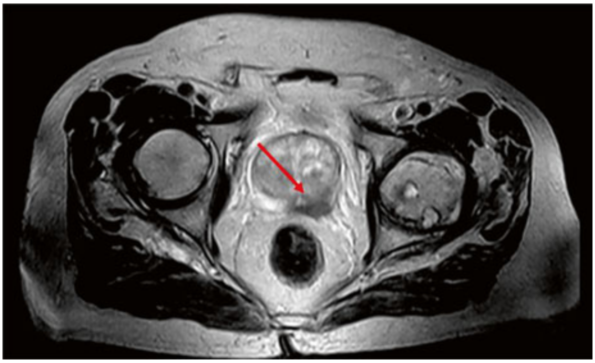

**Fig. 7.36** Prostate cancer (*arrow*). T2 axial image. Low-intensity area in the posterolateral exterior gland (Siemens Magnetom C! 0.35 T)

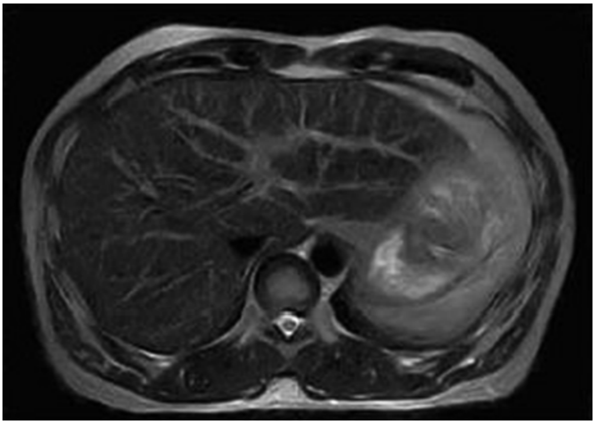

**Fig. 7.37** Liver imaging. T2-weighted spin echo sequence (Hitachi Aperto 0.4 T)

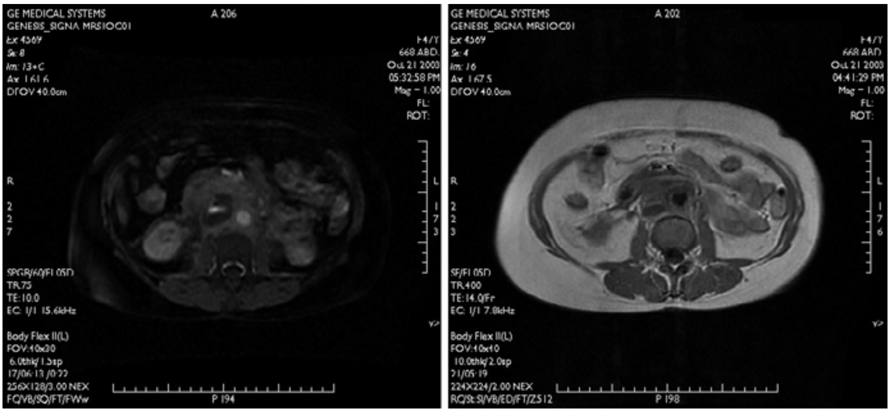


**Fig. 7.38** Retroperitoneal fibrosis. *Left*: contrast-enhanced spoiled gradient echo sequence (GE Signa Profile 0.2). *Right*: T1-weighted spin echo after contrast injection

**Fig. 7.39** Uterine myoma (Hitachi Aperto 0.4 T). *Left*: T2-weighted spin echo sequence. *Right*: contrast-enhanced T1-weighted spin echo sequence

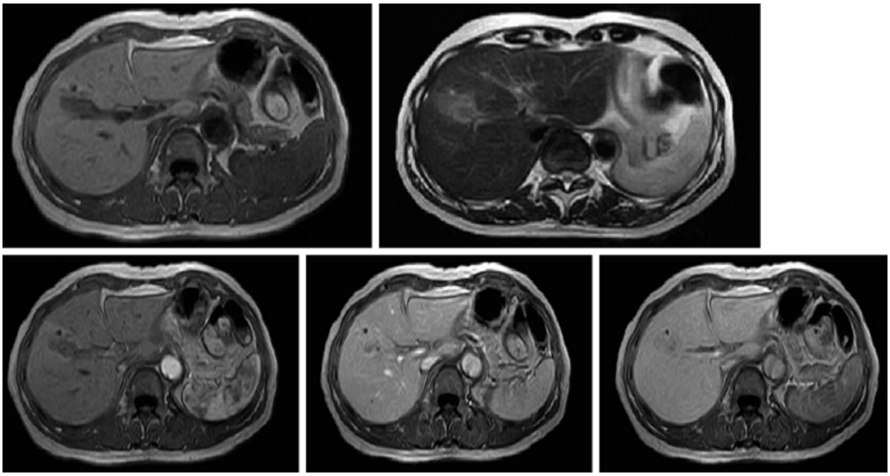

**Fig. 7.40** Hepatic liver tumor. Dynamic hepatic imaging (Hitachi Aperto 0.4 T). Gd-EOB DTPA (Primovist$^{R}$). *Upper row*: non-contrast T1 and T2 sequence (respiratory triggering). *Lower row*: dynamic contrast-enhanced T1-weighted gradient echo. 40 s, 70 s, 4 min

Breathhold imaging requires high scan speed for optimal body coverage in a breathhold time. This problem can be addressed by division of the scan volume in multiple slabs. Image quality of our low-field system was always very satisfactory in abdominal imaging (Fig. 7.40). Imaging of the hepato-biliary system can be performed without problems (Fig. 7.41).

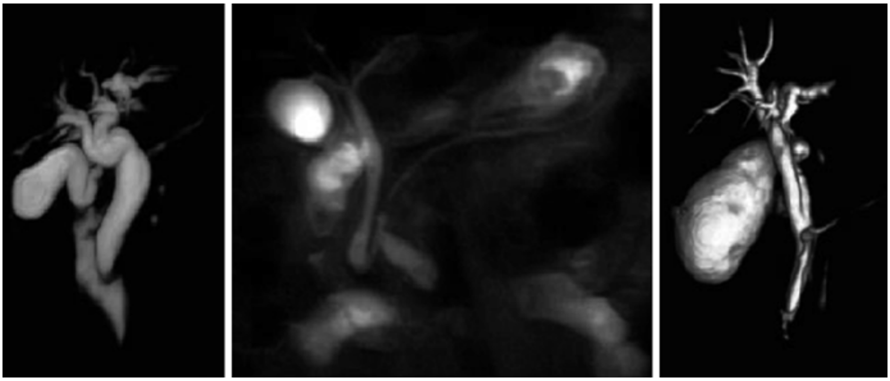

**Fig. 7.41** MR cholangiography (Hitachi Aperto Lucent 0.4 T). *Left*: single-shot scan, normal findings. *Middle*: volume rendering. Normal situation. *Right*: maximum intensity projection. Dilated common bile duct

Low-field MR systems were tested for dose planning in patients with prostate cancer (Petersch et al. 2004).

## 7.7 Vascular Imaging

There are only few reports on low-field MR angiography (PAVONE 1992). As discussed in Chap. 6, there are four types of MR angiography technique.

The most frequently used concept is time-of-flight imaging, which gives excellent arterial contrast in low- and high-field systems (Figs. 7.42 and 7.43). Phase-contrast angiography is equally well suited for all available field strengths.

CE MR angiography provides a very high SNR. The sequence technique needs a short echo time, which depends on the gradient performance. This prerequisite is given in modern low-field systems.

The shortened T1 time reduces the contrast effect of Gd-containing agents, which could be reducing image quality (Jager et al. 2000; Remonda et al. 2002). It could be shown that image quality of a CE MR angiography using low field strength can be comparable to a high-field system (Klein et al. 2008) (Figs. 7.44, 7.45, and 7.46).

## 7.8 Diffusion

Diffusion imaging is a valuable tool for detection of pathologic tissue changes. It is regularly performed using echo planar imaging. EPI sequences take profit from field strength. However, they can also be performed for head imaging on low-field scanners (Figs. 7.7 and 7.47). An advantage of low-field scanners is the reduction of susceptibility artifacts in the skull base.

For hepatic diffusion imaging, a combination of a diffusion-weighted HASTE sequence and a T1-weighted RARE or 2D spoiled gradient echo series has been proposed (Domalski and Klein 2006). It may be possible, to evaluate early necrotic

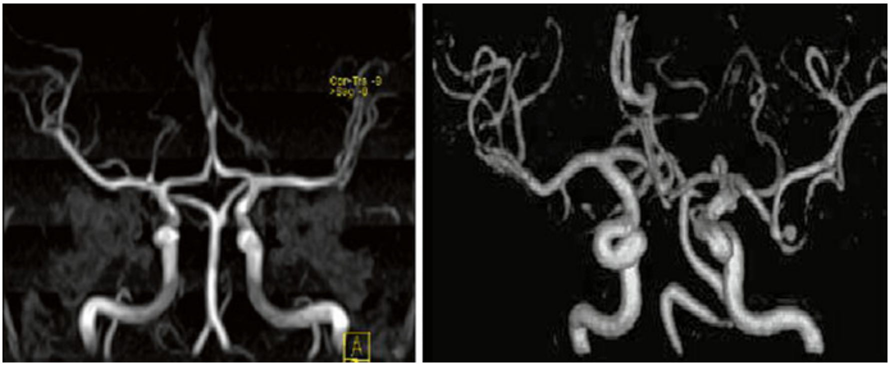

**Fig. 7.42** Time-of-flight MR angiography of the cranial vessels. *Left*: maximum intensity projection (Siemens Magnetom C!). *Right*: volume rendering (Hitachi Aperto 0.4 T)

**Fig. 7.43** MR angiography of the extracranial cerebral vessels. *Left*: Time-of-flight MRA of the carotid artery. MIP (Hitachi Aperto 0.4 T). *Right*: contrast-enhanced MRA. VRT reconstruction. 0.01 mmol/kg BW Gd-DTPA (Siemens Magnetom C! 0.35 T)

**Fig. 7.44** MR angiography of the thoracic aorta and supraaortic branches (Hitachi Aperto 0.4 T). Aneurysmatic widening. *Left*: MIP. *Left*: volume rendering

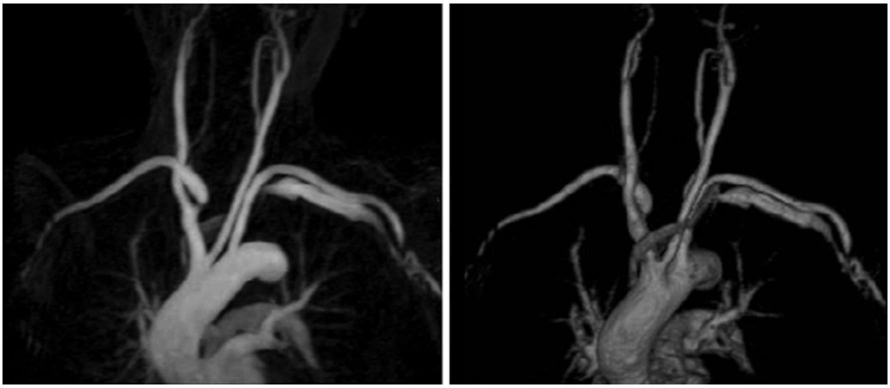

**Fig. 7.45** CE MR angiography of the aortic arch. Stenosis of the right subclavian artery (Siemens Magnetom C! 0.35 T)

**Fig. 7.46** Phase-contrast MR angiography of the portal venous system (Hitachi Aperto 0.4 T)

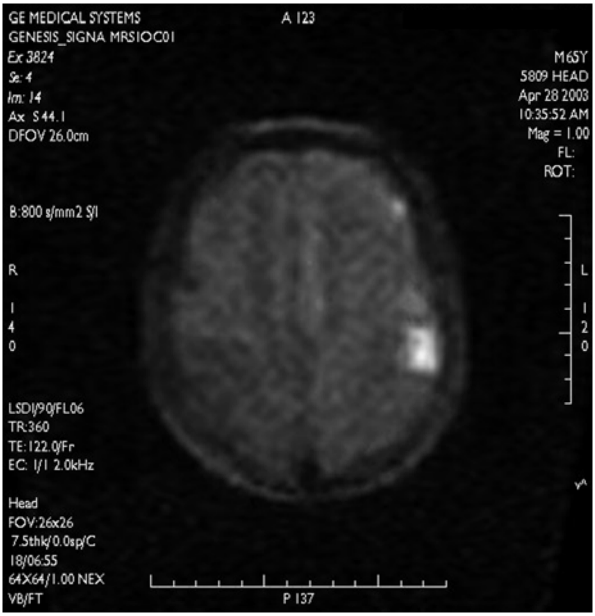


**Fig. 7.47** Acute ischemic damage in the left postcentral gyrus. Diffusion-weighted EPI sequence. GE Signa Profile 0.2 T

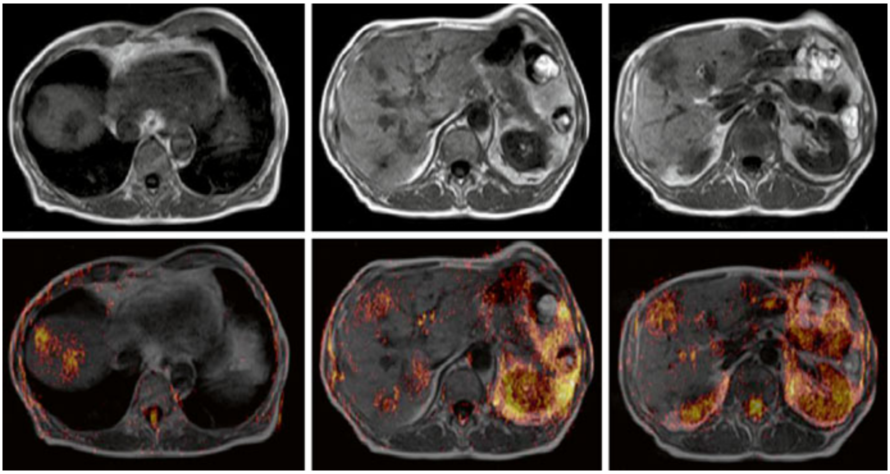

**Fig. 7.48** Body diffusion imaging. A patient with liver metastasis from colon carcinoma. *Upper line*: T1-weighted images demonstrate focal liver lesions (metastatic disease), *lower line*: the diffusion-weighted images are superimposed to the T1 images with color encoding

changes in liver tumors using this concept, but preliminary results suggest that at least 2 cm of lesion diameter is necessary to provide the minimal contrast–noise ratio (Fig. 7.48).

## 7.9 Functional Imaging

The effect of weight-bearing is most relevant for musculoskeletal diagnostic. There are special-purpose MR systems, enabling to examine patients in standing or sitting position. It is also possible to carry out the sequences during flexion or extension of a joint or the vertebral column (Harvey et al. 1998). This can contribute to the diagnosis of segmental spinal instability. The magnet design for these systems is either a permanent magnet (Esaote G-scan, 0.25 T) or a resistive magnet (Fonar Upright MRI, 0.6 T) (Fig. 7.49).

## 7.10 Whole Body

Using a four-channel HF receiver unit with a total of 13 coil elements, complete coverage of the head, neck, thorax, and abdomen is possible, providing a virtual whole-body imaging (Siemens Magnetom C! 0.35 T).

The images are merged using an image-composing tool (LEONARDO, Siemens Medical Solutions, Erlangen, Germany). The procedure is simple and impressive for demonstration (Fig. 7.50).

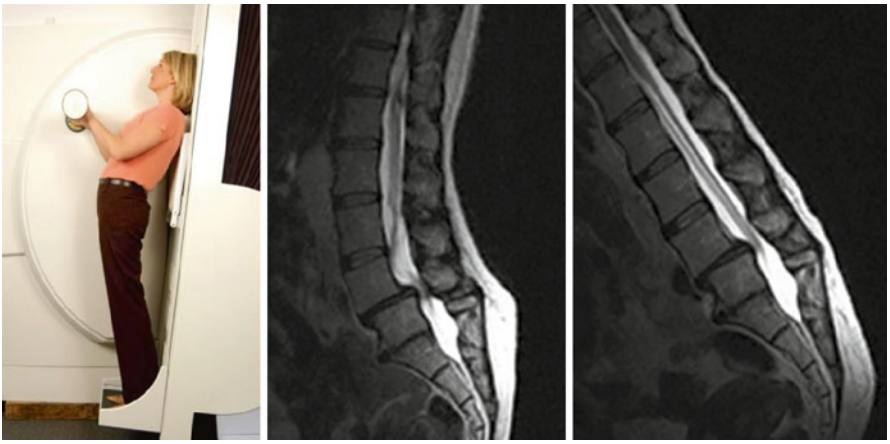

**Fig. 7.49** (**a**) The upright MRI facilitates examinations in standing position (weight-bearing). (**b**) In reclination, the spinal stenosis is aggravated. (**c**) In anteclination, the stenosis widens (Courtesy of FONAR Inc., Melville, USA)

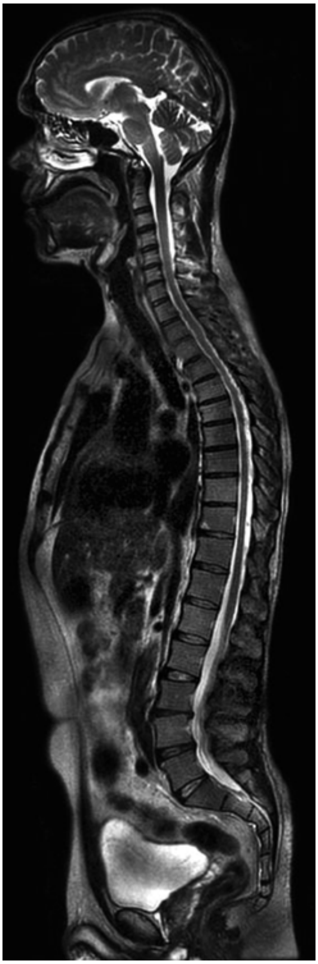

**Fig. 7.50** Whole-body imaging using a four-channel 0.35 T system (Siemens Magnetom C!). The circular polarizing head coil, the neck coil, and two body coils (for the thorax and abdomen) are combined. T2-weighted sagittal spin echo sequence in three scan positions. Image combination using a merging post-processing software

## 7.11 Cardiac Imaging

Magnetic resonance imaging has meanwhile become a widely used modality of cardiac diagnostic imaging.

The unrestricted visualization of cardiac anatomy, functional assessment including determination of ejection fraction, ventricular size, wall movement, wall thickness, and measurement of perfusion and mural contrast enhancement make cardiac MRI a valuable tool for the work-up of patients with myocardial ischemia or other disorders of the heart (Sandstede 2003; Lipton et al. 2002).

Perfusion and redistribution of contrast medium can be assessed using $^{201}$TI-SPECT. Disadvantage of nuclear medicine is the low spatial and temporal resolution of the images. Furthermore, radiation exposure for the patient is considerable. MRI can demonstrate myocardial perfusion with high spatial accuracy and good time resolution using segmented spoiled gradient echo sequences with phase sharing. Microvascular obstruction in ischemic areas, an important parameter for the prognosis of ischemic necrosis, can reliably be detected.

The first steps toward cardiac MRI were made in an era, where field strengths higher than 1 T were technically impossible. Systems with up to 0.35 T represented the standard (Herfkens et al. 1983; Gatehouse and Firmin 2000).

Today, cardiac MR imaging is usually performed using high-field systems. High field strength contributes to SNR, but is also the main cause of high examination costs.

Besides field strength, gradient and RF technique, coil design, acquisition sequences, and signal and image processing also have an important influence on image quality.

Furthermore, the higher resonance frequency at high field strength facilitates delineation of superficial structures. For body imaging, and therefore also cardiac imaging, lower field strength with lower resonance frequency and therefore better tissue penetration of the RF energy has physical advantages.

Heating of implanted material due to eddy currents, like implanted stents, is reduced at lower field strength (Klemm et al. 2000).

The open design of low-field systems is helpful for obese or handicapped patients (Rothschild et al. 1992).

In certain clinical situations, it can therefore be wishful to perform cardiac MR imaging on a low-field scanner.

We examined the potential of our low-field MRI, a Magnetom C! 0.35 T (Siemens, Erlangen, Germany) for cardiac imaging (Klein 2007).

The system possesses a software transfer option (PHOENIX, Siemens, Erlangen, Germany) which enables to use protocols from other Siemens systems. In our case, we simply transferred the cardiac sequences from our high-field system (Magnetom Symphony, Siemens, Erlangen, Germany). They worked on the low-field system without major changes.

We used parallel imaging technique in combination with a four-channel body–array coil. The gradient system operates at a slew rate of 55 T/m/s with a maximum gradient strength of 24 mT/m.

A three-channel ECG was used for triggering. After localizing the standard cardiac views using a gradient echo sequence, functional imaging series were acquired in short axis and two-chamber orientation. We used a slightly modified cine TrueFISP sequence in breathhold technique, derived from a 1.5 T system (Fig. 7.51). Echo time was TE = 2.16 ms, temporal resolution was TR = 47.71 ms, flip angle was 70°, one acquisition. Slice thickness was 8 mm with a 25 % gap. Matrix resolution was 128 × 128. The field of view was 300 mm. The acquisition window was automatically triggered at mean RR interval time.

No trigger delay was used to achieve data acquisition throughout the whole cardiac cycle.

All imaging data were analyzed using a specially designed software (ARGUS, Siemens Medical Solutions, Erlangen, Germany) on an image-processing workstation (LEONARDO, Siemens Medical Solutions, Erlangen, Germany).

## 7.11.1 Functional Imaging

Myocardial wall movement as a descriptor of heart function is routinely analyzed with echocardiography. MR can provide the advantages of ultrasound (noninvasive, comfortable and safe for the patient) and adds the advantage of standardized imaging planes and analysis, good reproducibility, and accuracy. Kaandorp and coworkers (Kaandorp et al. 2004) compared functional imaging with low-dose dobutamine stimulation (determination of the contractile reserve) and delayed enhancement imaging. They differentiated the patients (n = 48) regarding the percentage of

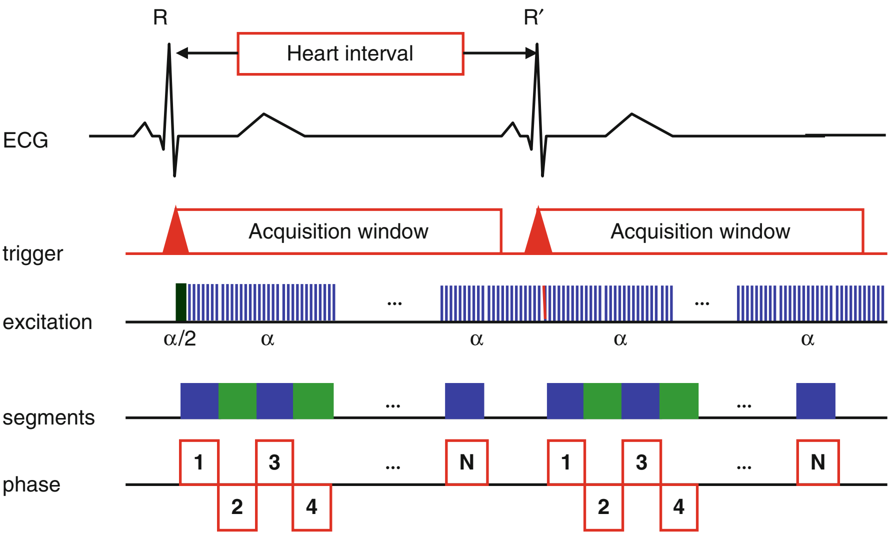


**Fig. 7.51** Schematic description of a segmented CINE TrueFISP sequence with continuous RF excitation

enhancing cardiac wall as parameter for the severeness of ischemic damage. For patients with small or large infarct areas, the results between functional deficit and ischemic area corresponded well. For medium infarct size (50–75 % of wall thickness), the correspondence between the two procedures was low, emphasizing the importance of late enhancement imaging as adjunctory procedure to functional imaging.

In our study, we found good results for myocardial functional assessment. A balanced fast gradient echo sequence was applied for functional imaging. The high signal-to-noise ratio at very low scan time makes this sequence ideally suited. The T2 contrast is known to be better in high-field settings. However, the cine TrueFISP sequence used in our protocol provides improved T2* contrast, which is absolutely adequate for delineation of myocardium and cardiac blood (Figs. 7.51 and 7.52).

## 7.11.2 Perfusion Imaging

Lund and coauthors (Lund et al. 2004) compared $^{201}$TI-SPECT and perfusion–redistribution MRI. They found MR imaging to be superior in terms of spatial resolution. Perfusion imaging revealed microvascular obstruction as predictor of nonrespondance to revascularization. Microvascular obstruction was also determined using delayed enhancement MRI. Probably, perfusion MR will have a more important role for diagnosis of microvascular occlusion. Catalano et al. (Catalano et al. 2005) found a systematic overestimation of infarct size with SPECT imaging.

We used a dynamic saturation recovery-prepared FLASH sequence (Fig. 10.11c, d) in short axis orientation. Echo time was TE = 1.61 ms, acquisition time of one slice was 295.1 ms, TI was 155 ms, flip angle FA = 50°, and matrix 128 × 77; 60

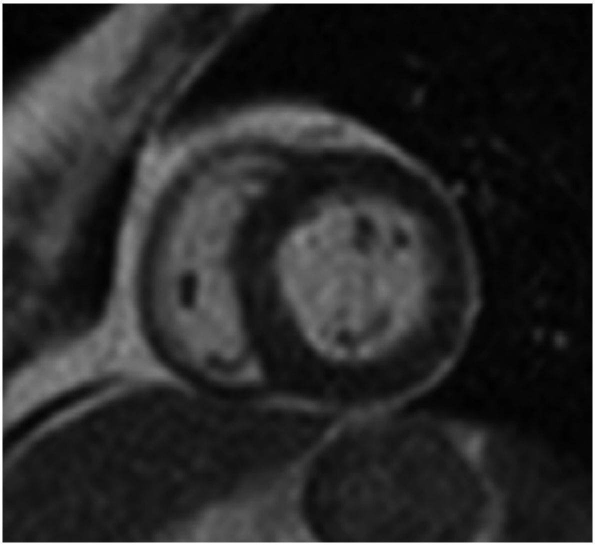

**Fig. 7.52** Short axis view. Cine TrueFISP imaging

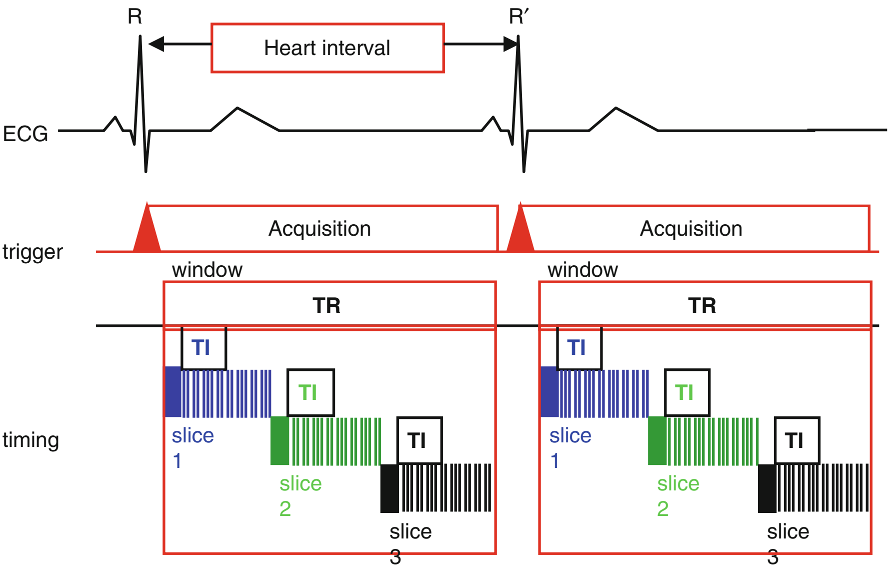


**Fig. 7.53** Schematic description of the multi-slice perfusion measurement with the SR-prepared FLASH sequence

**Fig. 7.54** Fat saturation recovery perfusion sequence. Subendocardial perfusion defect in the posteroseptal wall (*arrow*)

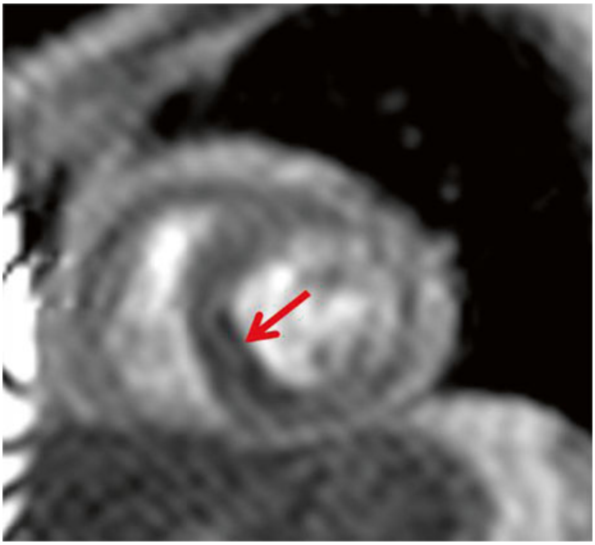

measurements were performed at a time interval equal to the R–R interval of the patient. The field of view was 360 mm. The sequence was started immediately after administration of 0.1 mmol Gd-DTPA/kg body weight (Magnevist, Schering, Berlin, Germany) in bolus technique (Figs. 7.53 and 7.54).

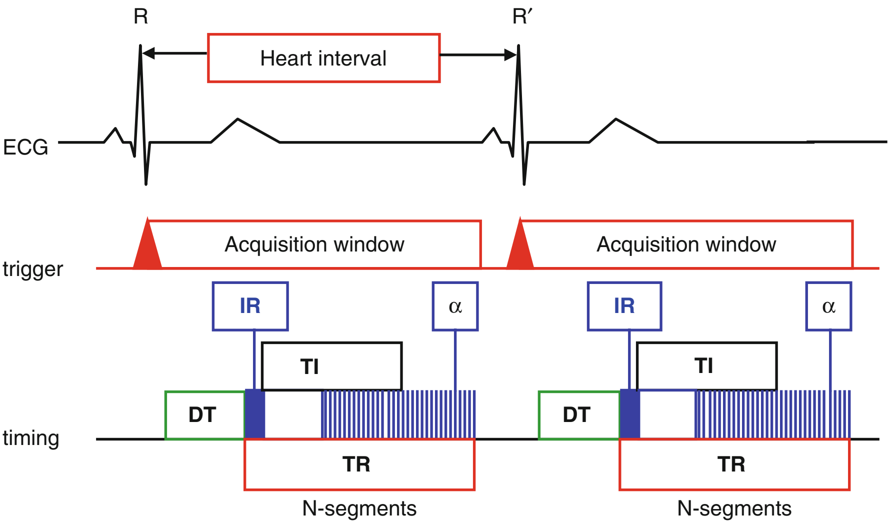


**Fig. 7.55** Schematic description of a segmented FLASH sequence with IR preparation (late enhancement)

### 7.11.3 Late Enhancement

The most sensitive method to determine the prognosis of myocardial ischemia is imaging of delayed contrast enhancement (DE-MRI). Lopez and coworkers (Lopez et al. 2004) found a strong correlation between the size of the contrast enhancing wall area and myocardial function after recovery. They furthermore detected that a wall thickness of less than 5.5 mm excluded the presence of vital myocytes.

In our study, imaging of delayed myocardial contrast enhancement was carried out 10 min after intravenous application of Gd-DTPA (Magnevist, Schering, Berlin, Germany) in a dosage of 0.1 mmol/kg. We used an IR-prepared fast gradient echo sequence in breathhold technique (Fig. 10.11e, f). FOV was 360 mm in short axis orientation. Echo time TE was 5.5 ms; trigger delay was maximum to achieve data acquisition in the end-diastolic phase. Flip angle FA was 35°. Field of view was 360 × 300 mm and matrix was 192 × 131; we performed one acquisition.

The MR sequence protocol uses an inversion recovery preparation for suppressing healthy, nonenhancing myocardium. This results in a reduced signal intensity, and therefore low signal-to-noise ratio, a crucial point for low-field imaging.

However, as could be demonstrated, image quality was surprisingly good. The reason may be that the IR-prepared gradient echo sequence is a pure T1 sequence (improved by lower field strength). Furthermore, the multichannel solenoid coil had an optimal sensitivity profile (perpendicular to the vertical magnetic field axis). And the improved RF penetration at lower field strength added additional signal power.

Optimal inversion time TI was determined by a pre-study and varied between 200 and 300 ms. Six consecutive images were acquired in short axis orientation in six positions from the valvular plane to the apex. Slice thickness was 8 mm with a 25 % gap (Figs. 7.55 and 7.56).

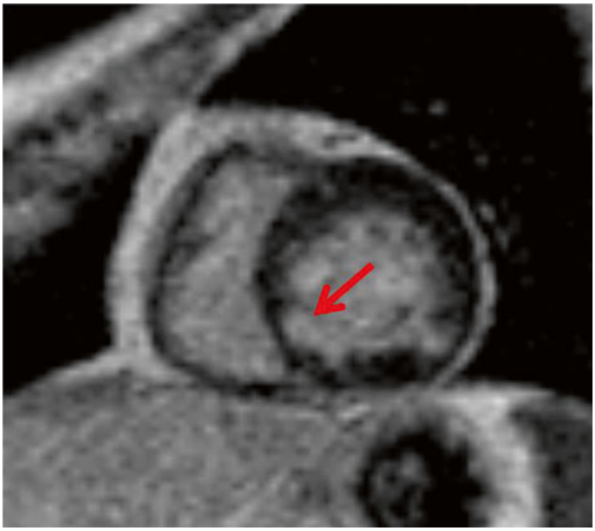

**Fig. 7.56** Late enhancement examination. IR-prepared gradient echo sequence. Subendocardial enhancement in the inferior and posterior myocardium (*arrow*), representing ischemic scarring

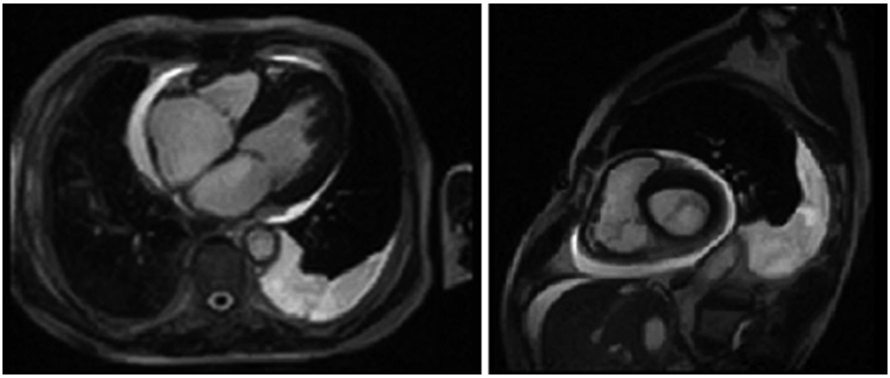

**Fig. 7.57** Pericardial and pleural effusion. Three-dimensional balanced steady-state acquisition with rewound gradient echo (3D BASG, Hitachi Aperto 0.4 T)

Cardiac imaging is also possible on low-field systems of other manufacturers. Hitachi Inc. provided an example of a clinical cardiac scan at 0.4 T (Fig. 7.57).

Our initial results could demonstrate that image quality in our routine cardiac low-field MRI setting is adequate for diagnosis of myocardial pathology. For functional imaging (cardiac wall kinetics) and late enhancement, it is even comparable to the results of high-field systems (Klein 2007).

However, since powerful gradients and RF transmitters, phased-array coil design, multichannel receivers, and much faster signal and image processors are available, further investigations concerning the role of cardiac low-field imaging are justified and necessary.

## 7.12 Implants

Biomedical implants can induce severe susceptibility artifacts in MR images. These artifacts depend mainly on the material and local field strength.

Using low-field MRI, these artifacts are markedly reduced (Sugimoto et al. 2003). It is important to consider further parameters that can influence susceptibility artifacts. The long axis of the prosthesis should be positioned in the direction of the readout gradient. Bandwidth and number of repetition echoes should be maximized. TE has to be minimized. Gradient power should be as high as possible (Figs. 7.58, 7.59, 7.60, and 7.61).

## 7.13 Interventional MRI

Open MRI facilitates interventional MR-guided procedures. These comprise mainly biopsies, pain therapy, and intraoperative MR scanning.

Using open MRI, the radiologist has permanent access to the patient; MRI exposes no x-radiation to patient and radiologist, and it offers excellent tissue contrast (Fig. 7.62). However, some restrictions have to be considered. The needle has to be angulated away from the (in permanent magnet systems vertically oriented) main field axis to become visible. Spatial resolution is limited. All instruments have to be MRI compatible (Tavernier and Cotten 2005).

Several companies have introduced MR-compatible needles and other instruments.

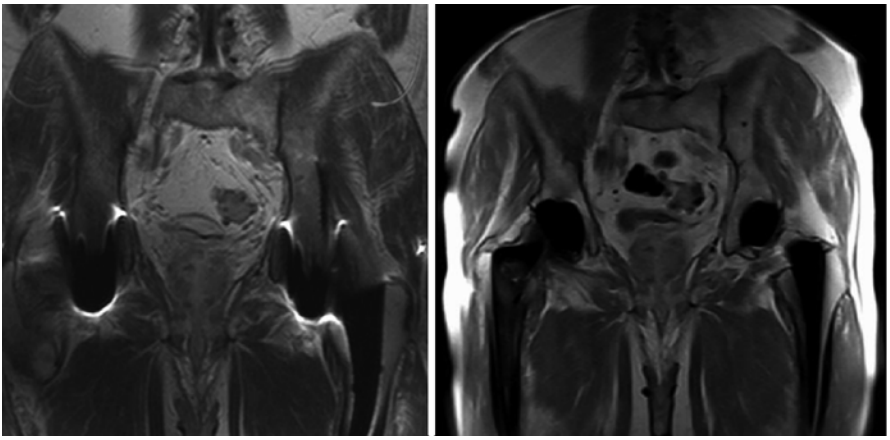

**Fig. 7.58** Metallic implants. Low-field systems provide reduced susceptibility artifacts. It is important to orient the readout gradient in the long axis of the implant. Gradient performance should be maximized. TE has to be set to minimum; bandwidth and turbo factor should be maximized. *Left*: volunteer patient with bilateral hip prosthesis. Severe artifacts obstruct evaluation of the periprosthetic area (Symphony 1.5 T, Siemens/Germany) TE 7 ms, TR 300 ms, TF 7, bandwidth 260 Hz/pixel, matrix 460×512, 5 mm slice thickness, time of acquisition 0:54 min. *Right*: same patient. Better delineation of the hip area at 0.35 T (Magnetom C!, Siemens/Germany) TE 8.9 ms, TR 515 ms, TF 7, bandwidth 260 Hz/pixel, matrix 384×512, 5 mm slice thickness, time of acquisition 1:40 min

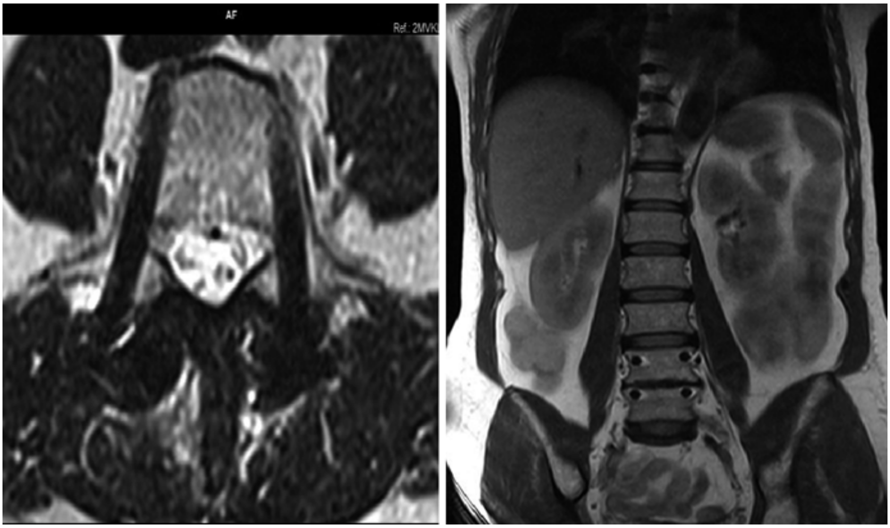

**Fig. 7.59** Axial T2-weighted SE sequence with pedicle screws after spondylodesis. Nearly no metal artifacts (Siemens Magnetom C! 0.35 T)

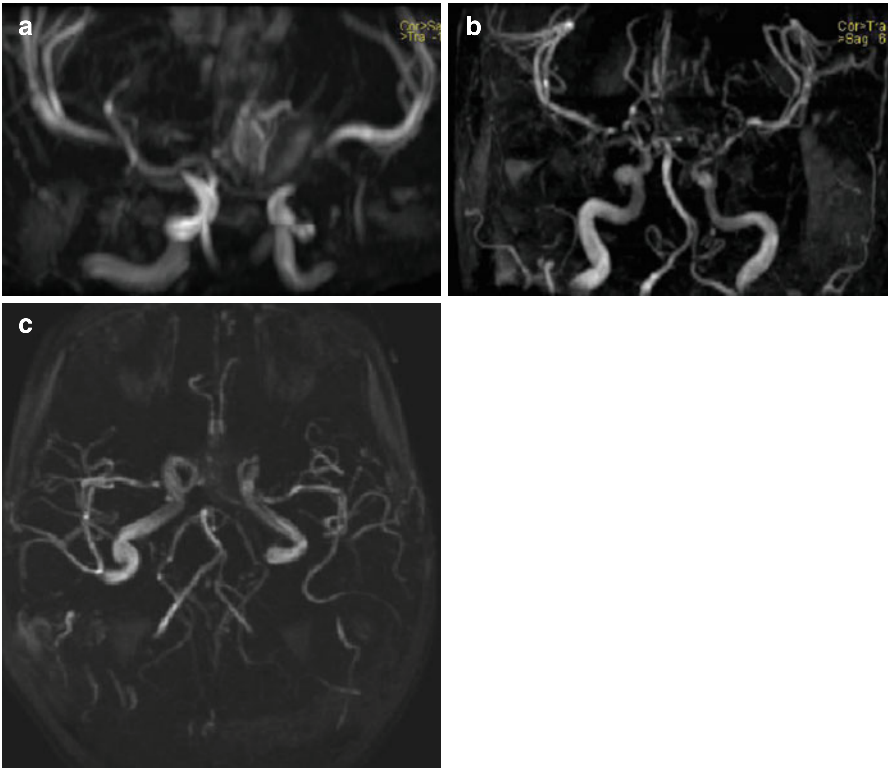


**Fig. 7.60** MR angiography in a 13-year-old boy after clipping of an ACA aneurysm. *Left*: 1.5 T (Siemens Magnetom Symphony 1.5 T). *Middle* and *right*: 0.35 T (Siemens Magnetom C!)

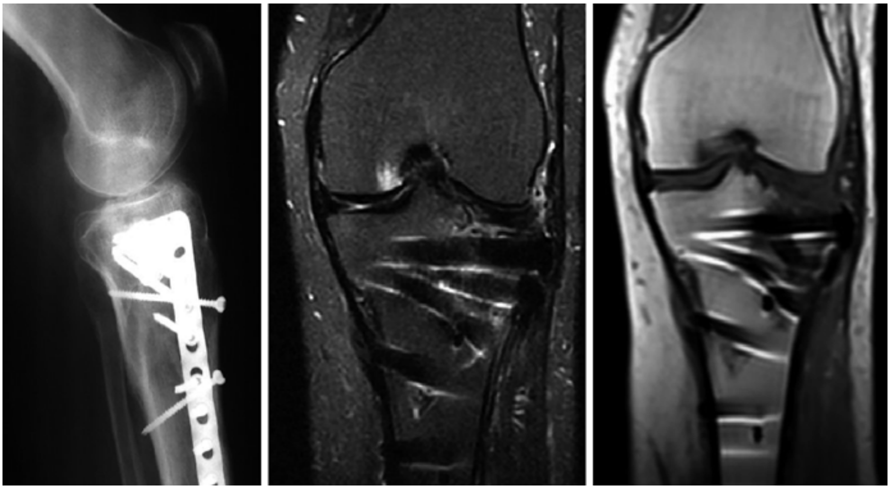

**Fig. 7.61** Knee pain after surgery for tibial head fracture. Despite metal components of the osteosynthesis, the small area of bone marrow edema can be delineated

**Fig. 7.62** MR-guided intervention in the knee joint (Hitachi)

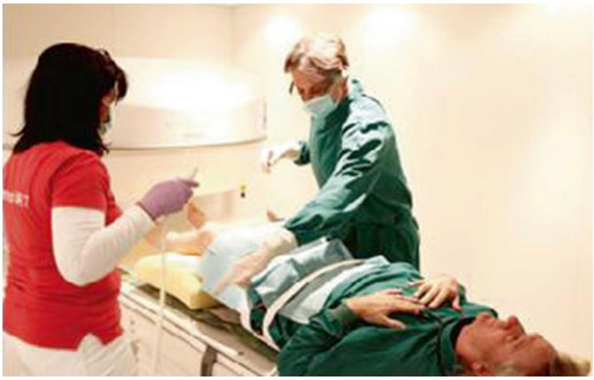

The first dedicated MRI for a surgical suite was the GE Signa SP (for: "surgical procedures"), an open 0.5 T system, consisting of two superconducting magnets in a "doughnut" combination.

Bootz and coworkers reported a series of operations in otorhinolaryngology. They appreciated real-time imaging. The demonstration of tissue changes during surgery is superior to conventional navigation techniques (Bootz et al. 2001). Bohinski used intraoperative MRI for guidance in transsphenoidal resection of pituitary adenomas (Bohinski et al. 2001).

Petersilge has proposed interventional MRI guidance for MR arthrography of the shoulder (Petersilge et al. 1997). MRI provides free angulation of the needle pathways and imaging without radiation exposure. However, compared with CT or fluoroscopy-guided procedures, there are some limitations.

Yamada described the use of an intraoperative low-field MRI scanner for MR-guided resection of intracranial malignant gliomas in 99 cases. Resection of the tumor bulk was guided by intraoperative MRI (0.3 T). The peripheral tumor extension was detected by additional staining with 5-aminolevulinic acid, a fluorescent marker (Yamada et al. 2015).

- Low-field MRI systems, with a field strength of less than 0.4 T and with a permanent magnet, are full-scale whole-body imaging machines
- The main drawback in routine imaging is the prolonged scan time on low-field systems, which is increased by about 40 %. Patient throughput is reduced about 20 % compared with a standard high-field scanner
- The most sensitive method for detection of fracture is MRI. Particularly in critical areas, like the scaphoid bone, low-field MRI can provide mandatory information for adequate clinical therapy
- Shoulder and elbow imaging in a closed-bore system means off-center positioning of the joint. In open low-field MRI, the joint can be positioned in the magnet center, resulting in improved image quality
- Breast imaging using low-field MR imaging has not been systematically evaluated
- Using respiratory-triggered SE sequences, high-quality images of the abdomen and pelvis are possible
- It could be shown that image quality of a CE MR angiography using low field strength can be comparable to a high-field system
- The effect of weight-bearing is most relevant for musculoskeletal diagnostic. There are special-purpose MR systems, enabling to examine patients in standing or sitting position
- Using a multi-coil approach, whole-body low-field MR imaging is possible
- Image quality in low-field MRI is sufficient for myocardial imaging
- To minimize metal artifact, the long axis of the prosthesis should lie in the direction of the readout gradient. Bandwidth and number of echoes should be maximized, TE minimized. Gradient power should be as high as possible
- Open MRI facilitates interventional MR-guided procedures

## References

Ahn JM, Kwak SM, Kang HS et al (1998) Evaluation of patellar cartilage in cadavers with a low field strength extremity-only magnet: comparison of MR imaging sequences, with macroscopic findings as the standard. Radiology 208:57–62

Assheuer J, Forutan F, Golfman C, Trümmler KH et al (2014) Do we need high field MR scanner for routine imaging of the lumbar spine? ISSLS, Seoul

Bohinski RJ, Warnick RE, Gaskill-Shipley MF et al (2001) Intraoperative magnetic resonance imaging to determine the extent of resection of pituitary macroadenomas during transsphenoidal microsurgery. Neurosurgery 49:1133–1143
Bootz F, Schulz T, Weber A, Scheffler B, Keiner S (2001) The use of open MRI in Otorhinolaryngology: initial experience. Comput Aided Surg 6:297–304
Bredella MA, Losasso C, Moelleken SC et al (2001) Three-point Dixon chemical-shift imaging for evaluating articular cartilage defects in the knee joint on a low-field-strength open magnet. AJR Am J Roentgenol 177:1371–1375
Catalano O, Antonaci S, Moro G et al (2005) Contrast- enhanced magnetic resonance imaging assessment of scar size in patients with chronic myocardial infarction. Ital Heart J 6:133–137
Cotten A, Delfaut E, Demondion X et al (2000) MR imaging of the knee at 0.2 and 1,5 T: correlation with surgery. Am J Roentgenol 174:1093–1097
Domalski S, Klein M (2006) MR-Diffusion imaging in liver and other body areas using HASTE and RARE technique. German Patent Application, DE 2006E21415
Friedman DP, Rosetti GF, Flanders AE et al (1995) MR imaging: quality assessment method and ratings at 33 centers. Radiology 196:219–226
Gatehouse PD, Firmin DN (2000) The cardiovascular magnetic resonance machine: hardware and software requirements. Heart 25:317–330
Harman M, Ipeksoy U, Dogan A et al (2003) MR arthrography in chondromalacia patellae diagnosis on a low field open magnet system. Clin Imaging 27:194–199
Harvey SB, Smith FW, Hukins DW (1998) Measurement of lumbar spine flexion-extension using a low-field open-magnet magnetic resonance scanner. Invest Radiol 33:439–443
Herber S, Kreitner KF, Kalden P, Low R, Berger S, Thelen M (2000) Low field MRI of the ankle joint: initial experience in children and adolescent using an open 0.2 T MR system. Rofo 172:267–273
Herfkens RJ, Higgins CB, Hricak H et al (1983) Nuclear magnetic resonance imaging of the cardiovascular system: normal and pathologic findings. Radiology 147:749–759
Jager HR, Moore EA, Bynevelt M, Kitchen N, Taylor W (2000) Contrast-enhanced MR angiography in patients with carotid artery stenosis: comparison of two different techniques with an unenhanced 2D time-of-flight sequence. Neuroradiology 42:240–248
Kaandorp TAM, Bax JJ, Schuijf JD et al (2004) Head- to- head comparison between contrast-enhanced magnetic resonance imaging and dobutamine magnetic resonance imaging in men with ischemic cardiomyopathy. Am J Cardiol 93:1461–1464
Kersting-Sommerhoff B, Hof N, Lenz M et al (1996) MRI of the peripheral joints with a low field dedicated system: a reliable and cost-effective alternative to high field units? Eur Radiol 6:561–565
Klang E, Aharoni D, Hermann KG et al (2014) Magnetic resonance imaging of pelvic entheses – a systematic comparison between short tau inversion recovery (STIR) and T1-weighted, contrast-enhanced, fat-saturated sequences. Skeletal Radiol 43:499–505
Klein HM, Meyners W, Neeb R, Trümmler KH (2007) Initial clinical results with cardiac MRI using an open low-field system. J Comp Assist Tomogr 31:430–434
Klein HM, Buchal R, Achenbach U, Domalski S (2008) CE-MRA of carotid and vertebral artery: open 0.35T vs. 1.5 T MRI. Clin Neuroradiol 18(2):107–112
Klemm T, Duda S, Machann J et al (2000) MR imaging in the presence of vascular stents: a systematic assessment of artifacts for various stent orientations, sequence types and field strengths. Magn Reson Imaging 12:606–615
Krampla W, Roesel M, Svoboda K et al (2009) MRI of the knee: how do field strength and radiologist's experience influence diagnostic accuracy and interobserver correlation in assessing chondral and meniscal lesions and the integrity of the anterior cruciate ligament? Eur Radiol 19(6):1519–1528
Kreitner KF, Hansen M, Schadmand-Fischer S, Krummenauer F, Runkel M (1999) Low-field MRI of the knee joint: results of a prospective, arthroscopically controlled study. Rofo 170:35–40

Kreitner KF, Loew R, Runkel M, Zöllner J, Thelen M (2003) Low-field MR arthrography of the shoulder joint: technique, indications, and clinical results. Eur Radiol 13(2):320–329

Lee RK, Griffith JF, Lau YY, Leung JH, Ng AW, Hung EH, Law SW (2015) Diagnostic capability of low- versus high-field MRI for lumbar degenerative disease. Spine (Phila Pa 1976) 40(6):382–391

Lipton MJ, Bogaert J, Boxt LM, Reba RC (2002) Imaging of ischemic heart disease. Eur Radiol 12:1061–1080

Loew R, Kreitner KF, Runkel M, Zoellner J, Thelen M (2000) MR arthrography of the shoulder: comparison of low field (0.2T) vs. High field (1.5T) imaging. Eur Radiol 10:989–996

Lopez MPL, Bodi V, Sanchis J, Garcia D, Pellicer M, Losada A et al (2004) Reliability of cardiac MRI indicators of myocardial viability for predicting the recovery of systolic function after a first acute myocardial infarction with a patent culprit artery. Rev Esp Cardiol 57:826–833

Lund GK, Stork A, Saeed M et al (2004) Acute myocardial infarction: evaluation with first- pass enhancement and delayed enhancement MR imaging compared with 201TI SPECT imaging. Radiology 232:49–57

Magee T, Shapiro M, Williams D (2003) Comparison of high-field-strength versus low-field-strength MRI of the shoulder. AJR Am J Roentgenol 181(5):1211–1215

Marti-Bonmati L, Kormano M (1997) MR equipment acquisition strategies: low-field or high field scanners. Eur Radiol 7:263–268

Mc Fain SB, Korosec FR, Holmes JH et al (2007) Functional lung imaging using hyperpolarized gas in MRI. J Magn Reson Imaging 25:910–923

Merl T, Scholz M, Gerhardt P et al (1999) Results of a prospective multicenter study for evaluation of the diagnostic quality of an open whole-body low-field MRI unit. A comparison with high-field MRI measured by the applicable gold standard. Eur J Radiol 30:43–53

Parizel PM, Dijkstra HA, Geenen GP et al (1995) Low field vs. High field MR imaging of the knee: a comparison of signal behavior and diagnostic performance. Eur J Radiol 19:132–138

Pavone P, Marsili L, Catalano C, Petroni GA, Aytan E, Cardone GP, Passariello R (1992) Carotid arteries: evaluation with low-field-strength MR angiography. Radiology 184(2):401–404

Pedersen JK, Lorenzen T, Ejbjerg B et al (2014) Low-field magnetic resonance imaging or combined ultrasonography and anti-cyclic citrullinated peptide antibody improve correct classification of individuals as established rheumatoid arthritis: results of a population-based, cross-sectional study. BMC Musculoskelet Disord 15:268

Petersch B, Bogner J, Fransson A et al (2004) Effects of geometric distortion in 0.2 T MRI on radiotherapy treatment planning of prostate cancer. Radiother Oncol 71:55–64

Petersilge CA, Lewin JS, Duerk JL, Haem SF (1997) MR Arthrography oft he shoulder: rethinking traditional imaging procedures to meet the technical requirements of MR image guidance. Am J Roentgenol 169:1453–1457

Raby N (2001) Magnetic resonance imaging of suspected scaphoid fractures using a low field dedicated extremity MR system. Clin Radiol 56:316–320

Reiser M (1997) MR mammography. Preoperative marking of non-palpable breast lesions with the magnetom open at 0.2 T. Radiologe 37(9):685–691

Remonda L, Senn P, Barth A, Arnold M, Lövblad KO, Schroth G (2002) Contrast-enhanced 3D MR angiography of the carotid artery: comparison with conventional digital subtraction angiography. AJNR Am J Neuroradiol 23:213–219

Riel KA, Reinisch M, Kersting-Sommerhoff B et al (1997) 0.2-Tesla magnetic resonance of internal lesions of knee joint: a prospective arthroscopically controlled clinical study. Knee Surg Sports Traumatol Arthrosc 7:37–41

Rössler E, Mattea C, Stapf S (2014) Feasibility of high-resolution one-dimensional relaxation imaging at low magnetic field using a single-sided NMR scanner applied to articular cartilage. J Magn Reson 251C:43–51

Rothschild PA, Domesek JM, Eastham ME, Kaufman L (1992) MR imaging of excessively obese patients: the use of an open permanent magnet. Magn Reson Imaging 9:151–154

Sandstede JJ (2003) Assessment of myocardial viability by MR imaging. Eur Radiol 13:52–61

Schäfer JF, Vollmar J, Schick F et al (2002) Imaging diagnosis of solitary pulmonary nodules on an open low-field MRI system – comparison of two MR sequences with spiral-CT. Rofo 174:1107–1114
Shellock FG, Bert JM, Fritts HM et al (2001) Evaluation of the rotator cuff and glenoid labrum using a 0.2-Tesla extremity magnetic resonance (MR) system: MR results compared to surgical findings. J Magn Reson Imaging 14:763–770
Sittek H, Perlet C, Herrmann K, Linsmeier E, Kolem H, Untch M, Kessler M, Reiser M (1997) MR mammography. Preoperative marking of non-palpable breast lesions with the Magnetom open at 0.2 T. Radiologe 37(9):685–691
Sugimoto H, Hirose I, Miyaoka E et al (2003) Low field strength MR imaging of failed hip arthroplasty: association of femoral periprosthetic signal intensity with radiographic, surgical, and pathologic findings. Radiology 229:718–723
Tavernier T, Cotten A (2005) High- versus low-field MR imaging. Radiol Clin North Am 43:673–681
Tung GA, Entzian D, Green A, Brody JM (2000) High-field and low-field MR imaging of superior glenoid labral tears and associated tendon injuries. Am J Roentgenol 174(4):1107–1114
Yamada S, Muragaki Y, Maruyama T, Komori T, Okada Y (2015) Role of neurochemical navigation with 5-aminolevulinic acid during intraoperative MRI-guided resection of intracranial malignant gliomas. Clin Neurol Neurosurg 130:134–139
Yu W, Feng F, Dion E, Yang H, Jiang M, Genant HK (1998) Comparison of radiography, computed tomography and magnetic resonance imaging in the detection of sacroiliitis accompanying ankylosing spondylitis. Skeletal Radiol 27:311–320

# Economy and Ecology

# 8

A responsible way of medical diagnosis and treatment is always an economical way. To waste resources means that fewer people are given the medical service they need.

The keyword is “value-based” payment. For several years, productivity-based payment will persist – but in the near future, not the procedure will be paid but the outcome, the value it has for the medical community: patient, insurer, hospital, referring physician, and government (Arenson 2015).

We may like it or not, we may call it in human or mechanistic, it is the way medicine is looked at by those who make the decisions all over the world.

It is wise, to prepare for this development. This requires two measurements:

- Use all rationalizing reserves. Optimize cost-effectiveness.
- If performance is paid, we have to define what performance is! (definitely the more difficult task).

To come back to our low-field MRI: what possible consequences could low-field MRI have on cost-effectiveness?

The term “effectiveness” is complex. To analyse it, we need public health studies on the costs/additional quality adjusted live year (QALY, see Chap. 1) for low- and high-field MRI for different indications.

The term “cost” is more easy: the best way to get an impression on the economical aspects of low-field magnetic resonance imaging is to establish a cost calculation, something everyone who goes in private MRI business has to do.

*All figures and calculation are estimated based on the conditions in the German health care and economic system and have to be adapted to the individual situation.*

The calculation has to consider the costs of investment:

- Location
- System components
- Installation
- Financing



H.-M. Klein, *Clinical Low Field Strength Magnetic Resonance Imaging: A Practical Guide to Accessible MRI*, DOI 10.1007/978-3-319-16516-5_8

And all operational costs:

- Room costs
- Energy
- Maintenance costs
- Employees
- Variable costs

We will compare the costs of a low-field imaging site with a high-field imaging site. The revenues are not discussed, since they are depending too much on the individual situation.

The calculation only addresses the MRI component of a diagnostic imaging institute.

Since such an institute can be understood as a modular combination of different modalities (X-ray, computed tomography, nuclear medicine, ultrasound, breast imaging, interventional radiology, and MRI), the assessment of one single module can be performed with sufficient exactness. As stated above, the given figures represent the conditions in Germany.

## 8.1 Investment

Before you invest time and money in a new imaging business, you have to answer multiple questions. The three most obvious ones are:

- Is there a need for this imaging site? (you will definitely know 1 year later)
- Where is the best location? (where would you like to go, if you would be a patient?)
- What is the right equipment?

### 8.1.1 Location

Sometimes, the location is already determined. This is true, if the imaging institute is part of a hospital.

If the location can be chosen deliberately, several prerequisites should be taken care of. Most important is good access to traffic and public transportation, as well as enough parking space.

The location in general should be attractive and comfortable for the patient. Convenience, a calm, competent atmosphere, is important. The location should be easy to find, and easy to access, particularly for handicapped patients (Fig. 8.1).

The size of the location defines the room costs. The minimum space, required for an open low-field MR imaging system, is about 40 $m^2$. This includes the room for the technical components, the scan room, control room, and dressing room for the patient. For a high-field system, the minimum space is larger, about 60 $m^2$, due to

**Fig. 8.1** Ambitious, patient-friendly design of an open MRI site (Radiological Institute Herne/Germany, Photography: Ulrich von Born, courtesy Hitachi Medical Imaging Inc.)

the larger dimensions of the system and the stronger field strength, extending the 0.5 mT safety line (see Chap. 3).

Additional space is needed for reception and waiting area, restrooms, storage, and reporting room. So the total minimum space, needed for an MR imaging practice, is about 100 $m^2$ for a low-field system and 150 $m^2$ for high-field system.

However, space is an important factor for convenience. Considering the high costs for the imaging equipment, space is comparatively cheap (except maybe in London or New York City).

The requirements of the manufacturer, concerning power supply, static conditions, network access, etc., have to be considered.

For further calculation, we use the costs of rented rooms, given in Sect. 8.2.1.

### 8.1.2 System Components

The main component is the MRI scanner. Additionally, a radiology information system is needed (RIS), including a picture archiving and communication system (PACS), with reporting stations, viewing stations, web server, storage device, and image printer.

The price of a whole-body low-field scanner depends on a variety of facts. Let us for this calculation assume the price to be €500,000.

The price of whole-body high-field scanners varies from about €700,000 for a standard 1.5 T system to more than €2 million for a high-end wide-bore 3 T scanner.

The price is influenced by a variety of facts, including local conditions for transport, infrastructure, and maintenance staff, and can only be used as a rough estimation.

The price of digital infrastructure (RIS, PACS) is even more variable. Let us assume the IT price for this single modality installation to be €100,000.

### 8.1.3 Installation

Before the system can be installed, the RF cabin has to be built. A high-quality cabin, including daylight window, ambient light, and maybe sound solution, has to be rated at about €100,000, depending on the size and equipment of the RF cabin.

For a high-field system, an additional high-power cooling system is needed, at a cost of about €80,000.

For practice equipment like furniture, room design, computer, printer, fax, and other installation costs, an additional €200,000 should be calculated.

### 8.1.4 Financing

With the above given figures, we have to calculate the MRI system costs (low field: €500,000, high field: €1 million), digital infrastructure (€100,000), RF cabin (€100,000, high field: additional air-condition €80,000), practice equipment, and additional costs (€200,000).

Total investment for the low-field setting will be €900,000 and for a high-field setting €1.48 million.

Interest rates are presently extremely low. Leasing costs are still about 5–7 % per year. For a cost calculation, we assume financing costs of 5 % per year for the whole investment. Due to decreasing annuity, the interest payment would be 2.5 % per year. The investment should be paid after 8 years. Total accumulated costs of finance are therefore 20 % of investment (low field: €180,000, high field: €296,000).

## 8.2 Operational Costs

### 8.2.1 Room Costs

The costs for building the rooms have already been calculated. Adequate rooms are rented; the total costs in Germany would be about 25 EUR/m$^2$/month, including heating and cleaning.

Therefore, the total minimum room costs per year would be €30,000 for low-field system, compared with about €45,000 for a high-field system.

### 8.2.2 Energy

The cost of electricity has grown dramatically during recent years. Presently, the costs per kilowatt hour are about €0.20, depending on the provider contract.

The standby power consumption of a high-field MR system, mainly caused by cooling of magnet, gradient amplifier, and other components, is about 20 kW. During operation, it goes up to about 100 kW. The total power consumption is about 370 MWh per year.

The standby power consumption of low-field MR system, mainly caused by a small heater of the magnet, is less than 2 kW. During operation, it can go up to about 10 kW. Total poor consumption is therefore called 40–50 MWh per year.

Total energy costs for high-field system are therefore about €75,000 per year and for low-field system about €10,000 per year.

### 8.2.3 Maintenance Costs

Regularly, to ensure operational safety and reliable system function, a maintenance contract is closed between manufacturer and customer. The annual fee for this maintenance contract, including all costs like helium, maintenance parts, and quality control, is about €80.000–140,000 for a high-field system.

For a low-field system, the prices are lower. Since these systems are extremely reliable, mainly due to the permanent magnet, it is possible, to restrict the maintenance contract only on quality control and the most expensive replacement parts, which cost about €20.000/year.

Maintenance of the IT system is regularly about 10 % of investment costs/year, therefore, about €10,000 per year.

### 8.2.4 Employees

Let us assume two radiology technicians and two administrative employees to be needed for organization and operation of the system. The accumulated salaries would add up to about €150,000 per year.

### 8.2.5 Variable Costs

There is a multitude of variable costs, as anyone who runs an imaging institute knows. Insurances, consulting (law, tax), teaching and training, cars: let us assume €100,000 for these issues.

### 8.2.6 Cost Calculation

The following table gives the estimated cost calculation of a stand-alone MR imaging site, compared for a high- and a low-field scanner. The costs of the low-field site are about 37 % lower, mainly due to lower scanner price, less maintenance requirements, and dramatically less power consumption.

The costs for RIS/PACS, practice design, employees, administration, and variable costs are not influenced by the system type. If these costs are neglected, the purely system (field strength)-related annual costs are €137,500 for the low-field system (31 %) compared with €384,500 for a high-field MR site, a difference of nearly €250,000/year.

| € | Low field | High field |
|---|---|---|
| MRI | 62,500 | 125,000 |
| RF cabin | 12,500 | 12,500 |
| Cooling, AC | | 10,000 |
| RIS/PACS | 12,500 | 12,500 |
| Practice installation | 25,000 | 25,000 |
| Energy cost | 10,000 | 75,000 |
| Room cost | 30,000 | 45,000 |
| Staff | 130,000 | 130,000 |
| Maintenance | 30,000 | 130,000 |
| Interest/leasing costs | 22,500 | 37,000 |
| Other | 100,000 | 100,000 |
| **Total costs/year** | **435,000** | **697,000** |

## 8.3 Effects on Ecology and Environment

To optimize a system concerning its environmental conditions, if done correctly, does also mean to optimize its economic performance.

Environmental optimization means reduced consumption of resources like helium or fossile energy sources, less production of trash, recycling of system parts, and repairing instead of replacement.

### 8.3.1 Helium

The first major advantage concerning protection of natural resources is the permanent magnet does not need helium for cooling. Helium is a rare gas, only found in very few places on earth as an element that cannot be synthesized. Since it is rare, it is also expensive, the price of helium gas is about €7,25/l, and a closed-bore conventional magnet has a volume of about 2000 l.

### 8.3.2 Magnet

The permanent magnet consists of a solid ridge of iron, holding two metal alloy magnet blocks, with the total weight of about 16 tons. There is no material loss: after the life cycle of the permanent magnet, the complete magnet can be reused. Power consumption for production of the iron magnet is about 500 kWh/t (8 MWh/magnet).

### 8.3.3 Electric Power Consumption

The most important environmental advantage of low-field magnetic resonance imaging systems is extremely reduced power consumption.

**Fig. 8.2** 300 $m^2$, 29.7 kWp PV installation producing about 10 % of my practice energy (30 MWh/year)

Gradient amplifiers and RF transmitters represent high-power components, but they need this high-power input only during the scan procedure.

It generally makes a lot of sense, to combine a radiology imaging site with some kind of alternative energy production.

At my practice, I have covered the roof with a 300 $m^2$ photovoltaic installation (30 kV peak). This installation produces up to 30 MWh per year (Fig. 8.2). I therefore can produce about 10 % of energy consumption by using the sunlight (which also represents the major part of my scan time). Actually, since alternatively produced energy is paid better in Germany, I can cover about 20 % of my energy costs with my own energy income. This represents a reduction of the electric energy costs from about €75,000 to €60,000 per year.

Energy, which is not needed by the imaging practice, can be used to support e-mobility (Fig. 8.3).

### 8.3.4 Heating Power

In an average building in Germany, the amount of energy for heating is 160 kWh/$m^2$/year, equivalent to 16 l of oil or 16 $m^3$ of gas.

For a new building, the standard is 70 kWh/$m^2$/year, equivalent to 7 l of oil or 7 $m^3$ of gas.

For a highly isolated "passive" energy house, 15 kWh/$m^2$/year is possible (1.5 l oil or 1.5 $m^3$ gas /$m^2$/year).

Another way to save energy is to combine heating of the house with cooling of the MRI magnet. Installing a heat transducer between magnet and cooling system can dramatically reduce the energy consumption of the cooling converters.

The heat, which is gained by the transducer, is stored in a 2500 l heat accumulator and used for heating of the house, including the showers in the sports club on the top floor (actually, they once called me on the phone and asked whether I could do some gradient echo scans, the showers were too cold – believe it or not…).


**Fig. 8.3** Tanja Mann, reloading her e-car. Tanja and Markus Mann own "Mann Naturenergie Inc.", providing us with the additionally needed, ecologically produced, electric energy

**Fig. 8.4** That is what our country, the "Westerwald", is known for: a long cold winter

Only during wintertime, our MRI "heating device" is supported by the gas heater (Fig. 8.4).

Our building has standard isolation (36 cm Bisotherm$^R$ walls, double glass with a K-value of 1.2); therefore, the expected gas consumption should be 7 $m^3/m^2$/year. At a size of 1800 $m^2$, this would mean 12,600 $m^3$/year.

The total gas consumption in 2012 was 5000 $m^3$ gas. Therefore, our practice building's specific heat energy value is 27 kW/$m^2$/year, or 39 % of the expected value.

And at 620 m altitude above sea level, we have cold winter.

With these procedures, using sun energy and saving power for the cooling system, we could reduce our electric energy costs to about €55,000 Euro in 2012.

At a gas price of 70 ct/m3, we saved €5,320 for gas in 2012.

If we take €75,000 for electricity as total energy cost/year and €55,000 as the real energy costs and subtract €5,320 savings for gas heating, we reduced our energy costs by about 34 %.

The investment for the photovoltaic installation and the heat transducer is amortized in 4 years.

- A responsible way of medical diagnosis and treatment is always an economical way. To waste resources means that fewer people are given the medical service they need
- The keyword is "value-based" payment. For several years, productivity-based payment will persist – but in the near future, not the procedure will be paid but the outcome
- The location in general should be attractive and comfortable for the patient. Convenience, a calm, competent atmosphere, is important. The location should be easy to find, and easy to access, particularly for handicapped patients
- The minimum space, for an open low-field MR imaging system, is about 40 $m^2$. For a high-field system, the minimum space is about 60 m
- The cost difference between a low- and a high-field MRI (price, financing, maintenance, power) is about 250,000 Euro/year
- Power consumption of a low-field system is only about 15 % of a high-field unit
- The use of heat exchangers and regenerative energy can lower the energy costs of a high-field MRI by nearly 40 %

## Reference

Arenson RL (2015) Gazing at the road ahead for radiology. RSNA News 25:4

# 9 Future Developments

Low-field MRI is a fallow-lying field. For decades, the technical developments mainly addressed MRI with higher field strength. Very few attempts have been made, to transfer this progress to systems with a field strength below 0.5 T.

To activate our fantasy, let us have a look on possible developments specifically for low-field MRI systems.

## 9.1 Technical Improvements

### 9.1.1 Magnet Design

There have been a lot of innovative designs. Toshiba developed the OPART, a 0.35 T system with a high-temperature superconducting magnet.

The four poles of the magnet enabled wide open access at a high mechanic stability. This system is no longer available.

The C-arm concept is most frequently used for permanent magnet systems. Mainly Hitachi and Siemens pursue this design (Fig. 9.1).

A variation of the C-arm concept is a tiltable magnet, realized by Esaote. The G-scan magnet can be tilted, to enable weight-bearing examinations, which are of importance in musculoskeletal imaging (Fig. 9.2).

Another innovative approach has been proposed by FONAR, with one magnet on the ceiling and one on the ground, resulting in a 360° open magnet. The MRI is installed as work in progress in Oxford/GB (Fig. 9.3).

The FONAR Upright MRI is an open 0.6 T system with a resistive electromagnet for functional imaging. It fills a small, but important market segment (Fig. 9.4). PARAMED Inc./Italy has combined an upright imaging concept with tiltable table/seat, providing new application options.

A very innovative approach is the development of single-sided MRI. It is used for the so-called magnetic particle imaging (MPI). In MRI, the influence of tissue substance on the relaxation properties of protons is measured. In MPI, the



H.-M. Klein, *Clinical Low Field Strength Magnetic Resonance Imaging: A Practical Guide to Accessible MRI*, DOI 10.1007/978-3-319-16516-5_9

**Fig. 9.1** Open C-arm Magnets: *Left* Siemens Magnetom C! 0.35 T. *Right*: Hitachi Aperto 0.4 T

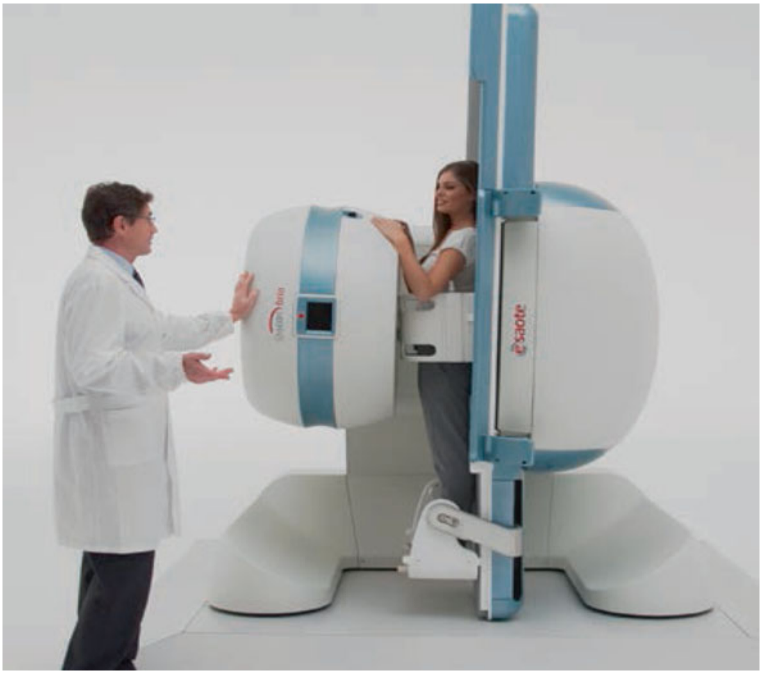


**Fig. 9.2** Esaote G-scan Brio with a field strength of 0.25 T

magnetization of the magnetic particles (magnetites, ultrasmall particles of iron oxide USPIO) is measured directly.

This method can produce extremely high-resoluted images in low magnetic fields (0.164 T) using the T1 relaxation time shortening. A vertical resolution of up to 20 μm is possible (Rössler et al. 2014). The magnetite particles are thermosensitive and can be used as nanothermometers, behaving as positive contrast agents in low-field MRI (Hannecart et al. 2015) (Fig. 9.5).

These different magnet designs give an impression of the variability of applications. Innovative magnet design is facilitated by low-field concepts.

**Fig. 9.3** The FONAR OPEN SKY MRI, with a field strength of 0.6 T. The system has 360° open access to the patient, ideally suited for interventional procedures (Courtesy FONAR Inc.)

**Fig. 9.4** Patient watching TV while scanned in a FONAR Upright MRI

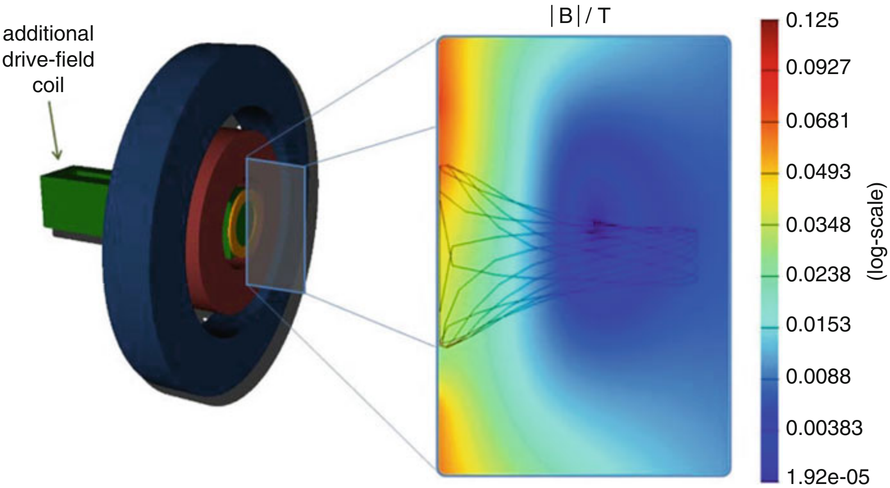


**Fig. 9.5** Single-sided magnetic particle imaging system (MPI)

### 9.1.2 Gradients

Gradient control technique and signal acquisition have experienced a small revolution with the introduction of silent scanning (Silent Scan$^{R}$, GE Healthcare). Until now, the technique does only work in a small number of high-field MRI (GE Optima MR 450w with GEM suite) (Alibek et al. 2014).

This new way of gradient control and data acquisition would represent an important improvement of convenience and patient comfort in low-field MRI as well.

### 9.1.3 Signal Production and Processing

High-quality RF transmitter and multichannel receiver can provide further improvement of image quality.

The newer concepts for analogous–digital conversion, at the start of the signal way right on the magnet (GE Optrix, Siemens) or even in the receive coil (Philips), are established in modern high-field systems. GE claims an SNR improvement of nearly 30 %. A concept ideally suited for low-field MR systems.

### 9.1.4 Coils

Coil design is a hot topic in MRI research and development. For high-field systems, the multiarray coil concepts of Siemens (TIM) and GE (GEM) and the similar products of Toshiba and Hitachi are meanwhile standard. They offer nearly whole-body coverage with multiple different coil combinations, suited for all organ regions.

There is no reason why solenoid coils could not be arranged in multi-coil arrays. However, only one low-field system has such an innovative array coil concept.

As said earlier, coil design is more an art, than a science, and there are only very few real specialists in this field (Underhill et al. 2010).

A novel approach, particularly facilitated by low-field systems, is high-temperature superconducting (HTS) coils.

Ma and coworkers (Ma et al. 2003) developed an HTS coil, consisting of a 7.62 cm YBa2Cur3O7 thin films on a $LaAlO_3$ substrate, cooled by liquid nitrogen.

This coil was compared at 0.2 T in a phantom measurement with a room temperature and a liquid nitrogen-cooled copper coil. SNR increased by 2.8 and 1.4, respectively. The technique comes from electromotor design and requires a lot of technical solutions.

## 9.2 Hyperpolarization

The magnetic force of spins lying parallel and antiparallel to the main magnetic field axis ($M_o$) neutralizes each other. Only some spins/million is the difference between parallel and antiparallel, and only these additional spins (net magnetization) contribute to the resonance signal.

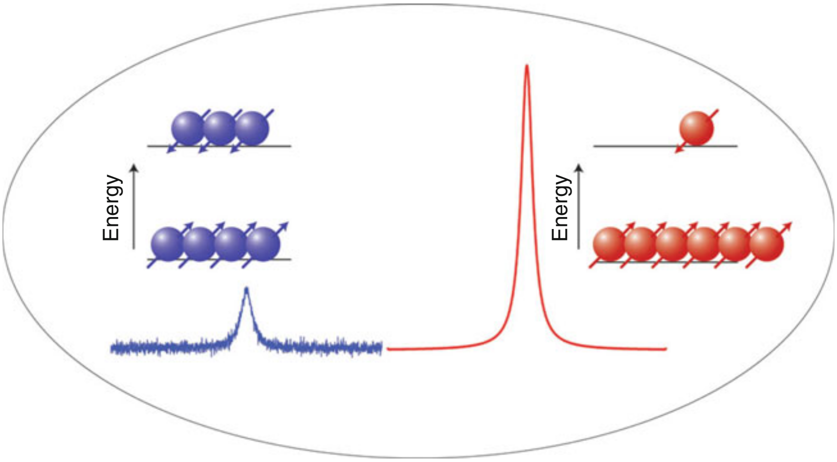


**Fig. 9.6** Net magnetization in thermal polarization and hyperpolarization and the resulting MRI spectra (Münnemann 2011)

Therefore, if the number of protons lying parallel to $M_o$ could be increased, this would have a huge impact on signal quality. One way to achieve this is hyperpolarization (Fig. 9.6).

Usually, this technique is based on $^{13}C$ spin resonance, not a common isotope for MR imaging (Münnemann and Spiess 2011). GE offers already a commercially available automated multichannel hyperpolarizer, The GE SpinLab for production of hyperpolarized carbon $^{13}C$ to view metabolic processes in the body with regular MRI systems. Low-field MR could have substantial advantages for this novel technique.

Recently, the use of hydrogen has been realized. If water-containing hyperpolarized hydrogen is injected and taken up by the body cells, the tissue metabolism can be monitored, opening completely new options for tumor diagnosis and molecular imaging. This method also facilitates lower-field-strength MRI and may create increased demand for these systems in the near future (Hövener et al. 2013; Gallagher et al. 2008a, b).

## 9.3 Zero-Energy MR Site

It is possible, using a permanent magnet low-field system, to build and operate an MR imaging site without external power supply, only driven by sun and wind: A "zero-energy practice".

The building has to be constructed as a "passive house." Minimized thermal losses during winter or heat accumulation in summer.

The roof has to be oriented to the direction of the highest sun intensity and completely covered with photovoltaic elements (Fig. 9.7).

We assume that the average power uptake of this practice would be 2 kW in standby and up to 10 kW during operation. In 8 h of service, this would mean about

**Fig. 9.7** Bungalow-type house with flat roof, tilted to sun direction (Courtesy: Holger Linke, Fingerhut Haus, Neunkhausen, Germany)

112 kWh/working day and 48 kWh/day without MR operation. With 220 working days in a year, the site would need 30,640 kWh/year.

For this activity, the zero-energy practice would need 300 $m^2$ of photoelements in Germany. In southern countries, where more solar energy can be gained per $m^2$, a smaller photoelectric collector area would be sufficient (or working days could be longer). Sun power can be combined with wind turbines.

To provide enough peak power for MR scanning, a battery or accumulator is necessary, buffering the solar energy. Battery technique is developing rapidly, since alternative energy always has the limitation of depending on wind and sun. Concepts like redox flow batteries are promising.

A zero-energy MRI site is possible, and may be an interesting solution, not only for remote areas with insufficient infrastructure.

At least, this makes clear how far the potential of MRI systems can reach, if we free ourself from the constraints of high field strength.

Sometimes, less can be more.

- Low-field MRI is a fallow-lying field with a lot of potential for improvement
- There is a variety of magnet designs for special purposes, facilitated by low-field concepts
- New gradient techniques like Silent Scan$^R$ could be useful for low-field MR systems
- Minimization of noise using high-quality active components for transmit and particularly signal receive, as well as AD conversion close to or in the coil, could improve SNR in low-field settings
- Compared with room temperature copper coils, HTS coils could provide three times better SNR at 0.2 T
- Hyperpolarization can increase net magnetization and thereby SNR, ideally suited for low-field MRI
- Using low-field MRI and optimized room construction combined with regenerative energy enables to build a "zero-energy practice" without external power supply

## References

Alibek S, Vogel M, Sun W et al (2014) Acoustic noise reduction in MRI using Silent Scan: an initial experience. Diagn Interv Radiol 20(4):360–363

Gallagher FA, Kettunen MI, Day SE et al (2008a) Magnetic resonance imaging of pH in vivo using hyperpolarized 13C-labelled bicarbonate. Nature 453:940–943

Gallagher FA, Kettunen MI, Day SE, Hu DE, Ardenkjaer-Larsen JH, Zandt R, Jensen PR, Karlsson M, Golman K, Lerche MH, Brindle KM (2008b) Magnetic resonance imaging of pH in vivo using hyperpolarized $^{13}$C-labelled bicarbonate. Nature 453:940–943

Hannecart A, Stanicki D, Vander Elst L et al (2015) Nano-thermometers with thermo-sensitive polymer grafted USPIOs behaving as positive contrast agents in low-field MRI. Nanoscale 7(8):3754–3767

Hövener JB, Schwaderlapp N, Lickert T, Duckett SB, Mewis RE, Highton LA, Kenny SM, Green GG, Leibfritz D, Korvink JG, Hennig J, von Elverfeldt D (2013) A hyperpolarized equilibrium for magnetic resonance. Nat Commun 4:2946

Ma QY, Chan KC, Kacher DF et al (2003) Superconducting RF coils for clinical MR imaging at low field. Acad Radiol 10:978–987

Münnemann K, Spiess HW (2011) The art of signal enhancement. Nat Phys 7:522–523

Rössler E, Mattea C, Stapf S (2014) Feasibility of high-resolution one-dimensional relaxation imaging at low magnetic field using a single-sided NMR scanner applied to articular cartilage. J Magn Reson 251C:43–51

Underhill HR, Yuan C, Hayes CE (2010) A combined solenoid-surface RF coil for high-resolution whole-brain rat imaging on a 3.0 Tesla clinical MR scanner. Magn Reson Med 64(3):883–892

# 10 Conclusion

A variety of factors contribute to image quality: field strength, gradient performance, homogeneity, coil design, signal- and image-processing techniques, and sequence tailoring.

Field strength is only one among many aspects of MR imaging quality.

However, technical development and scientific investigations have focused on high-field systems, which have a field strength of 1.5 to more than 9 T, using superconducting helium-cooled magnets. This aiming for higher field strengths has lasted for nearly three decades.

Only few systems with field strength lower than 0.5 T have survived this "field strength war."

The potential for high-definition low-field MR imaging has not been considered. Recent developments in low-field MRI, as a kind of "side effect" of the high-field imaging, have resulted in impressive imaging capacities.

It could be expected that there is some more potential in contemporary low-field systems, waiting to be explored.

Low field does not necessarily mean low cost. The reduced signal intensity in low-field systems requires a subtle handling of the signal. The quality of all signal conducting and processing parts has to be optimized to assure low noise level and signal loss.

There are many more positive aspects of low-field MR imaging systems. The permanent magnet does not need helium gas and cooling. An open, accessible design is possible. Dynamic joint examinations are possible. Missile effects are reduced. RF exposition is decreased. Given a comparable image quality, the application of low field strength may become an issue of patient safety.



H.-M. Klein, *Clinical Low Field Strength Magnetic Resonance Imaging: A Practical Guide to Accessible MRI*, DOI 10.1007/978-3-319-16516-5_10

To come back on our initial analogy: if you have a band, it is fun to play the whole spectrum. Systems with 1.5 T field strength are presently the standard and will probably continue to be. Three Tesla has a lot of good arguments on its side. Maybe dedicated high-field systems can combine the advantage of open access and high field strength/gradient performance. Systems with a field strength of less than 0.5 T need a redefinition. They add specific value to our imaging rationale and improve patient care.

# Index




H.-M. Klein, *Clinical Low Field Strength Magnetic Resonance Imaging: A Practical Guide to Accessible MRI*, DOI 10.1007/978-3-319-16516-5